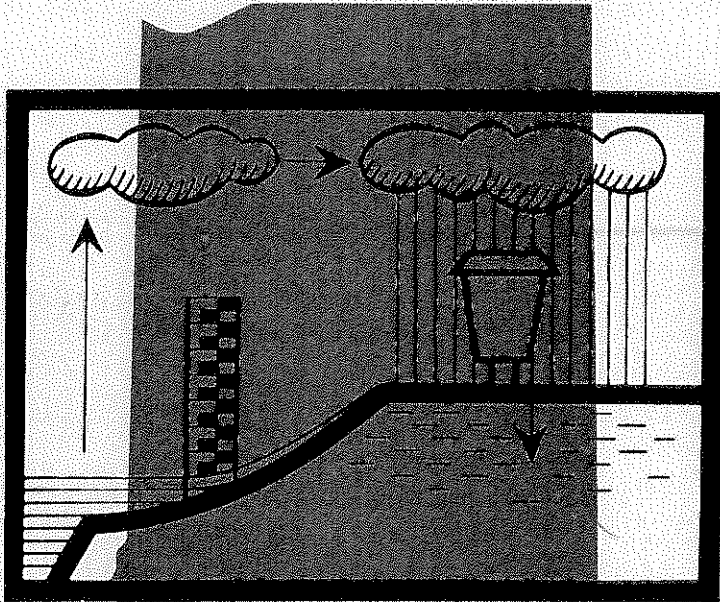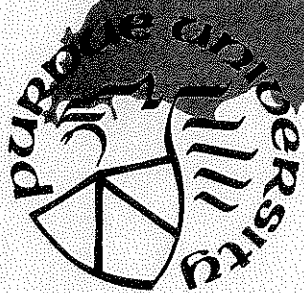*Systematic Development of Methodologies in*
Planning Urban Water Resources for Medium Size Communities

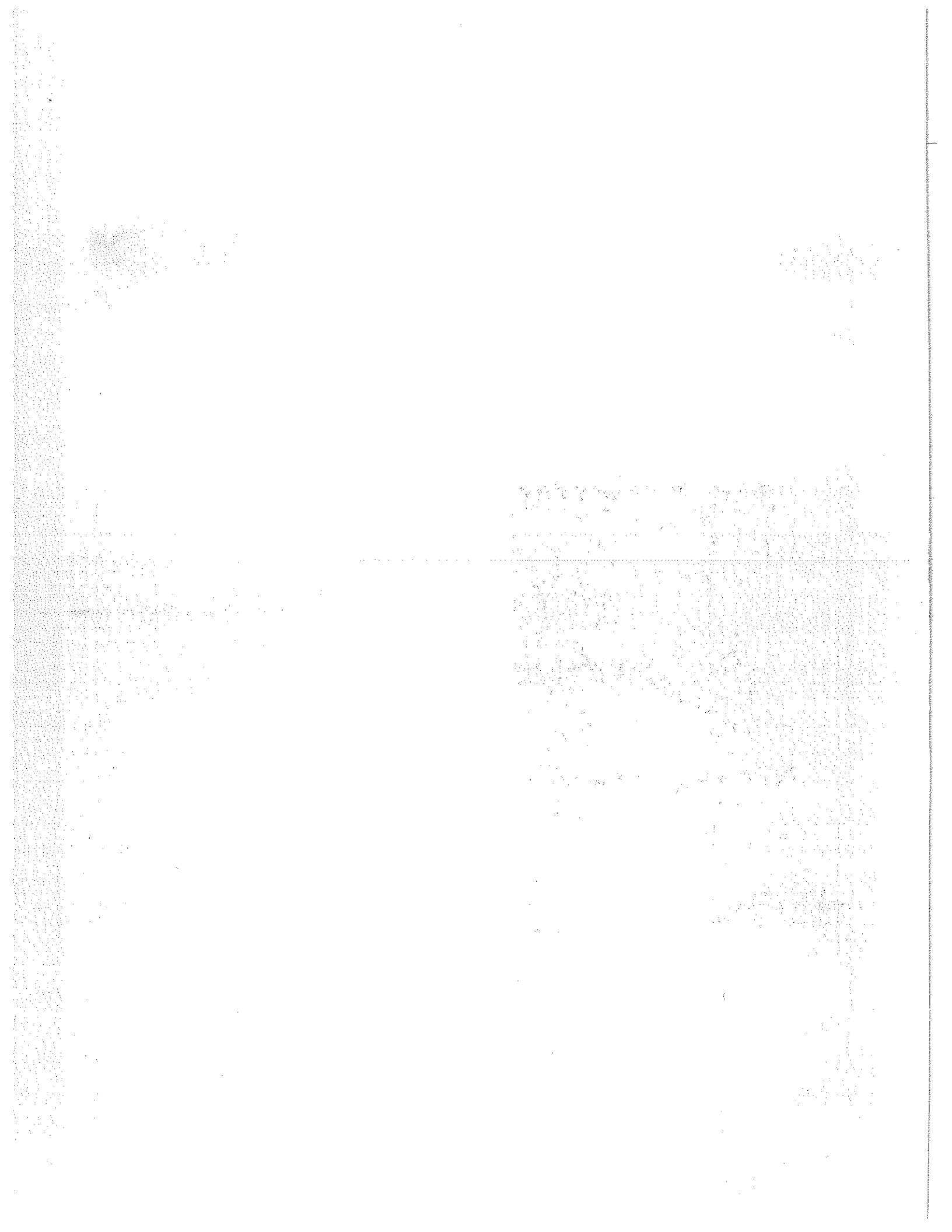# REGIONAL AQUIFER EVALUATION STUDIES
WITH STOCHASTIC INPUTS

by

Chenchayya T. Bathala

J. A. Spooner

A. Ramachandra Rao

February 1976

PURDUE UNIVERSITY
WATER RESOURCES RESEARCH CENTER
WEST LAFAYETTE, INDIANA

Water Resources Research Center

Purdue University

West Lafayette, Indiana

REGIONAL AQUIFER EVALUATION STUDIES WITH STOCHASTIC INPUTS
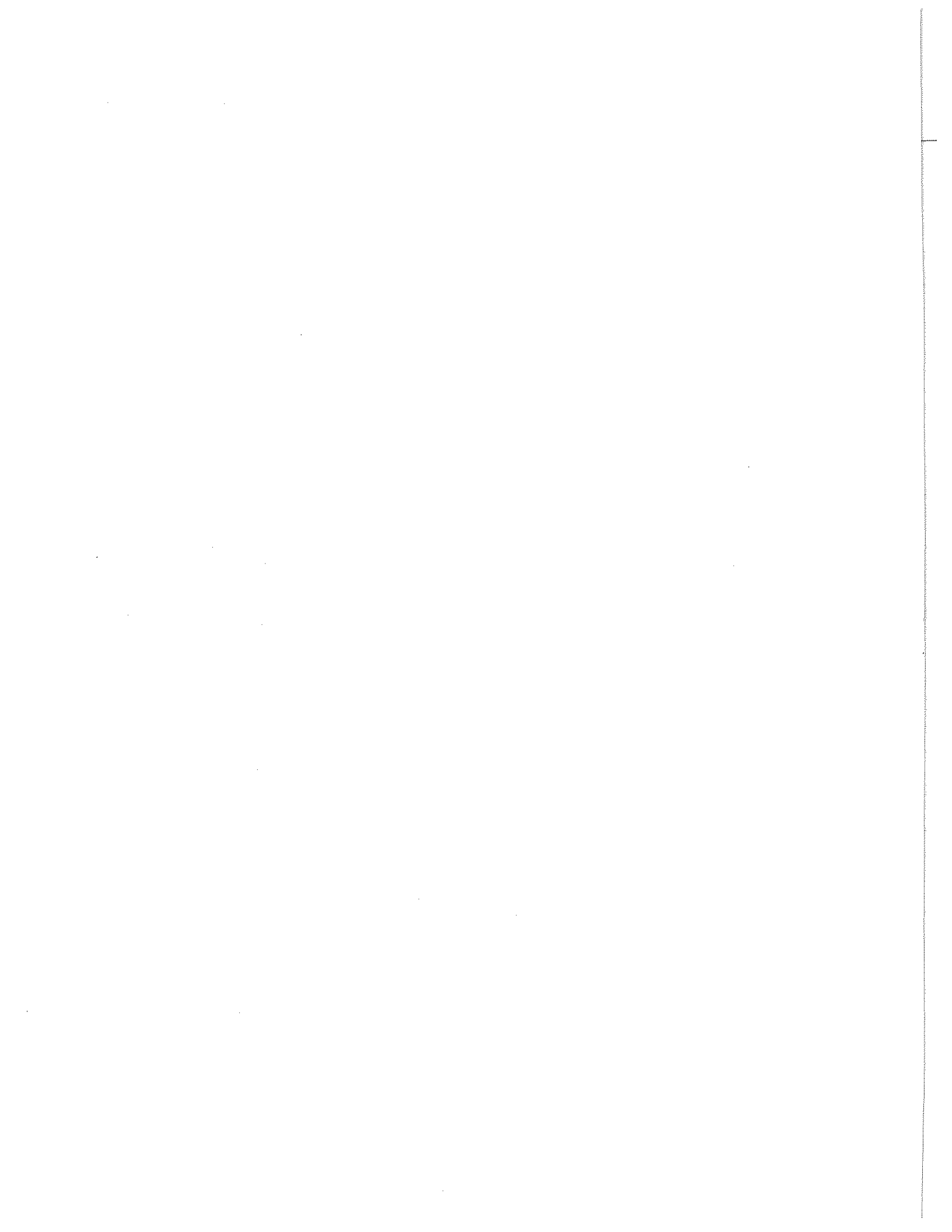
by

Chenchayya T. Bathala

J. A. Spooner

A. Ramachandra Rao

ACKNOWLEDGEMENTS
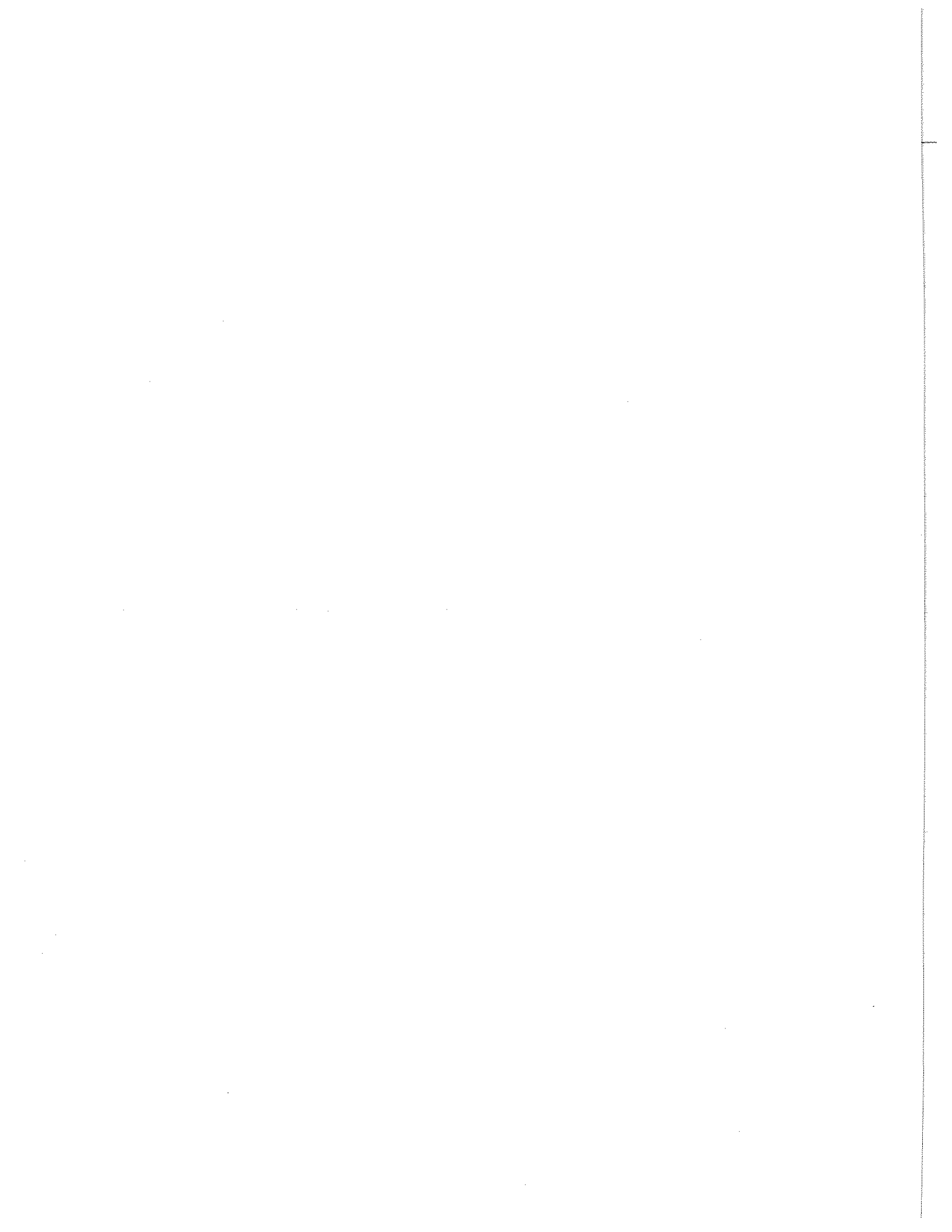
ABSTRACT

The main objective of the present study is the development of a deterministic digital model representing the glacial aquifers underlying medium size communities so that the water resources planning and development of these communities can be better accomplished. Another general purpose of the study is to obtain further insight into the techniques of groundwater modeling in order to develop better models for evaluating groundwater resources. The following are the specific objectives:

(1) To explore the feasibility of developing digital models representing the glacial aquifers underlying medium size communities and to point out the limitations of the approach.

(2) To formulate and calibrate the digital model by using historical data available from past records.

(3) To estimate the aquifer capacity by using stochastic inputs under increasing water demand.

The glacial aquifer underlying Lafayette and West Lafayette, Indiana, was selected as a test site. The digital model was formulated by using the finite difference method. Initial estimates of recharge from ponds and base flow into streams were obtained from a flow net analysis. Cross correlations and time lags between rainfall, river stages and groundwater levels were examined to introduce net recharge due to rainfall into the model and to establish the hydraulic interaction between the rivers and the aquifer. The digital model was calibrated by using a parameter adjustment procedure. The values of hydraulic conductivity, storage coefficient, net recharge due to rainfall and base flow into the streams were suitably adjusted to simulate the observed historic water levels. Stochastic difference equation models were fitted to the historic input time series of rainfall and river stages and these models were used to provide inputs to estimate the aquifer capacity under increased water demand.

The following principal results were obtained from the study. The cross correlation studies were quite useful in introducing recharge due to rainfall and in examining the hydraulic connection between the rivers and the aquifer. The vertical leakage from the overlying aquitards and the induced streambed infiltration were included in the digital model as lumped quantities without considering the physical properties of the overlying aquitards and the streambed. Lack of suitable data and funds were the major limitations in formulating and calibrating the digital model in the present study. Due to the above limitations, the results presented herein must be interpreted with caution. The results indicated the need for developing less expensive and more flexible methods of evaluating groundwater resources for medium size communities.

TABLE OF CONTENTS

LIST OF TABLES

LIST OF FIGURES

LIST OF SYMBOLS

Symbol	Description	Units
a	Distance from pumped well to recharge boundary	ft.
d_j	Serial correlation coefficient at lag j	
h	Head	ft.
ho	Head at the end of previous time step	ft.
h_T	Total potential drop	ft.
i	Column number of a node	
j	Row number of a node	
K	Hydraulic conductivity	gpd/ft^2 or ft/day
K	Total number of lags	
m	Saturated thickness of aquifer	ft.
N	Sample size	
n	Number of parameters	
n_d	Number of potential drops	
n_f	Number of flow channels	
p	Number of autoregressive terms	
Q	Pumping rate	gpm
Q	Test statistic in Portmanteau test	
q	Number of moving average terms	
R_A	Stochastic model for monthly precipitation at Agronomy Farm	
r	Distance from pumped well to observation point	ft.
r_w	Nominal radius of well	ft.
S	Storage coefficient	
S_W	Stochastic model for mean monthly stage in the Wabash River	
S_{WC}	Stochastic model for mean monthly stage in the Wildcat Creek	
s	Drawdown	ft.
Δs	Drawdown intercept per log cycle	ft.
T	Transmissivity	gpd/ft or ft^2/day
t	Time since pumping started	day
Δt	Time increment	day
$W(U)$	Well function	
$W(\cdot)$	Random variables	
$\overline{W}$	Mean of $W(\cdot)$	

<u>Symbol</u>	<u>Description</u>	<u>Units</u>
$x(\cdot)$	Values of the variate X	
x,y	Rectangular coordinates	ft.
$\Delta x,\Delta y$	Finite difference grid lengths in x and y directions	ft.
$y(\cdot)$	Values of the variate Y	
$\bar{y}$	Mean of $y(\cdot)$	
$z(\cdot)$	Values of the variate Z	
α	Level of significance	
α,β,γ	Parameters to be estimated in stochastic models	
$\zeta(\cdot)$	Random input values	
ν	Number of degrees of freedom	
σ	Standard deviation	
$\hat{\sigma}$	Estimate of standard deviation	

I. INTRODUCTION

1.1 General

The demand for water is rapidly increasing due to growth in population and urbanization. In many regions, groundwater is an important source to meet this increased demand, and hence proper regional planning and utilization of groundwater resources demand our attention. During the past few years considerable effort has been directed toward the analysis of these groundwater resources. In view of the large expenditures involved in these aquifer evaluation studies, better aquifer modeling techniques are of vital importance.

Digital models, based on either finite difference or finite element approximations, are often formulated for groundwater resource evaluation. Although the principles of groundwater flow and the techniques of numerical modeling are well established, the limitations imposed by the data and manpower requirements and computational expenditure on the development of these models are not well understood. These limitations play a major role if a digital model is to be developed for aquifers underlying medium size communities. Some additional limitations in terms of data requirements and methods of analysis arise if these are glacial aquifers. Therefore, it is desirable to explore the feasibility of constructing a digital model for the aquifers underlying medium size communities and to point out the limitations of the approach.

Rainfall and stream flow are the major sources of recharge and/or discharge to aquifers and therefore, these variables are commonly used as inputs in digital models. However, rainfall and runoff processes are stochastic in nature. Thus these processes should be simulated by using appropriate stochastic models. The simulated inputs should be used when the digital model is applied to estimate aquifer capacity under future water demands. This aspect needs further investigation for a better understanding of the behavior of the various input variables in groundwater models.

1.2 Objectives

In view of the foregoing, the specific objectives of the present study are as follows:

(1) To explore the feasibility of constructing a digital model for the glacial aquifers underlying medium size communities and to explore the difficulties that may arise due to limitations on the data, computational expenditure and availability of skilled manpower.

(2) To study the location and characteristics of the aquifers which are potential sources of water supply to the community.

(3) To formulate and calibrate the digital model using historical data available from past records.

(4) To develop stochastic models for rainfall and river stage processes.

(5) To estimate the aquifer capacity using stochastic inputs under increasing water demand.

1.3 Report Organization

The report is organized as follows. The basic principles of groundwater flow, the techniques of numerical formulation and the general procedure for the development of stochastic models for the input variables are discussed in Chapter II. A case study pertaining to the glacial aquifers underlying Lafayette and West Lafayette in Tippecanoe County, Indiana is presented in Chapter III. This chapter deals with the data used in the study, the location and characteristics of aquifers and the stochastic models developed for the rainfall and river stages in the area. The development of the deterministic digital model, the method of calibration and the estimation of aquifer capacity are discussed in Chapter IV. The limitations regarding the formulation of the digital model and the difficulties encountered in terms of data requirements and computing expenses are elaborated in Chapter V. Results of the study indicate the need for other ways of evaluating groundwater resources of medium size communities.

II. MODELING HYDROGEOLOGIC SYSTEMS

The cause-and-effect relations governing the flow of groundwater are complicated and a direct field investigation of these relationships is highly expensive and time consuming. Consequently, several types of analog models and digital computer techniques have been devised for the study of the cause-and-effect relationships of hydrogeologic systems. In the past few years, digital computer models have become quite popular for evaluating groundwater resources.

2.1 Formulation of Digital Computer Models

The principles of numerical modeling of the groundwater flow systems are well established. Two basic approaches; finite difference equations and finite element formulations have been used.

The basic concepts of numerical modeling by using the finite difference techniques are discussed in detail by *Remson, et al* (1971). Several investigators (*Stallman, 1956; Skibitzke, 1963; Prickett and Lonnquist, 1968; and Pinder and Bredehoeft, 1968*) have developed digital computer models by using the finite difference method for the evaluation of groundwater resources.

In the recent past, the finite element method has become popular as an efficient tool for the evaluation of groundwater flow systems. The finite element method and its application to several engineering problems are explained in *Zienkiewicz* (1971). *Remson, et al* (1971) have briefly described the application of finite element method to groundwater flow problems. *Guymon* (1973) presented a general procedure for the solution of fluid flow problems by using finite elements. *Javandel and Witherspoon, 1968; and Neuman and Witherspoon, 1970* have used the finite element method for the analysis of transient flow through porous media. A general algorithm for handling a variety of regional groundwater problems using finite elements, such as steady or unsteady flow, confined or unconfined flow was developed by *Wiggert* (1974).

Finite elements have several advantages over finite differences, especially when attempting to model irregular boundaries. The size of the "finite elements" can be varied readily, viz. small elements may be used in areas of rapid change and large elements may be used where variations are less severe. The inhomogeneities and anisotropy within the physical aquifer are taken into account quite easily in the finite element method. Of course all the above modifications may also be achieved by using finite difference techniques, by introducing approximations and special formulas. However, the basic concepts of the finite element method as applied to hydrogeologic systems analysis are not yet fully developed. For example, problems such as transition of flow from artesian to water table conditions is still under investigation.

In most of the groundwater resource evaluation studies using digital computer models, the historical record of input variables are often used for the calibration of the model as well as for the estimation of aquifer capacity under future water demand. The hydrological and meteorological variables such as

rainfall, stream flow, and temperature contribute to the net recharge into the aquifer and, therefore, constitute most of the input variables into the digital computer model. These input variables change from time to time and their occurrence is uncertain. Alternatively, these variables are said to be stochastic in nature. In the past few decades, statistical methods and the theory of stochastic processes were found to be efficient tools in understanding and forecasting such processes. Consequently, when the future behavior of certain input variables into the digital computer model is uncertain, the use of historical variables for the future predictions appears to be unrealistic. An alternative and a more realistic approach would be to use the historical input variables only for the calibration of the model. The historical input variables may then be analyzed stochastically and the simulated values may be used as inputs into the digital computer model for the estimation of aquifer capacity under future water demand. Thus, the critical situations, such as low rainfall and low stream flows that might show up in the future will also be taken into account during the estimation of aquifer capacity.

In the light of the foregoing discussion, one of the primary objectives of the present study is to demonstrate the use of statistical methods and stochastic processes in the development of digital computer models for the long range determination of aquifer capacity. Consequently, the digital computer technique developed by *Prickett and Lonnquist (1968)* using the finite difference method was used in the present study without regard to the relative merits of the different methods of numerical formulation. However, the above approach may also be used, even when the problem is formulated by using the finite elements. Only a two-dimensional analysis was considered in the present study. The basic concepts of the finite difference approximations are briefly explained below.

2.1.1 *Derivation of Finite Difference Equations*

The fundamental equation governing the unsteady state, two-dimensional flow of water in an anisotropic nonhomogeneous, confined aquifer is given by Eq. 2.1.

$$\frac{\partial}{\partial x}\left(T_x \frac{\partial h}{\partial x}\right) + \frac{\partial}{\partial y}\left(T_y \frac{\partial h}{\partial y}\right) = S \frac{\partial h}{\partial t} + Q \tag{2.1}$$

where,

x, y = rectangular coordinates

T_x, T_y = transmissivities in the x and y directions

h = piezometric head

t = time

S = storage coefficient

Q = net groundwater withdrawal rate per unit area

The following assumptions are made in deriving Eq. 2.1 (*Bear, 1972*):

(1) The flow in the aquifer is in the laminar range obeying Darcy's law.

(2) The flow in the aquifer is approximately two-dimensional in the horizontal plane.

(3) The fluid is homogeneous and slightly compressible.

(4) Water is instantaneously released from storage upon a decline in piezometric head.

There is no general closed form solution to the nonlinear partial differential equation presented in 2.1. However, a numerical solution can be obtained through a finite difference approach, which involves replacing the continuous differential equation by an equivalent set of discrete difference equations. As a first step in obtaining a finite difference solution to Eq. 2.1, a gird is superimposed over a map of an aquifer in the x-y plane as illustrated in Fig. 2.1. The intersections of grid lines are called nodes and are referenced with a column (i) and row (j) coordinate system collinear with the x and y directions. The differentials, ∂x and ∂y are approximated by the finite lengths Δx and Δy respectively. The area of each mesh, $\Delta x \Delta y$ should be small compared to the total area of the aquifer so that the discrete model is a reasonable representation of the continuous system. The aquifer is thus subdivided into volumes having dimensions $m\Delta x\Delta y$ where m is the thickness of the aquifer. The mathematical derivation of the finite difference approximation to the governing differential equation, 2.1 may be found in *Prickett and Lonnquist (1971)*. The final form of the finite difference approximation is given below as Eq. 2.2

$$T_{x,i-1,j}(h_{i-1,j}-h_{i,j})/\Delta x^2 + T_{x,i,j}(h_{i+1,j}-h_{i,j})/\Delta x^2 + T_{y,i,j}(h_{i,j+1}-h_{i,j})/\Delta y^2 + T_{y,i,j-1}(h_{i,j-1}-h_{i,j})/\Delta y^2$$

$$= S(h_{i,j}-ho_{i,j})/\Delta t + Q_{i,j}/\Delta x\Delta y \qquad (2.2)$$

where,

$\Delta x, \Delta y$ = finite difference grid lengths in x and y directions.

i,j = column and row numbers of a node.

$Q_{i,j}$ = net withdrawal rate at the node i,j.

Δt = time increment elapsed since last calculation of heads.

$ho_{i,j}$ = calculated head at node i,j at the end of the previous time increment Δt.

$h_{i,j}$ = calculated head at the present time increment at node i,j.

Equation 2.2 is valid for flow through a nonhomogeneous confined aquifer where the transmissivities are different in the x and y directions. On the other hand, if the aquifer is assumed to be homogeneous, and horizontally isotropic we have,

$$T_{x,i,j} = T_{y,i,j} = T_{i,j} \qquad (2.3)$$

where,

$T_{i,j}$ = the transmissivity at the node i,j.
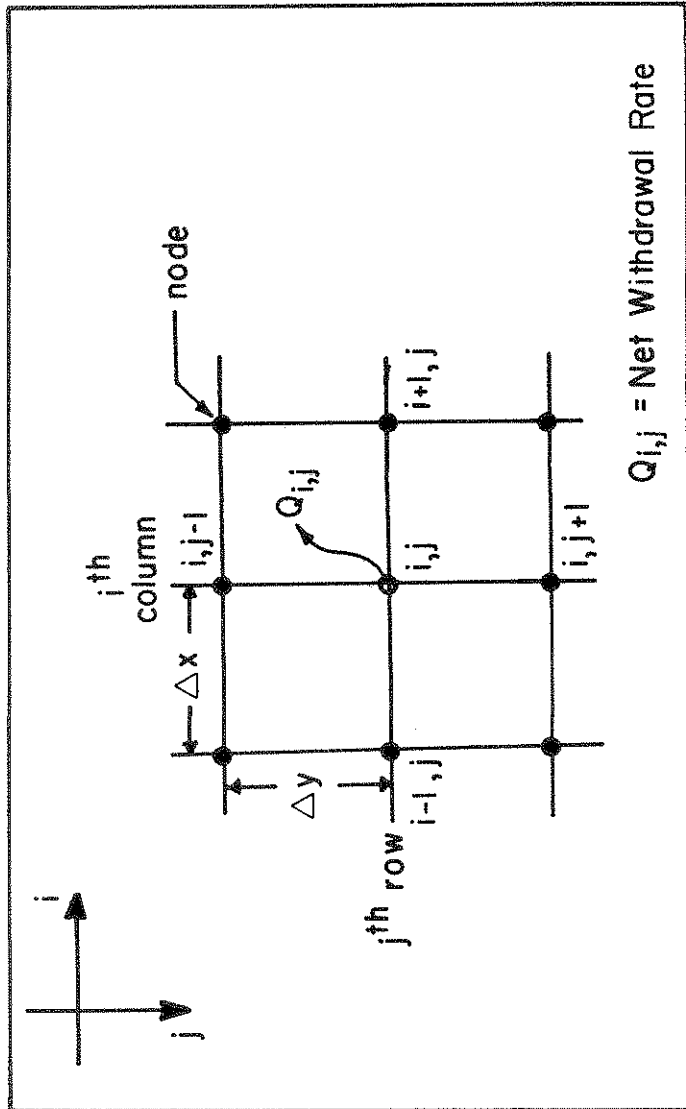
FIGURE 2.1   FINITE DIFFERENCE GRID

By substituting Eq. 2.3 into Eq. 2.2, the final form of the finite difference approximation governing the two-dimensional flow of groundwater in an isotropic, homogeneous confined aquifer can be expressed as in Eq. 2.4.

$$T_{i-1,j}(h_{i-1,j}-h_{i,j})/\Delta x^2 + T_{i,j}[(h_{i+1,j}-h_{i,j})/\Delta x^2 + (h_{i,j+1}-h_{i,j})/\Delta y^2] + T_{i,j-1}(h_{i,j-1}-h_{i,j})/\Delta y^2$$

$$= S(h_{i,j}-ho_{i,j})/\Delta t + Q_{i,j}/\Delta x \Delta y \tag{2.4}$$

An equation of the form 2.4 is written for every node of the finite difference grid superimposed on the area of interest. Thus, there will be as many equations as the number of nodes. These equations must be solved simultaneously for the principal unknowns, $h_{i,j}$. As there will be a large number of simultaneous equations, special iterative techniques are usually required to obtain a solution, even employing a digital computer.

2.1.2 Solution of Finite Difference Equations

There are several iterative techniques available in the literature for the solution of the finite difference approximations such as Eq. 2.4. Among these, the successive over-relaxation (SOR) method (Young, 1954) and the alternating direction implicit (ADI) method (Peaceman and Rachford, 1955) are the most commonly used. In the present study we have used a modified form of the ADI method as applied by Prickett and Lonnquist (1971) in the aquifer simulation program. The method is briefly described below.

The ADI method involves first, for a given time increment, the reduction of a large set of simultaneous equations to a number of small sets. This reduction is achieved by solving the finite difference equations of an individual column of the model by Gauss elimination while all terms related to the nodes in adjacent columns are held constant. The set of column equations is then implicit in the direction orthogonal to the column alignment. The solution of the set of column equations is then reduced to a straight forward process by incorporating, what Peaceman and Rachford termed G and B arrays, applied to a tri-diagonal matrix. After all column equations have been processed, column by column, the node equations of an individual row are solved again by Gauss elimination while all terms related to adjacent rows are held constant. Finally, the solution of all the equations row by row completes an "iteration". The above procedure is repeated a sufficient number of times until the solution converges. This completes the calculations for the given time step. The calculated heads are then used as initial conditions for the next time step. Peaceman and Rachford (1955) point out that the ADI method is unconditionally stable regardless of the size of the time step. Also the use of the G and B arrays greatly reduces both the computer core storage and execution time. The procedure for solving Eq. 2.2 by the ADI method is explained in Prickett and Lonnquist (1971). An example is also illustrated for the calculation of heads by using G and B arrays.

2.2 Boundary Conditions

The existence of geohydrologic boundaries limits the continuity of most aquifers in one or more directions to distances from a few hundred feet or less to a few miles or more. The geohydrologic boundaries may be divided into two types. These are, the (i) barrier boundaries and the (ii) recharge boundaries. Barrier boundaries are lines across which there is no flow and they may consist of folds, faults or relatively impervious deposits (aquiclude) such as shale or clay. Recharge boundaries are lines along which there is no drawdown and they may consist of rivers, lakes and other bodies of surface water hydraulically connected to aquifers. Most of these geohydrologic boundaries are not clear-cut straight line features but are irregular in shape and extent.

When a particular area is selected for investigation by using a simulation model, the first step is to fix the boundaries of the model based on the information regarding the location of geohydrologic boundaries in the neighborhood of the study area. For example, a river in the study area may be treated as a recharge boundary to the simulation model. Similarly, a line of bedrock outcrop may be considered as a barrier boundary. Thus the analysis of the problem would be greatly simplified if the boundaries of the model could be made to coincide with the geohydrologic boundaries. On the other hand, if the geohydrologic boundaries are located far away from the area of investigation, the groundwater system may be isolated, for modeling purposes, by introducing some arbitrary boundaries stipulated by the specific problem. These may be designated as "mixed boundaries", and there would be flow crossing the boundaries which should be taken into account in the simulation model.

All the boundary conditions pertinent to the study area must be introduced mathematically into the digital computer model before the simulation is started. A barrier boundary can be formed in a digital computer model (*Prickett and Lonnquist, 1971*) either by assigning zero transmissivities outside the boundary of interest or by introducing modified transmissivities and storage coefficients along the boundary according to vector volume concept. A recharge boundary can be simulated (*Prickett and Lonnquist, 1971*) by setting the storage coefficients of the nodes along the position of the boundary to extremely large values. A mixed boundary problem may be handled by introducing the estimates of flow across the boundaries at the respective nodes with an appropriate sign convention. However, these estimates may need to be modified until the simulated heads near the boundaries compare with the observed heads within certain limits.

2.3 Input Variables

The primary variables that constitute the inputs to the digital computer model are the aquifer properties, initial water levels, pumping rates, recharge and evapotranspiration. The aquifer properties, viz. the transmissivity and the storage coefficient at different locations in the study area are generally estimated from field pumping tests and geological information. The initial water levels are obtained from observation wells and also from the records of wells drilled in the past. Therefore,

the aquifer properties and the initial water levels may be considered as constant inputs into the digital model. However, when the aquifer properties are questionable, they may need to be modified during the process of calibration of the digital model. The input variables such as pumping rates, recharge and evapotranspiration are subject to changes which depend on several factors. The pumping rates are based on the yield capacity of the aquifer and the demand for water from the community. In the recent past, the demand for water in most of the communities has been steadily increasing due to growth in population and urbanization. Recharge to the aquifer essentially depends on the magnitude of rainfall and the infiltration characteristics of the soil. With the growth in urbanization more of the exposed areas are paved, thus decreasing the amount of seepage into the aquifers. The magnitude of evapotranspiration depends on temperature and humidity and the type of vegetation. The streams, lakes and other bodies of surface water also contribute to recharge as well as evaporation. Most often both recharge and evapotranspiration take place simultaneously and therefore, it is sufficient if the net recharge into the aquifer is considered in the formulation of the digital model.

In an urban area such as the one presently selected for investigation, the areal distribution of infiltration characteristics of the soil is rather complicated. However, the areal distribution of rainfall and temperature may be considered uniform over a small area. Moreover, the information on rainfall, temperature, river stages,etc. for most of the places in the U.S.A. are extensively documented whereas, the infiltration characteristics of the soil are not so readily available. Consequently, the net recharge into the groundwater system can be incorporated into the digital model considering the cause-and-effect relation without regard to the infiltration characteristics of the soil. The time series of rainfall, temperature, river stages, etc. are therefore considered as primary input variables into the model. As these variables change from time to time, and are mostly "chance dependent", they are treated as "stochastic" variables. However, the historical values of rainfall, temperature, etc. may be directly used as inputs into the digital model during the period of calibration. But these variables need to be simulated in order to use them as inputs into the calibrated digital model for the long range determination of aquifer capacity. The reason being that this procedure should include some of the critical situations to groundwater yield such as low rainfall, low river stages and high temperatures that might occur in the future. The general procedure adopted for the construction of stochastic models and the simulation of the input variables is presented in the next section.

2.4 Construction of Stochastic Models

In the present study we have considered the stochastic difference equation models of the hydrologic or the meteorologic features such as, precipitation, temperature, stream flow and stream stages. The general form of the stochastic difference equation which can be used to model most of the above processes is explained below.

Let $y(k)$ represent the mean value of the variate Y in the kth instant, $k = 1,2,3, \ldots, N$.
Let the variate Y be significantly correlated with the other variates, say X and Z. In a physical sense,
we may consider that the variate Y represents the mean monthly stages in a river, whereas the variates
X and Z stand respectively for the mean rainfall and the mean monthly groundwater levels in the vicinity
of the stream gaging station. A general representation for $y(k)$ is a stochastic difference equation which
relates $y(k)$ to its past values, $y(k-1)$, $y(k-2)$, $\ldots$ and the past values of the variates X and Z as
shown in Eq. 2.5.

$$y(k) = \alpha_0 + \sum_{j=1}^{n_0} \alpha_j \, y(k-j) + \sum_{j=1}^{n_1} \alpha_{n_0+j} \, X(k-j) + \sum_{j=1}^{n_2} \alpha_{n_0+n_1+j} \, Z(k-j) + \zeta(k) \qquad (2.5)$$

In Eq. 2.5, $\zeta(k)$ is the random input and is represented as shown in Eq. 2.6.

$$\zeta(k) = \sum_{j=1}^{n_3} \alpha_{n_0+n_1+n_2+j} \, W(k-j) + W(k) \qquad (2.6)$$

where,

$n = n_0+n_1+n_2+n_3+1$ = the total number of parameters, and

$W(\cdot)$ = independently and identically distributed random variables with zero mean.

The integers n_0, n_1, $\ldots$ and the coefficients α_j, $j = 0, 1, 2, \ldots$, in eq. 2.5 are unknown and
may be slowly varying functions of   time k. The random input $\zeta(k)$ may be attributed to that part
of the variate Y which is not accounted for by the variates X, Y or Z. Once again, in a physical sense,
$\zeta(k)$ could stand for the unexplained components of the physical process such as evaporation and induced
infiltration,   which also influence the stages in a river to some extent. Since the random input
$\zeta(k)$ may be subsequently correlated, at least to a lesser degree, with $y(k)$, it is customary to represent
it as in Eq. 2.6. In Eq. 2.6 the sequence $W(\cdot)$ consists of independently and identically distributed
random variables with zero mean. Usually the probability distribution of $W(\cdot)$ is not normal. The
coefficients α_j and the integers n_i, $i = 0,1, \ldots$ have to be estimated with the aid of the observed
values of the variates Y, X and Z.

If the variate Y exhibits significant periodicities, then it is customary to include the sinusoidal
trend functions in the stochastic difference equation 2.5 as shown below in Eq. 2.7.

$$y(k) = \alpha_0 + \sum_{j=1}^{n_0} \alpha_j \, y(k-j) + \sum_{j=1}^{n_1} \alpha_{n_0+j} \, X(k-j) + \sum_{j=1}^{n_2} \alpha_{n_0+n_1+j} \, Z(k-j) + \sum_{j=1}^{n_3} \alpha_{n_0+n_1+n_2+j} \, W(k-j) +$$

$$\sum_{j=1}^{n_4} \left[\beta_j \, \sin\left(\frac{2\pi jk}{12} \right) + \gamma_j \, \cos\left(\frac{2\pi jk}{12} \right) \right] + W(k) \qquad (2.7)$$

The relationship shown in Eq. 2.7 is a general stochastic difference equation that can be used
to represent most of the hydrologic and meteorologic processes. The commonly used autoregressive
(AR), moving average (MA), and the autoregressive-moving average (ARMA) models are all special forms

of the general stochastic difference equation, 2.7.

The simplest dynamic model for $y(k)$ which is related only to its past value $y(k-1)$ and which exhibits significant annual periodicities may be written as shown in Eq. 2.8.

$$y(k) = \alpha_0 + \alpha_1 \, Y(k-1) + \beta_1 \sin \frac{2\pi k}{12} + \alpha_1 \cos \frac{2\pi k}{12} + W(k) \qquad (2.8)$$

where, $W(k)$ is the ideal one step-ahead prediction error encountered in predicting $y(k)$.

2.4.1 *Parameter Estimation*

The unknown coefficients α_j, β_j and γ_j, $j = 1, 2, \ldots$ and the integers n_i, $i = 0, 1, 2, \ldots$ can be estimated from the given observations $y(k)$, $k = 1, 2, \ldots N$ using a suitable criterion of performance. In the present study the least square criterion is selected. The method used for parameter estimation is discussed in *Kashyap and Rao (1973, 1976)*.

For modeling a given process, a number of models are analyzed with different values of the integers n_i, $i = 0,1,2, \ldots$ in the general stochastic difference equation, 2.7. Appropriate sinusoidal trend functions are included on the basis of the results obtained from the autocovariance and the power spectral analysis of the observed values $y(k)$, $k = 1, 2, 3, \ldots N$. The coefficients α_j, β_j, and γ_j, $j = 1, 2, \ldots$ for each model are estimated by using the real time recursive prediction algorithm discussed by *Kashyap and Rao (1973, 1976)*. The residuals and the estimated parameters from the different models are tested for statistical significance by using several validation tests. The general criteria for validating the models is explained next.

2.4.2 *Validation of Models and Selection Criteria*

A model can be considered as validated if it adequately represents the process for which it is designed (such as forecasting). However, the validity of a model can be specified only in relative terms and in comparison with other models considered for the process. We can envision two different approaches to the problem of validation. The first of these has analytical basis behind it whereas the second approach is based on simulation results.

In the first approach, the validity of the assumptions underlying the model is tested by using the usual theory of hypothesis testing. In many cases, the only important assumption is that the disturbance sequence $W(\cdot)$ be of zero mean and uncorrelated sequence. The estimates of the disturbances or equivalently the residuals are obtained by using the given model and the available observations. The assumption that the residuals are uncorrelated is checked after reformulating the problem as a choice between two hypotheses H_0 and H_1. The hypothesis H_0, usually called the null hypothesis, declares the residuals to be independent and of zero mean. The hypothesis H_1, usually called the alternate, declares the successive residuals to be dependent and obey an autoregressive process. If the hypothesis

H_0 is accepted at a suitable prespecified level of significance, then the corresponding model is accepted. On the other hand, if H_1 is accepted, the model is considered to be unsatisfactory. The residuals are also analyzed to discover the nature of the serial dependence among them. If there is a sinusoidal trend component in the residuals, then this information can be used to modify the model, by including additional sinusoidal trend functions. The details of the specific methods of hypothesis testing used in the presnet study are explained in Chapter III.

In the second approach used to validate a model, we can compare the characteristics of the model output, such as correlograms, spectral densities and extreme value characteristics, with the corresponding characteristics of the observed data. The various statistical characteristics of the model output can be obtained either by analysis or by simulation. The model is accepted if the discrepancy between the characteristics of the simulated and the observed data is within one or two standard deviations of the corresponding characteristics.

For a given process, there may be more than one model that satisfies all the validation tests. Under such circumstances some criteria are needed for the model choice. In the present study, the final models were selected on the basis of the following criteria. (i) The number of parameters in the model should be as few as possible, but at the same time the residuals and the estimated parameters should satisfy all the validation tests. (ii) If $\hat{\sigma}_W^2 = \frac{1}{N} \sum_{k=1}^{N} (\hat{W}(k))^2$ is the residual variance and $\hat{\sigma}_s^2 = \frac{1}{N} \sum_{k=1}^{N} (y(k)-\bar{y})^2$ is the variance of the signal, then the ratio $\hat{\sigma}_W^2/\hat{\sigma}_s^2$ should be as small as possible.

III. CASE STUDY: LAFAYETTE-WEST LAFAYETTE AREA, INDIANA

3.1 General

3.1.1 *Location*

Lafayette and West Lafayette are the two major cities located in the central part of Tippecanoe County, Indiana. Lafayette, the county seat is situated 60 miles (96.5 kilometers) northwest of Indianapolis and 130 miles (209 kilometers) south-southeast of Chicago. The study area used in the modeling is 4.35 miles (7.02 km) wide west to east, and 6.06 miles (9.75 km) north to south. It is bounded on the north by latitude $40^{\circ}28'35"$ N., on the east by longitude $86^{\circ}50'52"$ W., on the south by latitude $40^{\circ}23'17"$ N. and on the west by longitude $86^{\circ}55'52"$ W. The above area chosen for investigation envelops most of the municipal and the industrial well fields located in Lafayette and West Lafayette. The location of the study area and the city limits of Lafayette and West Lafayette are shown in Fig. 3.1.

3.1.2 *Geography*

The twin cities, Lafayette and West Lafayette are separated by the Wabash River which flows southwestward from the northeastern corner of Tippecanoe County. Wildcat Creek is the major tributary to the Wabash River in the study area. The creek flows from east to north and enters the Wabash river in the northeast corner of the area under investigation. Burnett Creek is another very small tributary which drains into the Wabash River at the northern boundary of the study area.

The land surface of the study area is flat to rolling except where the Wabash River and Wildcat Creek cut deeply into the ground surface. The northwestern and the southeastern parts are relatively at a higher altitude than the Wabash River flood plain which lies in the northeast-southwest direction. The maximum relief in ground elevation is about 210 feet (64 m).

The climate is characteristic of the northern midcontinent region. The average annual precipitation is about 36 inches (91 centimeters) and is nearly uniformly distributed throughout the year. The average annual air temperature is about $52^{\circ}F(11^{\circ}C)$. The coldest month is January and the warmest month is July.

The population of Lafayette and West Lafayette, according to the 1970 census (Bureau of Census, 1970), was 64,112 persons. In addition to this, Purdue University located in West Lafayette has a student population of 27,000. The economy of the region is based mainly on agriculture and industrial production.

3.2 Data Used in the Present Study

The data used in the present investigation can be broadly classified into three catagories. These are, (i) geological data, (ii) hydrological data, and (iii) pumping data. The geological data consist mainly of driller's logs for various wells drilled within the study area. These data give essentially the geological information of the area. The static water levels measured in the observation wells and
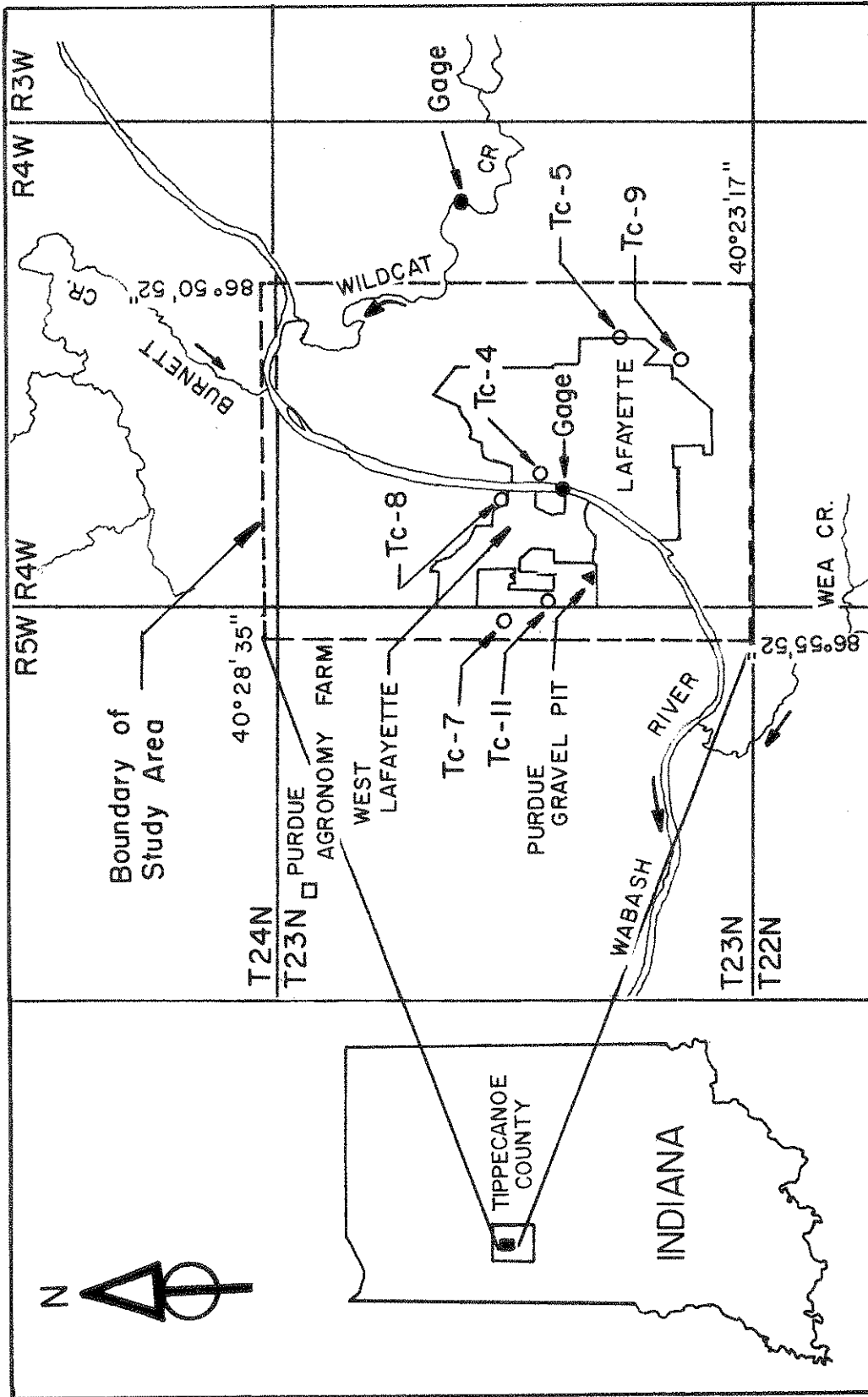
FIGURE 3.1 STUDY AREA

the ponds located in the study area, rainfall values and the river stages constitute the hydrological data. The pumping records report information on the volume of water withdrawn during different periods from various pumping centers in the study area. The above data were collected from Purdue University and federal, state and local municipal agencies.

3.2.1 *Geological Data*

Most of the geological information on the location and the driller's logs of various wells drilled in Lafayette, West Lafayette and the vicinity were collected from the Groundwater Unit, Department of Natural Resources, State of Indiana, and also from *Maarouf and Melhorn* (1975). Some of the information on wells drilled before 1956 were obtained from the basic data compiled by *Rosenshein and Cosner* (1956). The above data provided the location of wells by township, range and section numbers and listed the well logs at the time of drilling.

3.2.2 *Hydrological Data*

The monthly average values of static water levels at different locations in the study area were obtained from the observation wells maintained by the U.S.G.S. The location of these wells are shown in Fig. 3.1 and are designated TC-4, TC-5, TC-7, TC-8, TC-9 and TC-11. Although these wells are never used for pumping, the static water levels from these wells are significantly affected by pumping in the neighboring wells. The water levels from these wells are measured with reference to the land surface datum. Four to five readings of water levels taken over a month were averaged to obtain the monthly water level readings. The above records are available for varying periods of time since 1944. The details of the observation wells and the exact period of the available data are given in Table 3.1. The elevation of the land surface datum of each well below which the water levels were measured is also indicated. Plots of monthly average water levels from observation wells TC-4, TC-7 and TC-9 are presented in Fig. 3.2 as the data from these wells are available for a considerably longer period of time than for the other observation wells.

There are several ponds in the study area. In terms of recharge, the most important among these is the gravel pit located in the Purdue University campus. It receives most of the storm drainage water from the campus, and was found to be a steady source of recharge to the groundwater basin (*Bjelke, 1960*). The monthly average water levels in the gravel pit are available from June 1957 to December 1959. As the period of record is very small, only the average water level (545 ft. (166 meters) above mean sea level) is used in the present investigation. The location of the gravel pit is shown in Fig. 3.1.

The rainfall data used in the present study were measured at the Purdue Agronomy Farm which is situated in the northwest side of West Lafayette (Fig. 3.1). The raingage is located at $40^{\circ}28'$N. latitutde and $87^{\circ}00'$W. longitude. The monthly rainfall data from the Purdue Agronomy Farm were obtained
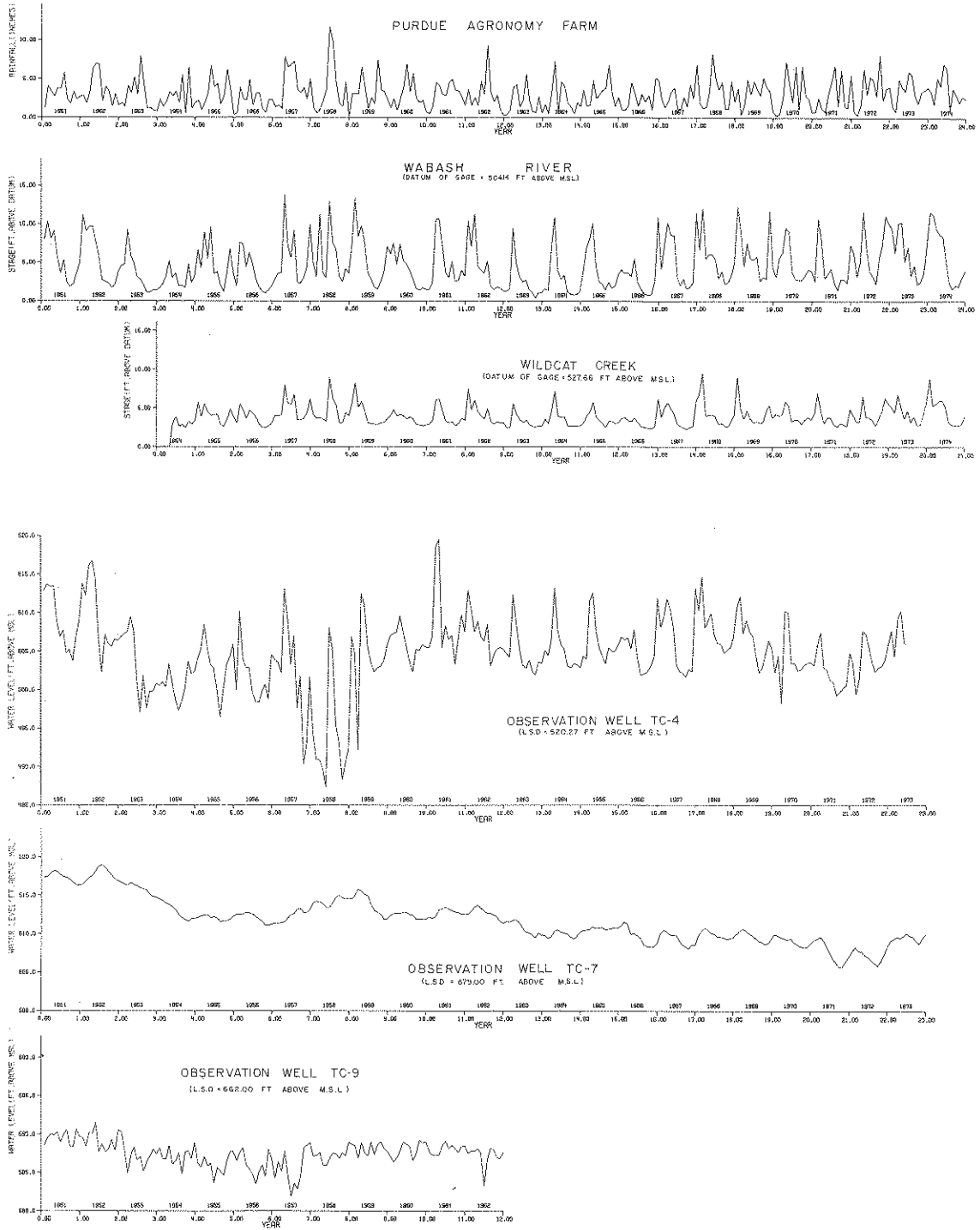
FIGURE 3.2 HYDROLOGICAL DATA

TABLE 3.1

DETAILS OF WATER LEVEL DATA FROM OBSERVATION WELLS

(LSD = Land Surface Datum)

OBS. WELL	OWNER	LOCATION	PARTICULARS	L.S.D. (Ft. above M.S.L.)	AVAILABLE DATA
TC 4	Lafayette Water Works, Lafayette	T23N, R4W, Sec. 20 NE¼ SW¼ NE¼ East bank of Wabash River near Canal St. Well 7 at City Well Field.	Unused drilled well, dia. 12", depth 127 ft.	520.87	1944-present
TC 5	Fairfield Manufacturing Co., Lafayette	T23N, R4W, Sec. 27 SE¼ NW¼ Earl Ave. & Wallace St.	Unused drilled well. Dia. 8", depth 124.4 ft.	671.00	1944-1957
TC 7	Purdue Uni., W. Lafayette	T23N, R5W, Sec. 13 SE¼ SE¼ Research housing pumphouse.	Abandoned drilled well, dia. 8", depth 206.5 ft.	679.00	1945-present
TC 8	W. Lafayette Water Co., W. Lafayette	T23N, R4W, Sec. 17 SE¼ SW¼ Happy Hollow Rd. and No. River Rd.	Abandoned drilled well, dia. 12", depth 57.9 ft.	533.00	1945-1949
TC 9	Aluminum Co. of America, Lafayette	T23N, R4W, Sec. 34 NW¼ NW¼ Earl Ave & U.S. Highway 52	Drilled unused well, dia. 16", depth 160 ft.	662.00	1947-1962

from "Climatological Data", published by the U.S. Department of Commerce. The data, which is available since 1953 is plotted in Fig. 3.2. In Fig. 3.2, the data for the years 1951 and 1952 were taken from the monthly rainfall records of Purdue University Airport.

The Wabash River stages were measured at the gage located in Lafayette near the Brown Street Levee. The location of the gage is shown in Fig. 3.1. The datum of the gage is 504.14 ft. (153.66 m.) above mean sea level. The mean monthly stages were collected from the "Daily River Stages" (Weather Bureau, U. S. Dept. of Commerce) and the data dates back to 1914. A plot of the mean monthly stages since 1951 are shown in Fig. 3.2.

The mean monthly stages of the Wildcat Creek were obtained from the Geological Survey, U.S. Dept. of the Interior. The gage on the Wildcat Creek is located 2.5 mi. (4 km) upstream of its confluence with the Wabash River (Fig. 3.1). The datum of the gage is 527.66 ft. (160.83 m.) above M.S.L. and the data is available since May 1954 and a plot of this data is presented in Fig. 3.2.

3.2.3 *Pumping Data*

There are three major pumping centers in the study area. These are, (i) the Lafayette Water Works, (ii) the West Lafayette Water Company and (iii) Purdue University. The Lafayette Water Works and the

West Lafayette Water Company supply most of the water used for domestic purposes by the Lafayette and West Lafayette communities. Purdue University supplies campus water requirements.

The well field for the Lafayette Water Works is located in Lafayette on the east bank of the Wabash River near Canal Street. About 75% of the water pumped from this well field is first conveyed to the storage tanks located in the Columbian Park. The water is again pumped from these tanks into the distribution system. The well field owned by the West Lafayette Water Company is situated on the west bank of the Wabash River near Happy Hollow Road in West Lafayette. In effect, these two pumping stations draw most of their water from the Wabash River. The wells which supply water to the Purdue University campus are situated at different locations in the campus. Only those wells which yield large quantities of water are considered in the present study. The location of the well fields operated by the above three agencies are shown in Fig. 4.1.

Annual pumpage data from the Lafayette Water Works and the West Lafayette Water Company are available since 1916. However, detailed information on the monthly pumpages are available only since 1961. The above data were obtained from the Public Service Commission, State of Indiana. The monthly pumpage data from Purdue University are available since 1954. The plots of the pumping records from the above three stations and the booster pumping at the Columbian Park are shown in Fig. 3.3 for the years 1961 onward. There has been a steady increase in the demand for water in the Lafayette and West Lafayette communities since 1961. The pumping record from the Purdue University also shows a steady increase until 1971, and drops slightly from 1972 onwards.

There are several industries located in and around Lafayette. A few of these industries, which use large quantities of water, maintain their own well fields. Among these, the Aluminum Company of America, Eli-Lilly & Company and Duncan Electric Company are the three industrial agencies which pump considerable amount of water. The location of these well fields are shown in Fig. 4.1. At present, the pumpage data from the above industries are not available. In addition, there are quite a few domestic wells in the study area. The pumpages from these wells are very small in comparison to that from municipal or industrial well fields. Consequently, the domestic pumpage was not included in the present study.

3.2.4 *Limitations on the Available Data*

Although we could get information regarding the location and driller's logs on more than about 500 wells in the study area, the data is inadequate from the standpoint of groundwater modeling. The location of wells given by township, range and section number are insufficient to pinpoint their exact location. The drillers logs do not clearly distinguish between clay, silt and till. The distinction between coarse sand and small gravel is also not noted by most drillers. Most of the wells are partially penetrating. Consequently, the total thickness of the aquifers in the area cannot be defined
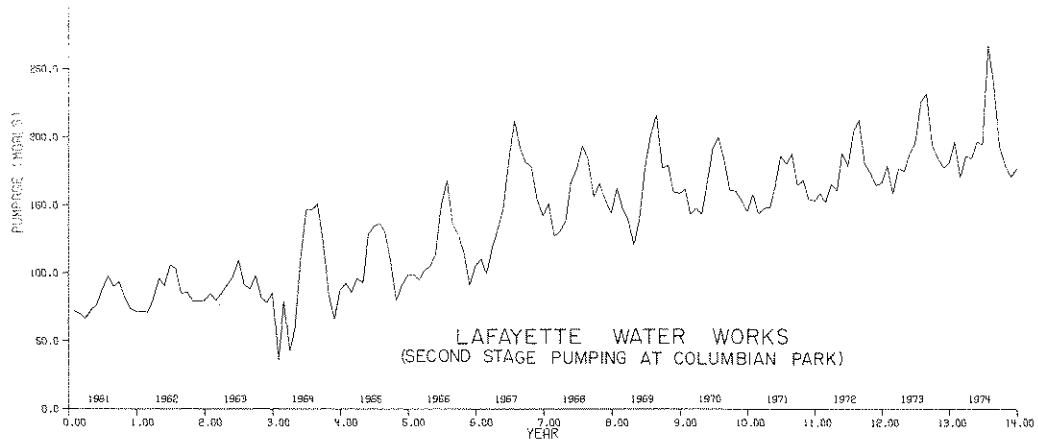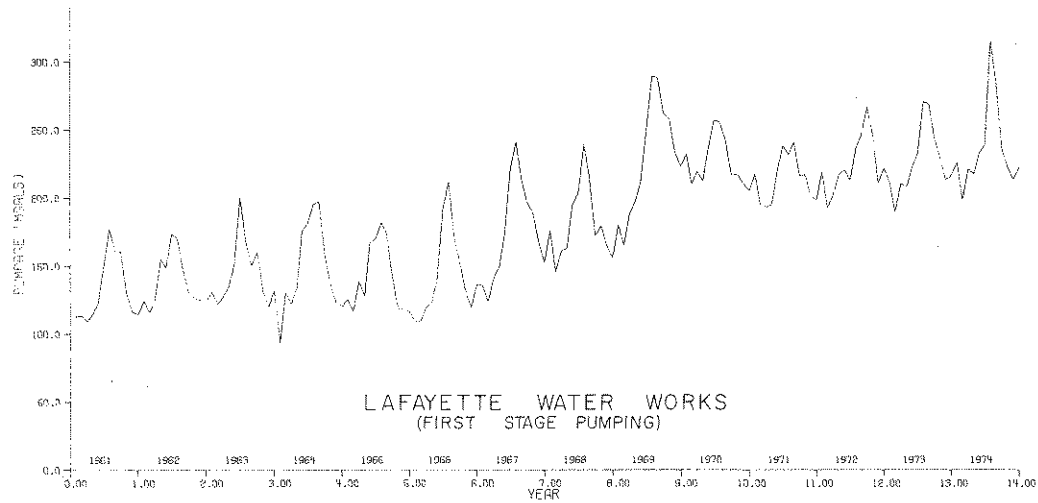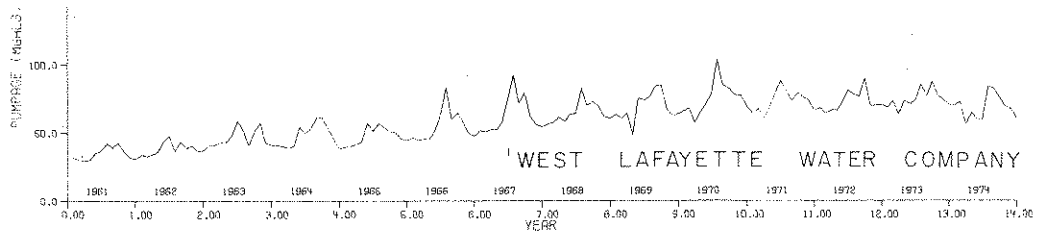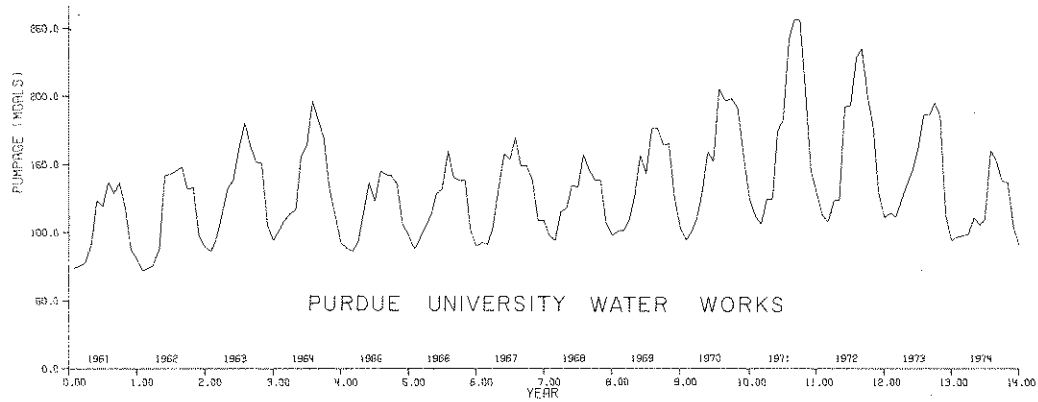
FIGURE 3.3 PUMPING DATA

completely. There is very little pumping information available in the above records. A few of the well logs contain information on pump tests carried out for 3 or 4 hours. Usually a single value of drawdown is recorded at the end of the test period. The above pumping data is of little value even to obtain a rough estimate of the hydraulic conductivity and storage coefficient of the aquifer.

Almost all the observation wells in the study area are located very near the pumping centers. Consequently, the static water levels measured from these wells were seriously affected by the daily fluctuations in pumpage.

Efforts to collect pumping information from private groundwater users has not been successful. Consequently, estimated values of pumpage at these pumping centers were used in the model. The resulting drawdowns near these pumping centers may not be realistic.

3.3 Location and Characteristics of the Aquifers

3.3.1 Geology and Hydrogeology

The geology of Tippecanoe County was first described by *Gorby* (1886). *Leverett and Taylor* (1915) briefly outlined some of the glacial features of the County. The groundwater resources of the area were briefly described by *Harrell* (1935). The groundwater resources and hydrogeology of Tippecanoe County have been investigated in greater detail during the past two decades. *Rosenshein and Cosner* (1956) compiled the basic data on several hundred wells located in the county prior to 1956. *Rosenshein* (1958) analysed and interpreted the basic data (*Rosenshein and Cosner, 1956*) and presented the first detailed report on the groundwater resources of Tippecanoe County. *Maarouf and Melhorn* (1975) investigated the hydrogeology of glacial deposits in Tippecanoe County. A brief description of the geology and hydro-geology of the study area summarized from the above investigations is presented below.

The study area is entirely covered by a heavy mantle of uniconsolidated deposits, mostly glacial drift. A few small bedrock outcrops are seen near the boundaries. The salient feature of the glacial drift is that it ranges in depth from a thin veneer to about 435 ft (133 m.) in an irregular manner. Bedrock is Paleozoic consisting of mostly shales, limestones and siltstones. The configuration of bedrock surface in the study area is shown in Fig. 3.4 (*Maarouf and Melhorn, 1975*).

Glacial outwash is the principal source of groundwater in the study area. However, shallow bed-rock, sand and gravel lenses within the till and the Holocene alluvium can yield some water for domestic and stock purposes. The alluvial deposits lying along the buried preglacial Teays valley has the highest groundwater potential.

3.3.2 Occurrence of Groundwater

Groundwater occurs under leaky artesian as well as semi-watertable conditions in the study area. Although distinct boundaries do not exist between the leaky artesian and the semi-watertable conditions, the investigations made by *Maarouf and Melhorn* (1975) and *Rosenshein* (1958) have revealed that the aquifer to the east of the Wabash river mostly underlying Lafayette is under leaky artesian conditions
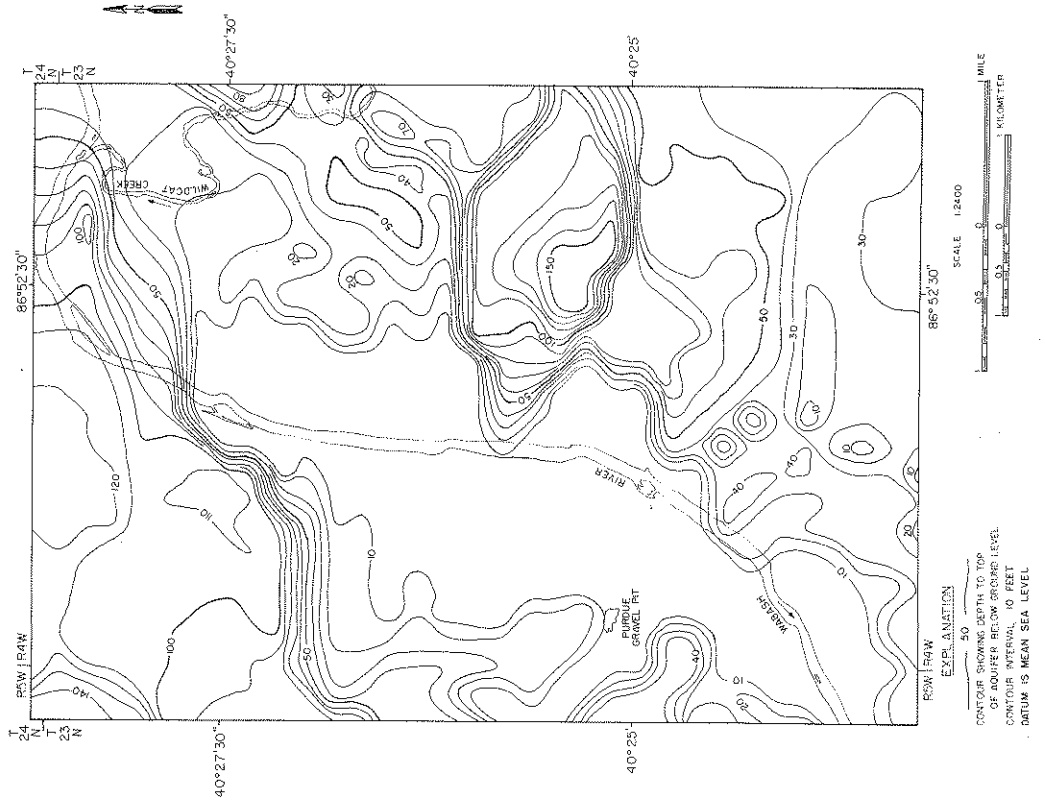
FIGURE 3.5 DEPTH TO TOP OF AQUIFER
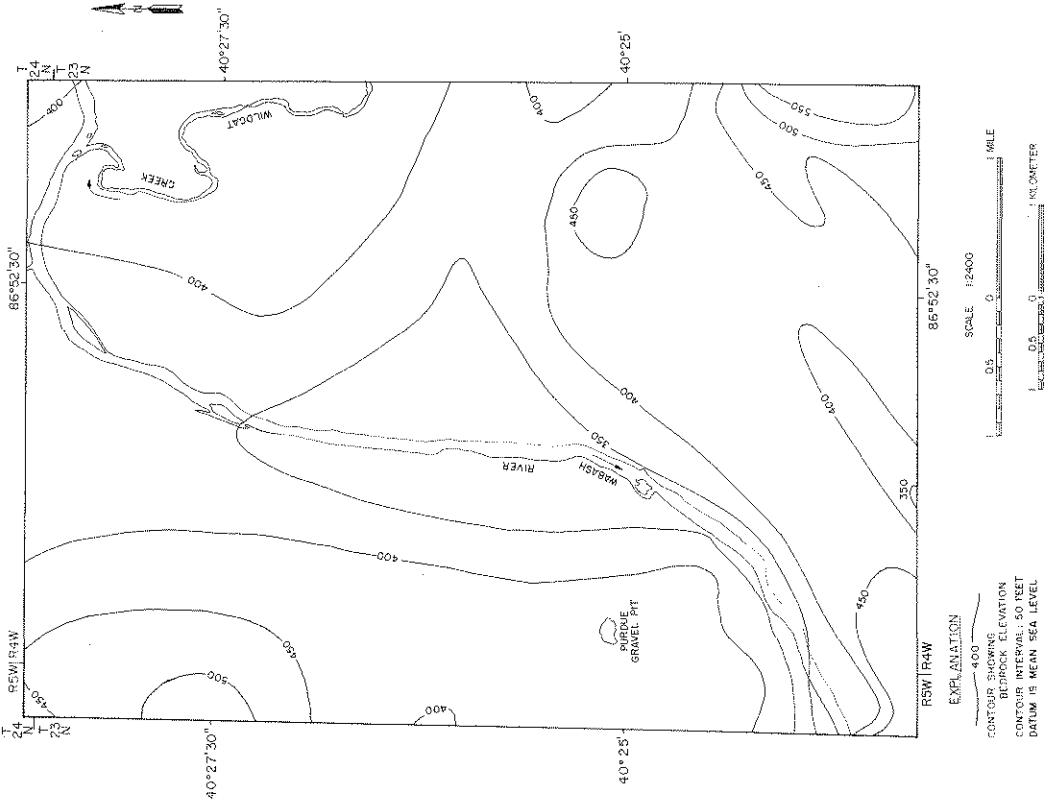
FIGURE 3.4 CONFIGURATION OF BEDROCK SURFACE

in general and that on the west side of the river underlying West Lafayette and the Purdue University campus is under watertable conditions. Information regarding depth to the top of the aquifer and the thickness of the aquifer at different locations in the study area were obtained from *Maarouf and Melhorn (1975)* and are respectively plotted in Figs. 3.5 and 3.6.

3.3.3 *Hydrologic Properties of the Aquifer*

The properties that primarily control the movement of water in an aquifer are the hydraulic conductivity (K) and the storage coefficient (S). The basic definitions and the methods of computation of the above properties are explained in many text books on groundwater hydrology (*Todd, 1959., DeWiest, 1965., and Walton, 1970*). For given values of hydraulic conductivity and storage coefficient, the yield into a well is directly proportional to the saturated thickness of the aquifer. Alternatively, the yield into a well is directly dependent on the transmissivity (T) of the aquifer. There are several methods available to estimate the hydraulic conductivity and the storage coefficient of an aquifer from field data. These methods range from the rigorous pumping test analysis (type curve methods, *Jacob, 1940*) to approximate solutions by using one drawdown (*Logan, 1964*). In practice, it is not possible to carry out pumping tests in a study area such as the one discussed here because of large expenditures involved. Consequently, in the present study we have limited ourselves to using the data which is already available from the past records.

The hydraulic conductivity and the storage coefficient of the aquifer at a few locations in the study area were computed by analyzing the pumping test data available from the past records. These locations are, (i) West Lafayette Water Company, (ii) Eli-Lilly & Co., and (iii) Aluminum Company of America (Fig. 3.1). The pumping test data from the above locations were obtained from the Groundwater Unit, Department of Natural Resources, State of Indiana. The details of the pumping test analyses for the data from the above stations are presented in Appendix A. The computed values of the aquifer parameters are shown in Table 3.2.

In addition, the specific capacity information from 24 wells located in different parts of the study area were analyzed to estimate the hydraulic conductivity. The method of estimation is explained below.

The theoretical specific capacity of a well discharging at a constant rate in a homogeneous, isotropic, nonleaky artesian aquifer infinite in areal extent is given by eq. 3.1 (*Theis, 1963*).

$$\frac{Q}{s} = \frac{Tt}{264 \; \log_{10}\left(\frac{Tt}{1.87 \; r_w^2 \; S}\right) - 65.5} \tag{3.1}$$

where,

$\frac{Q}{s}$ = specific capacity, in gpm/ft

TABLE 3.2 AQUIFER PROPERTIES

SERIAL NUMBER	WELL LOCATION			DEPTH TO BEDROCK (FT. BELOW G.L.)	DEPTH OF WELL (FT. BELOW G.L.)	AQUIFER THICKNESS (FT)	WELL RADIUS (FT)	PUMPING RATE (GPM)	PUMPING PERIOD (DAY)	DRAWDOWN (FT)	SPECIFIC CAPACITY (GPM/FT)	STORAGE COEFFICIENT	TRANSMISSIVITY (FT²/DAY)	HYDRAULIC CONDUCTIVITY (FT/DAY)	REMARKS
	TOWNSHIP	RANGE	SECTION & WELL NO.												
1	2	3	4	5	6	7	8	9	10	11	12	13	14	15	16
1	22N	4W	4-6	214	60	32	0.17	10	0.04	3	3.33	0.0005	788	25	SPQ
2	22N	4W	4-7	214	62.5	34	0.17	11	0.05	2.5	4.40	0.0005	1082	32	SPQ
3	22N	4W	6-7	225	64	56	0.25	15	0.42	2	7.5	0.001	1503	27	SPQ
4	22N	4W	6-8	215	84	9	0.18	15	0.17	10	1.5	0.001	250	28	SPQ
5	22N	5W	1-7	260	134	5	0.17	10	0.08	3.5	2.86	0.001	491	98	SPQ
6	23N	4W	2-3	186	78	4	0.17	10	0.04	2	5.00	0.05	63	16	SPQ
7	23N	4W	9-4	138	129	73	0.42	425	0.17	4	106.25	0.001	29392	403	SPQ
8	23N	4W	9-4	138	129	73	0.42	305	0.17	3	101.67	0.001	28056	384	SPQ
9	23N	4W	17-6	165	88	61	1.50	1302	0.06	14	93.00	0.1	7615	125	PT
10	23N	4W	17-11	165	88	61	1.50	1302	0.33	14	93.00	0.1	15365	252	SPQ
11	23N	4W	19-15	242	173	170	0.25	56	0.33	3	18.67	0.1	3707	22	SPQ
12	23N	4W	20-11	130	85	67	1.75	2100	0.33	26	80.77	0.05	13694	204	SPQ
13	23N	4W	20-7	130	101	66	2.00	2461	0.22	18	136.72	0.05	22712	344	SPQ
14	23N	4W	20-12	130	98	61	1.75	1600	0.33	26	61.54	0.05	10220	168	SPQ
15	23N	4W	20-13	130	91	76	1.75	2100	0.33	13	161.54	0.05	29392	387	SPQ
16	23N	4W	20-14	130	96	71	1.75	2100	0.33	22	95.45	0.05	16700	235	SPQ
17	23N	4W	21-1	166	82	38	0.42	300	0.33	6	50.00	0.001	15364	404	SPQ
18	23N	4W	27-9	260	260	54	1.75	825	0.33	14.33	57.57	0.0005	7461	138	PT
19	23N	4W	28-1	263	127	30	0.33	240	0.25	7	34.29	0.001	9319	311	SPQ
20	23N	4W	29-13	153	91	53	0.42	183	0.04	3	61.00	0.001	15030	284	SPQ
21	23N	4W	30-22	170	125	72	1.75	2020	0.33	41.5	48.67	0.1	7315	102	SPQ
22	23N	4W	30-25	150	120	25	0.25	40	0.21	13	3.08	0.1	498	20	SPQ
23	23N	4W	30-25	150	120	25	0.25	55	0.21	16	3.44	0.1	561	22	SPQ
24	23N	4W	32-6	214	71	36	0.17	7	0.06	18.17	7.00	0.05	1373	38	SPQ
25	23N	4W	34-4	247	247	42	1.75	700	0.37	25.5	38.53	0.0005	8574	357	PT
26	23N	4W	34-8	247	247	42	1.75	718.6	0.76	10	28.18	0.0005	6112	146	PT
27	23N	5W	1-8	215	161	21	0.17	8	0.13	12	0.8	0.0001	207	10	SPQ
28	23N	5W	36-2	-	155	45	0.25	50	0.25	2	4.17	0.10	7869	175	PT
29	23N	4W	35-1	-	127	21	0.18	152	0.21		76.00	0.05	18370	875	SPQ

SPQ: *Results from specific capacity data;* PT: *Results from pumping test.*
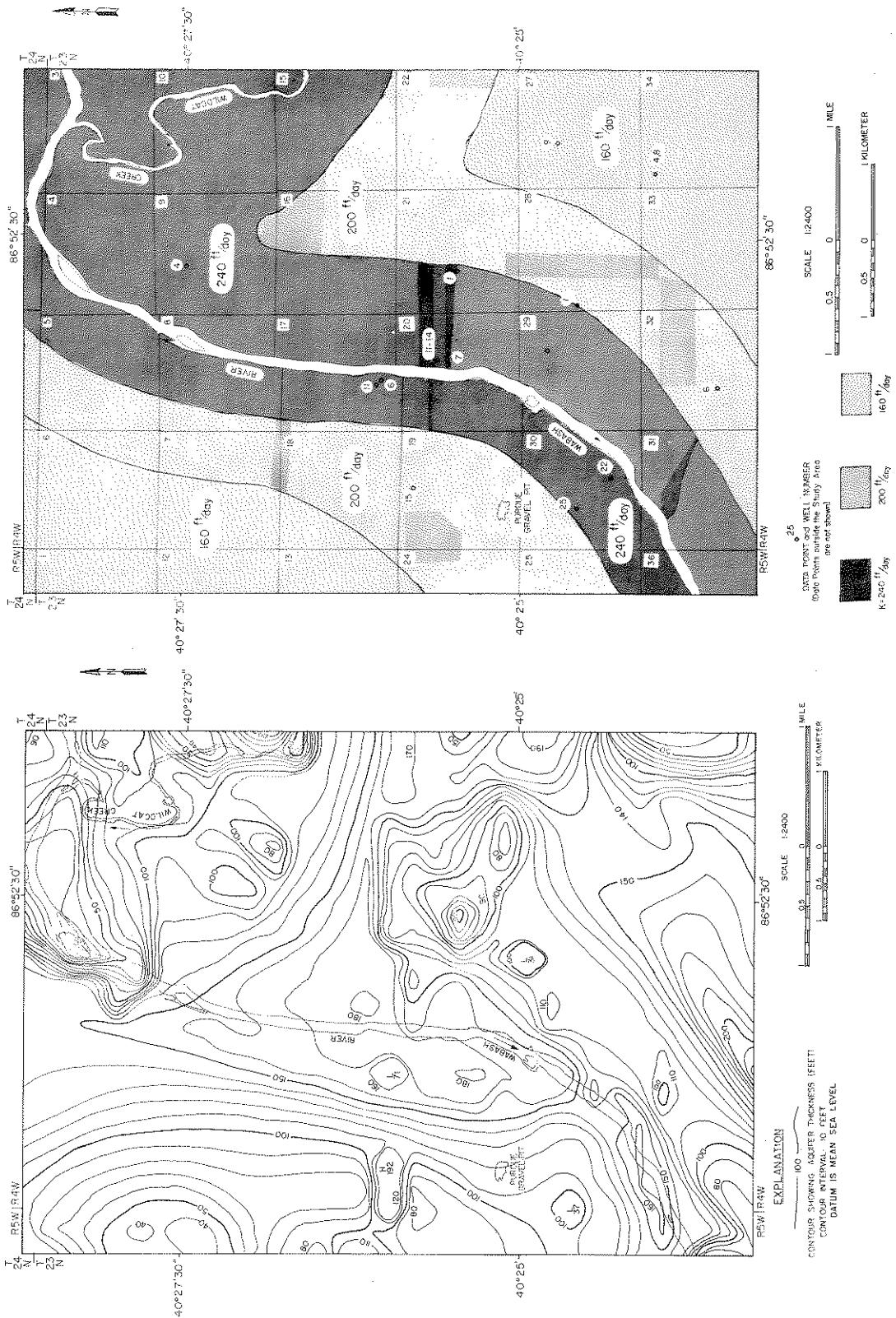
FIGURE 3.7   AVERAGE HYDRAULIC CONDUCTIVITY
OF THE AQUIFER

FIGURE 3.6   MAP OF AQUIFER THICKNESS

Q = pumping rate, in gpm

s = drawdown, ft

T = transmissivity, in gpd/ft

S = storage coefficient, fraction

r_w = nominal radius of well, in ft

t = time since pumping started, in days

Equation 3.1 was derived from the Theis non-equilibrium equation after incorporating Jacob's approximation. The assumptions made in deriving Eq. 3.1 are, (1) the production well penetrates, and is uncased, through the total saturated thickness of the aquifer, (2) well loss is negligible, and (3) the effective radius of the production well has not been affected by the drilling and development of the production well and is equal to the nominal radius of the production well.

There is no direct method of obtaining transmissivity from Eq. 3.1 for a given value of specific capacity. However, there are several approximate solutions and graphical methods available (Ogden, 1965., Hurr, 1966., and Narasimhan, 1967) for computing the transmissivity from Eq. 3.1. In all the above methods, a reasonable value is assumed for the storage coefficient either from previous knowledge of the geology of the aquifer or from the pumping test results from similar neighboring areas. Because the specific capacity varies inversely as the logarithm of 1/S in Eq. 3.1, even large errors in the assumed values of storage coefficient will result in comparatively small errors in the computed values of transmissivity. Thus we can obtain estimates of transmissivity from Eq. 3.1.

In the present study we have prepared graphs showing the relationships between the specific capacity and the transmissivity for the most commonly used values of S and for different values of r_w^2/t. These graphs are presented in Appendix B for the values of S ranging from 0.2 to 0.0001 and for r_w^2/t ranging from 0.1 to 100.

The graphs shown in Appendix B were used to compute the transmissivity at different locations in the study area by using the observed specific capacity information and the estimates of storage coefficient. The hydraulic conductivity values were then obtained by dividing the computed T values with the aquifer thickness at the respective locations. The results are shown in Table 3.2. The values of hydraulic conductivity presented in Table 3.2 can only be considered as approximations since the specific capacity information derived from water well records were often affected by partial penetration, well loss and by the presence of hydrologic boundaries. In addition, the pumping period used in most wells was not long enough to reach steady state conditions.

The aquifer parameters estimated with the above information were then used to arrive at the average values of hydraulic conductivity and the storage coefficient over the entire study area as shown in Figs. 3.7 and 3.8. Briefly, the hydraulic conductivity near the Wabash River and the Wildcat Creek is

FIGURE 3.9 PIEZOMETRIC SURFACE MAP OF MAY 1954
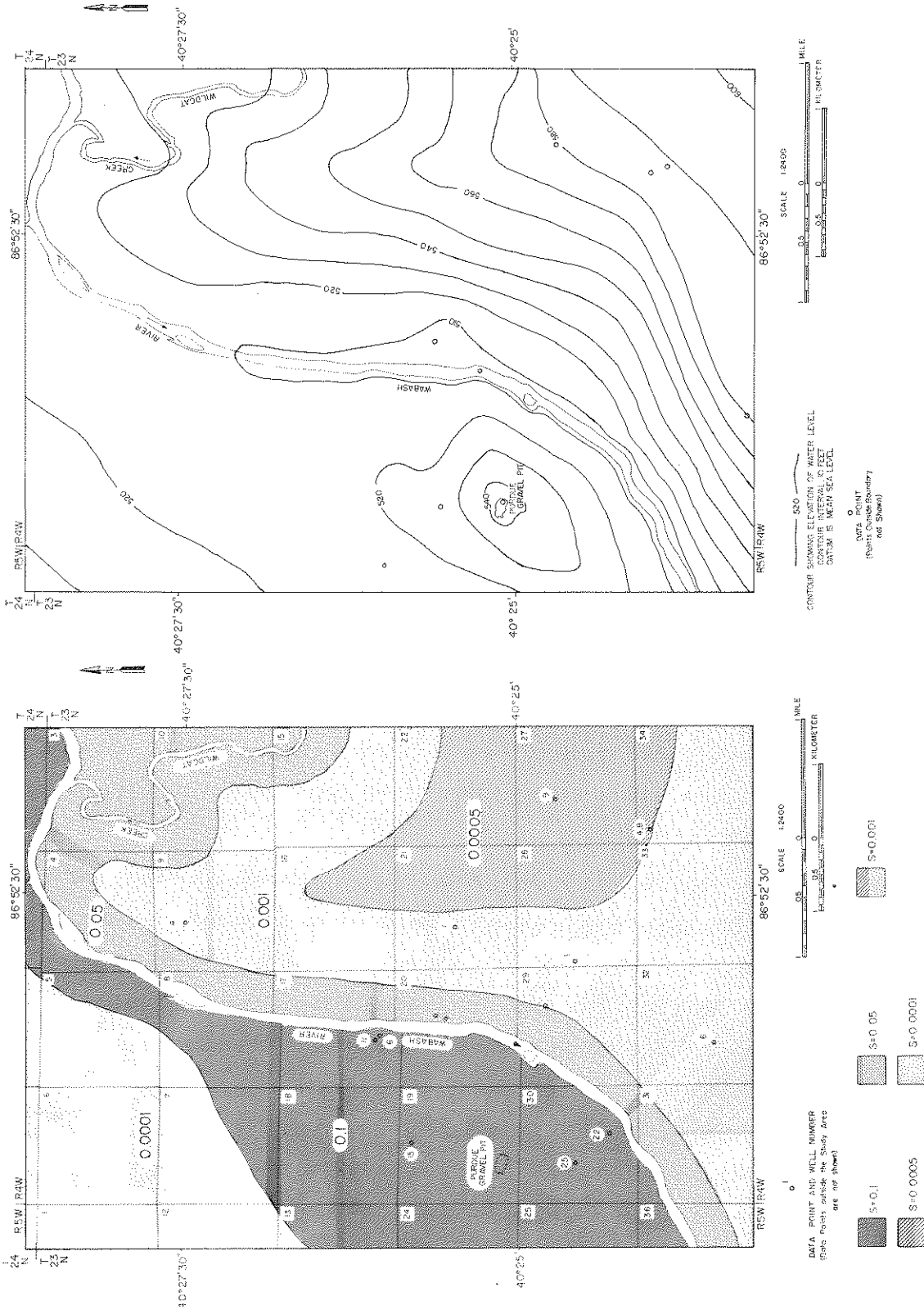
FIGURE 3.8 AVERAGE STORAGE COEFFICIENT

OF THE AQUIFER

about 240 ft/day (73 m/day). The value reduces to about 160 ft/day (49 m/day) away from the Wabash River on both sides. The storage coefficient was found to be about 0.05 on the east side of the Wabash River for a few hundred feet and decreased to about 0.0005 away from the river towards the east. There was no appreciable change in the storage coefficient for the aquifer underlying West Lafayette and the value was about 0.1.

3.3.4 *Piezometric Surface Maps*

As described in Sec. 3.3.1, the thickness of the glacial drift underlying Lafayette and West Lafayette ranges from a thin veneer to about 435 ft. (133 m.) and the geologic formation is highly heterogeneous. Thus it is very hard to distinguish between artesian and the water table conditions in the study area. For example, the water table condition at a location may change into artesian condition when the water level goes below an intermittent clay layer. Similarly, the piezometric surface at one location may show up as a phreatic surface at a different location which is a few hundred feet away. Consequently, in the present study no distinction has been made between the phreatic surface and the piezometric surface. The water level contour maps prepared for the study area are therefore called "piezometric surface maps" throughout this report.

Both long term changes and seasonal fluctuations can be envisioned in the piezometric surface at any location. In the present study, the above aspects were investigated using piezometric surface maps prepared for different time periods.

Piezometric surface maps for different time periods were prepared by using water levels observed at different observation wells in the study area. As there are very few observation wells over the entire area, static water levels measured from the wells at the time of drilling were also used. In addition, the measured stages in the Wabash River, the Wildcat Creek and the Purdue Gravel Pit were also considered in the preparation of the maps. Once again, the available data were insufficient for preparation of the maps at regular intervals of time. Consequently, those time periods during which there were several data points distributed over the area were selected. These time periods are, May 1954, November 1959, and November 1962. The piezometric surface maps for the above time periods are shown in Figs. 3.9, 3.10 and 3.11. The maps are similar to each other except for some minor distortions in the contour lines due to local fluctuations in water levels. For example, the piezometric surface elevation at the northwest corner of the study area is approximately in the range between 530 ft. (161.5 m.) and 540 ft. (165 m.) above mean sea level in all the three maps. Similarly, the piezometric surface elevation in the southeast corner is close to 600 ft. (183 m.) above mean sea level. However, there are some apparent differences in the contours which are very close to the rivers. These differences may be attributed to the fluctuations in the river stages. From the above results it can be concluded that there are no significant long term changes in water levels in the study area.

FIGURE 3.11 PIEZOMETRIC SURFACE MAP OF
NOVEMBER 1962

FIGURE 3.10 PIEZOMETRIC SURFACE MAP OF
NOVEMBER 1959
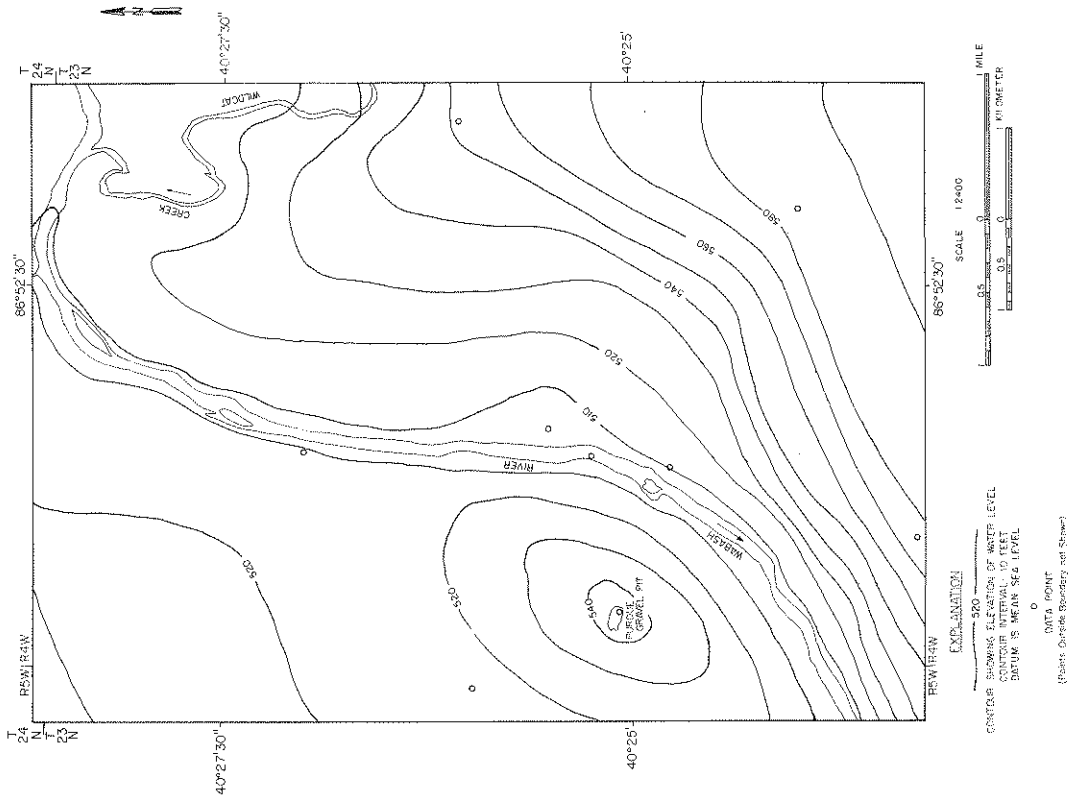
In order to investigate the seasonal fluctuations, the average piezometric surface maps were prepared for the months of January and July using water level information available during the period 1953-1972. The obvious reason for selecting the above months is that January is the coldest month and July is the warmest month in the study area. The average piezometric surface maps for the months of January and July are shown in Figs 3.12 and 3.13. There is close agreement between the piezometric surface contours in the two maps. However, there may be some significant seasonal fluctuations in drawdowns in the neighborhood of the major pumping centers. But because of lack of information, these local fluctuations are not apparent in the piezometric surface maps.

From the foregoing analysis of piezometric surface maps it can be concluded that the piezometric surface in the study area does not fluctuate very much with time.

3.3.5 *Recharge into the Aquifer*

The principal sources of recharge into the aquifer in the study area are rainfall, the influent seepage from rivers and ponds. The average annual precipitation over the area is about 36 inches (91 cm). The stream valleys and the terraces are the areas which are most favorable for recharge due to rainfall in the study area. However, the presence of intermittent clay lenses in the aquifer may decrease the amount of recharge. *Rosenshein* (1958) and *Maarouf and Melhorn* (1975) have mapped the surface and near-surface conditions related to recharge in different regions of Tippecanoe County. Based on the above investigations, the infiltration characteristics of the study area may be classified into four catagories as shown in Fig. 3.14. These are labelled Zones I-IV, and their different characteristics are explained in Fig. 3.14. The above classification yields qualitative information on the recharge capacity of different locations in the study area. The interaction of rainfall and groundwater levels may be investigated using stochastic models (*Rao, et al.*, 1973, 1975). The cross correlation properties between rainfall, Wabash River stages and water levels in wells TC-4 and TC-7 are discussed in detail by *Rao, et al.* (1975).

A plot of the cross correlogram between water levels in TC-7 and rainfall at Agronomy Farm is shown in Fig. 3.15. The highest cross correlation coefficient between rainfall and groundwater levels is 0.124 at a lag of eight months which indicates that the present change in groundwater levels is primarily influenced by the rainfall that had occurred about eight months previously. The cross correlations at other lags (Fig. 3.15) lie within the 2-standard error limits given by $\pm 2/\sqrt{N}$ with 95% probability (*Box and Jenkins*, 1970). Consequently, we can conclude that the aquifer which consists mostly of intermittent clay and till lenses acts as a low pass filter and it takes a long time, such as eight months for the infiltrated water to reach the water table.

It can be inferred from Fig. 3.2 that water levels in observation well TC-4, located on the east bank of the Wabash River, fluctuate as the stage in the river. Similar fluctuations are also observed from the water level record of well TC-8 located on the west bank of the Wabash River. A
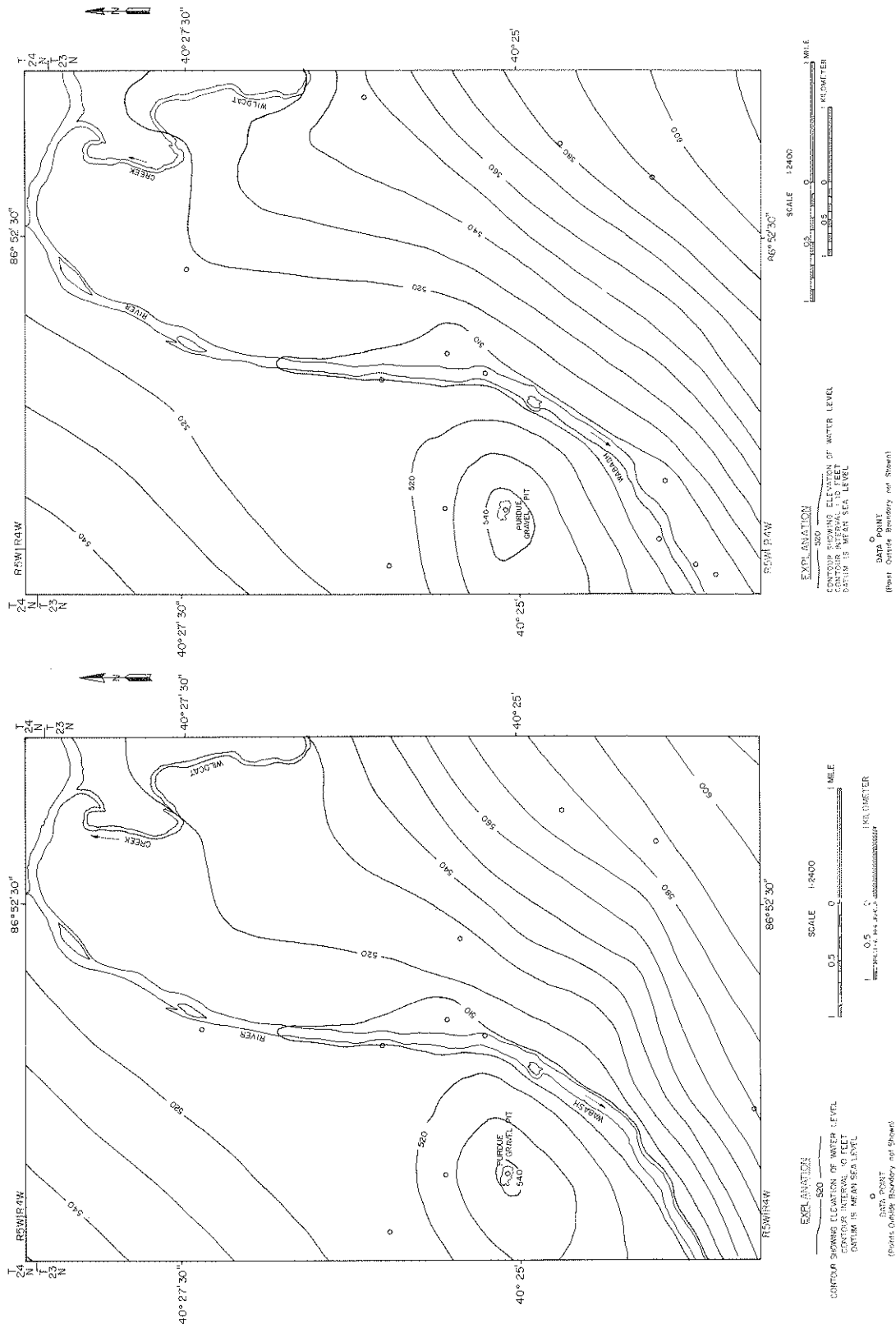
FIGURE 3.13 AVERAGE PIEZOMETRIC SURFACE
MAP OF JULY (1953-'72)

FIGURE 3.12 AVERAGE PIEZOMETRIC SURFACE
MAP OF JANUARY (1953-'72)

FIGURE 3.15 CROSS CORRELATIONS BETWEEN
RAINFALL AND WATER LEVELS IN WELL Tc-7
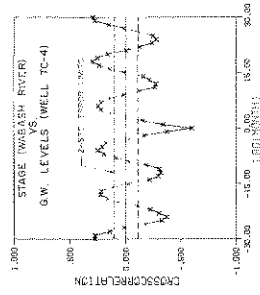
FIGURE 3.16 CROSS CORRELATIONS BETWEEN
WABASH RIVER STAGE AND WATER LEVELS IN WELL Tc-4

FIGURE 3.14 INFILTRATION CHARACTERISTICS
OF THE STUDY AREA

study of the cross correlations between the mean monthly stages in the Wabash River and the mean monthly water levels in well TC-4 is presented in Fig. 3.16 along with the confidence limits given by $\pm 2/\sqrt{N}$, where N is the number of data points. The cross correlogram (Fig. 3.16) indicates significant positive correlations at lags of 6, 18 and 30 months and negative correlations at lags of 0, 12 and 24 months. However, the cross correlation at lag zero is the most predominant of all, which indicates that the water levels in well TC-4 and the river stages are in phase. From the foregoing analysis, it can be concluded that the Wabash River is hydraulically connected to the aquifer. This is also evident from the contours of the piezometric surface maps (Figs. 3.9 - 3.13) which indicate that there is considerable base flow contribution into the Wabash River from the underground reservoir. However, some recharge to the groundwater reservoir may take place as a result of influent seepage from the Wabash River during periods of high stage. At present, the data available is not sufficient to investigate the response of groundwater levels to changes in Wildcat Creek stages. An examination of the glacial formation in the vicinity of the Wildcat Creek has shown less favorable conditions for hydraulic connection between the creek and the aquifer. However, some leakage may take place through the clay and till lenses from the creek to the aquifer and vice versa depending on the relative water levels.

In addition to the above sources of recharge and discharge, the investigations made by *Bjelke (1960)* have shown that the gravel pit in Purdue University campus is hydraulically connected to the aquifer and forms a steady source of recharge to the groundwater basin.

The initial estimates of recharge from the gravel pit and the net baseflow into the Wabash River were obtained from a flow net analysis. These estimates were suitably modified during the calibration of the digital model.

3.3.6 *Flow Net Analysis*

The use of graphical analysis of flow nets in estimating the groundwater flow is explained in *Ferris, et al. (1962)*. Flow through the full thickness of the aquifer may be computed by using flow net and Eq. 3.2 (*Ferris et al., 1962*).

$$Q_N = \frac{n_f}{n_d} \; K \; h_T m \qquad\qquad (3.2)$$

where,

Q_N = discharge through the full thickness of the aquifer, in gpd

n_f = number of flow channels

n_d = number of potential drops

K = hydraulic conductivity, in gpd/sq ft

m = saturated thickness of aquifer, in feet

h_T = total potential drop, in feet

The above approach was used in the present study for estimating the recharge into the gravel pit and the base flow contribution into the Wabash River. Since the piezometric surface does not fluctuate very much with time the average piezometric surface for the month of January (Fig. 3.12) was considered as a base map for flow net analysis. The flow net for the study area and the computational details are presented in Appendix C. The following results were obtained.

The average elevation of the water surface in the gravel pit is 545 ft. (166 m.) above mean sea level which is about 36 ft (11 m.) above the average water level in the Wabash River near the gage in Lafayette. The average hydraulic gradient towards the Wabash River is 0.0056 ft/ft. From the flow net analysis (Appendix C), the average recharge from the gravel pit was estimated to be about 14.2 mgd (54000 m^3/day). The above value was obtained by assuming an average hydraulic conductivity of 200 ft/day (61 m/day) and an average aquifer thickness of 80 ft (24 m). This value is about twice the average recharge value estimated by *Bjelke* *(1960)*. It will be seen later that the recharge from the gravel pit computed from the digital model is in close agreement with the value estimated from the flow net. It can be observed from the flow net in Appendix C that most of the recharge from the gravel pit eventually provides base flow into the Wabash River.

The average base flow contribution into the Wabash River in its 8.2 miles (13.2 km) reach in the study area was estimated to be about 55.8 mgd (212000 m^3/day). An average hydraulic conductivity of 230 ft/day (70 m/day) was assumed in the flow net analysis and the details are shown in Appendix C.

3.4 Stochastic Models for Rainfall and River Stages

The need for the development of stochastic models for the input variables such as rainfall and river stage data and the procedure for the construction of the same were explained in Secs. 2.3 and 2.4. In this section, the statistical characteristics of the input variables and the specific models fitted to them are discussed. We have also discussed several tests used for the validation of the above models.

The monthly rainfall values measured at the Purdue Agronomy Farm during the years 1954-1972 (Fig. 3.2) were used for the development of the stochastic model for the precipitation process. The mean monthly stages in the Wabash River during the period 1931-1970 and those of the Wildcat Creek for the period 1954-1970 (Fig. 3.2) were considered for simulating the river stages. The statistical characteristics of the above data and the construction of the stochastic models are presented next.

3.4.1 *Characteristics of the Data*

Some of the elementary statistics of the input variables used in the analysis are presented in Table 3.3. The standard deviations of monthly precipitation values and of the mean monthly stages

TABLE 3.3
STATISTICS OF OBSERVED RAINFALL AND RIVER STAGES

STATISTIC	RAINFALL (IN) (AG. FARM)	RIVER STAGE (FT. ABOVE DATUM)	
		WABASH	WILDCAT
Period of Data	1954-72	1931-70	1954-70
Mean	3.020	4.295	3.949
Std. Dev.	2.034	3.028	1.371
Skewness Coefficient	1.094	1.213	1.218
Kurtosis	4.281	4.028	5.583
Minimum	0.080	0.400	2.26
Maximum	11.700	17.600	9.520

Datum of gage above mean sea level:
    Wabash River at Lafayette = 504.14 ft.
    Wildcat Creek near Lafayette = 527.66 ft.

in the Wabash River are approximately two-thirds of their respective means, which indicate a wide
variability of the processes. On the other hand, the standard deviation of the mean monthly stages
in the Wildcat Creek is only about one-third of its mean, indicating lesser variability of the Wildcat
Creek stages. The values of the coefficients of skewness and kurtosis for the three sets of data are
positive and are large.

The means and standard deviations of the precipitation data and of the river stages in individual
months are plotted in Fig. 3.17. In the results presented in Fig. 3.17 the first month is January
and the last month is December. The monthly means of the precipitation data and of the river stage
data can be seen to change over the year (Fig. 3.17). Consequently, a seasonal pattern exists in
the above processes. The monthly standard deviations of the Wabash River stages also exhibit a
seasonal pattern. However, the standard deviations of the precipitation data and of the Wildcat
Creek stages for the individual months do not exhibit any pronounced seasonality

The histograms of the precipitation data and of the river stages are shown in Fig. 3.18. All
the histograms are highly skewed. There is a predominance of months when the precipitation is less
than about 4.0 in. (10.2 cm.). Similarly, the frequencies of Wabash River stages being less than
about 5 ft. (1.5 m.) and that of Wildcat Creek being less than about 4 ft. (1.2 m.) are high. The
probability of occurrence of more than 6 in. (15 cm.) of rainfall in any month can be seen to be
small. Similarly, the probabilities of the mean monthly stage being greater than 6 ft. (1.8 m.) in
the Wabash River and being greater than 5 ft. (1.5 m.) in the Wildcat Creek are also very small.

The autocovariance and the power spectral densities of the monthly precipitation data and of
the mean monthly river stage data were also examined. The computational details of the estimation
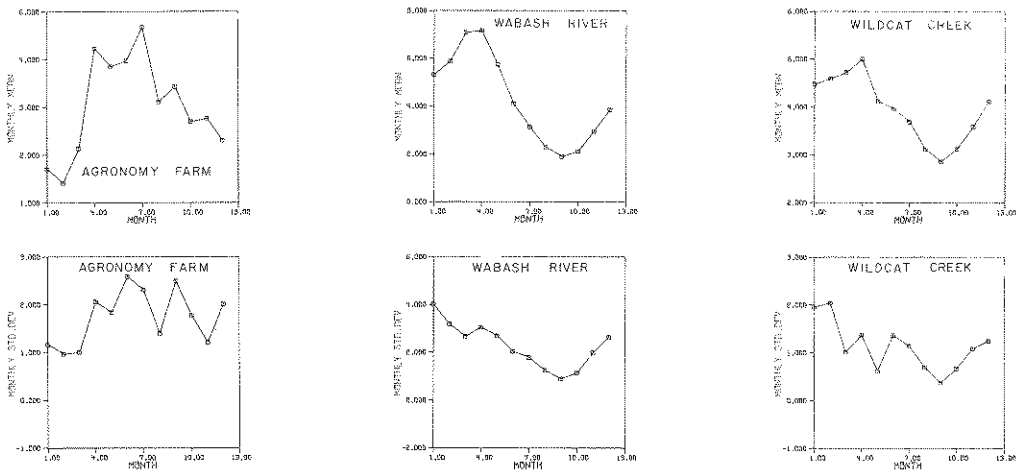
FIGURE 3.17   MONTHLY MEANS AND STANDARD DEVIATIONS OF OBSERVED DATA
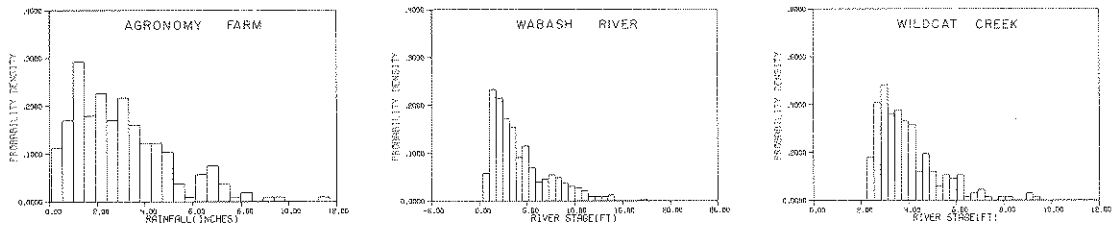
FIGURE 3.18   HISTOGRAMS OF OBSERVED DATA
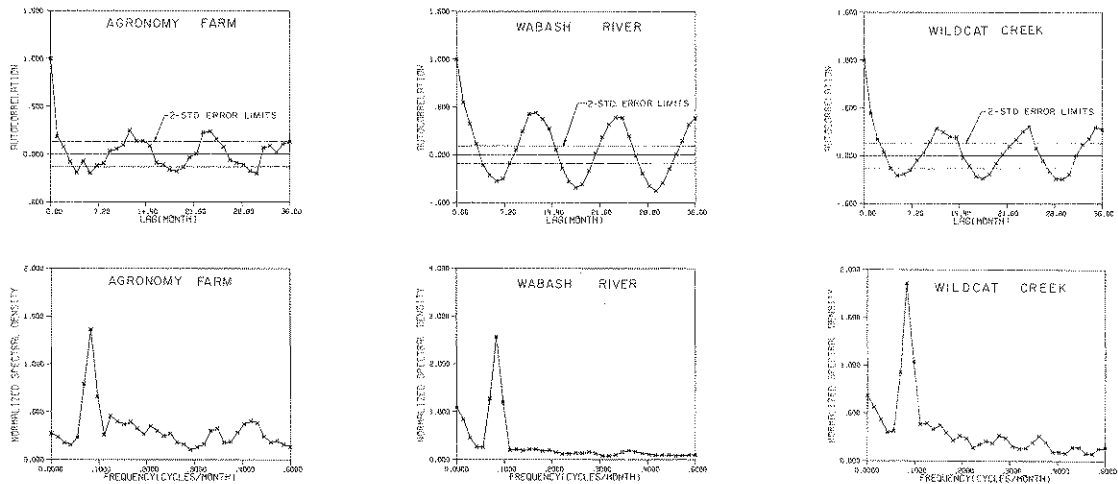
FIGURE 3.19   AUTOCORRELATIONS AND POWER SPECTRAL DENSITIES OF OBSERVED DATA

of autocovariances and power spectral densities are found in *Jenkins and Watts* (1968), and are also discussed by *Dixon* (1971). The autocovariances and the power spectral estimates were normalized by dividing each of the values by the variance of the appropriate series. The resulting correlograms and power spectral densities are plotted in Fig. 3.19. The correlograms indicate significant correlation, in the sense that these coefficients at certain lags are greater than twice standard error given by $\pm 2/\sqrt{N}$, where N is the number of months of the data used in the computation (*Box and Jenkins*, *Sec. 8.2, 1970.*, and *Anderson, 1942*). For example, there are strong positive correlations at lags of 12,24 and 36 months and negative correlations at approximate lags of 6, 18 and 30 months. The periodicities shown by the correlograms are also evident from the power spectral density plots shown in Fig. 3.19. The annual periodicity is perhaps the most strongly defined cycle that could be seen in the power spectral density plots. The obvious conclusions from a study of the power spectral density plots is that any model developed for the precipitation and the river stage data must necessarily account for these periodicities.

3.4.2 *The Stochastic Models*

Stochastic models were fitted to the input variables, rainfall and river stages as explained in Chapter II. Appropriate sinusoidal trend functions were included in the stochastic difference equations in order to preserve the significant periodicities (Sec. 3.4.1) that were observed in the precipitation and the river stage data. The best fitted models for the monthly precipitation at Agronomy Farm and for the mean monthly stages in the Wabash River and the Wildcat Creek are presented in Table 3.4.

Table 3.4

STOCHASTIC MODELS FITTED TO MONTHLY PRECIPITATION AND RIVER STAGE DATA

SYMBOL	DATA	STATION	FITTED MODEL $y(k+1) =$
R_A	Precipitation	Purdue Agronomy Farm	$2.904 + 0.057\ y(k) - 0.01\ y(k-1)$ $+0.284\ \sin \omega_1 k - 1.180\ \cos \omega_1 k$ $-0.410\ \sin \omega_2 k - 0.135\ \cos \omega_2 k + W(k)$
S_W	Stage	Wabash River at Lafayette	$2.701 + 0.305\ y(k) + 0.093\ y(k-1) + 1.461$ $\sin \omega_1 k$ $+1.293\ \cos \omega_1 k + 0.176\ \sin \omega_2 k$ $-0.175\ \cos \omega_2 k + W(k)$
S_{WC}	Stage	Wildcat Creek near Lafayette	$2.59 + 0.34\ y(k) + 0.414\ \sin \omega_1 k$ $+0.522\ \cos \omega_1 k + W(k)$

$\omega_1 = 2\pi/12, \quad \omega_2 = 2\pi/6$

In the model R_A for monthly precipitation at Agronomy Farm (Table 3.4) the coefficient of $y(k-1)$ is very small in comparison to that of $y(k)$. Consequently, it can be concluded that the monthly

precipitation in the (k+1)-th month is essentially dependent on the precipitation in the k-th month and on the seasonal trend functions with periodicities of 12 and 6 months. The ratio of the variance of the residuals $(\hat{\sigma}_w^2)$ to the variance of the signal $(\hat{\sigma}_s^2)$ is 32.8%. Thus the model explains 67.2% of the variance of the residuals $W(\cdot)$.

The model S_W for the mean monthly stages in the Wabash River (Table 3.4) shows that the stage at any given month is influenced by the stage in the preceding two months and also by the seasonal trend functions with 12 and 6 months periodicities. On the other hand, the mean monthly stage in the (k+1)-th month of the Wildcat Creek (model S_{WC}, Table 3.4) is only dependent on the stage in the previous month and the sinusoidal trend functions with annual periodicity.

The ratio $\hat{\sigma}_w^2/\hat{\sigma}_s^2$ for the model S_W of the Wabash River is 16.7% indicating that the model explains 83.3% of the residual variance. The variance of the residuals explained by the model S_{WC} for the mean monthly stages in the Wildcat Creek is 80.1%.

3.4.3 *Validation Tests for Residuals*

We can obtain the residuals $\bar{W}(k)$ from the models R_A, S_W and S_{WC} by using the available observations and the respective stochastic difference equations shown in Table 3.4 For example, the residuals of model S_{WC} can be obtained from Table 3.4 as shown in Eq. 3.3. The tests

$$\bar{W}(k) = y(k+1) - 2.59 - 0.34\, y(k) - 0.414 \sin \omega_1 k - 0.522 \cos \omega_1 k \qquad (3.3)$$

pertaining to the validation of the residuals $\bar{W}(\cdot)$ are discussed below.

(i) Correlogram Test

We have assumed previously that the sequence $W(\cdot)$ are made up of independent random variables. The above assumption will be valid if the residuals $\bar{W}(\cdot)$ are independent. This aspect will be tested by computing the correlation coefficients $d_j(w)$ of the residuals at different lags $j=1,2,\ldots,M$.

$$d_j(w) = r_j(w)/r_0(w)$$

$$\qquad (3.4)$$

$$r_j(w) = \frac{1}{N-j} \sum_{k=j+1}^{N} \bar{W}(k)\, \bar{W}(k-j)$$

If $[\bar{W}(\cdot)]$ is white with zero mean the correlation coefficients $d_j(w)$ should be small in comparison with unity and must lie within the range of $\pm 2/\sqrt{N}$ with 95% probability (*Box and Jenkins, 1970*). The values of confidence limits for the correlation coefficients of the different processes are listed in Table 3.5. The plots of the correlograms for the residuals of the models R_A, S_W and S_{WC} are shown in Fig. 3.20 along with the confidence limits which are shown as 2-standard error limits. The residual correlation coefficients are within the confidence limits. Consequently, we can conclude that the residuals are uncorrelated.

TABLE 3.5

CONFIDNECE LIMITS AND CRITICAL VALUES FOR VALIDATION TESTS ON RESIDUALS

| STATION | SAMPLE SIZE N | CONFIDENCE LIMITS | | | | |
| | | CORRELOGRAM TEST | | CUM.PERIODOGRAM TEST | | |
		α	$2/\sqrt{N}$	α	q	$k_\alpha/\sqrt{q}$
Rainfall Ag. Farm	228	0.05	0.132	0.25	113	0.097
Stage Wabash R.	480	0.05	0.091	0.25	239	0.067
Stage Wildcat Cr.	228	0.05	0.132	0.25	113	0.097

P O R T M A N T E A U   T E S T   (C R I T I C A L   V A L U E S)

| Lag K | α | RAINFALL (AG.FARM) (p=2, q=0) | | STAGE(WABASH R.) (p=2, q=0) | | STAGE(WILDCAT CR.) (p=1, q=0) | |
		ν	Critical Statistic	ν	Critical Statistic	ν	Critical Statistic
5	0.05	3	7.815	3	7.815	4	9.488
10	0.05	8	15.507	8	15.507	9	16.919
15	0.05	13	23.362	13	23.362	14	23.685
20	0.05	18	28.869	18	28.869	19	30.144
25	0.05	23	35.172	23	35.172	24	36.415
30	0.05	28	41.337	28	41.337	29	42.557

F - T E S T   A N D   C H I - S Q U A R E   T E S T   (C R I T I C A L   V A L U E S)

LAG K	α	F-TEST CRITICAL STATISTIC	CHI-SQ. TEST CRITICAL STATISTIC
5	0.05	2.21	11.070
10	0.05	1.83	18.307
15	0.05	1.67	24.996
20	0.05	1.59	31.410
25	0.05	1.51	37.652
30	0.05	1.46	43.773

α = significance level

q = (N-2)/2 if N is even
  = (N-1)/2 if N is odd

K_α = 1.02 for α = 0.25

P = no. of autoregressive terms

q = no. of moving average terms

ν = no. of degrees of freedom

(ii) Cumulative Periodogram Test

The cumulative periodogram test is performed to detect the presence of any deterministic sinusoidal components in the residuals (Bartlett, 1955). The periodogram $I(f_k)$ of the residuals [$\hat{W}(\cdot)$] is defined in Eq. 3.5.
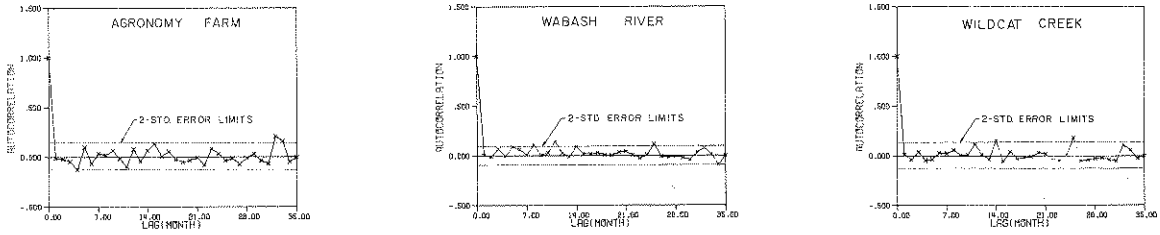
FIGURE 3.20   CORRELOGRAMS OF RESIDUALS
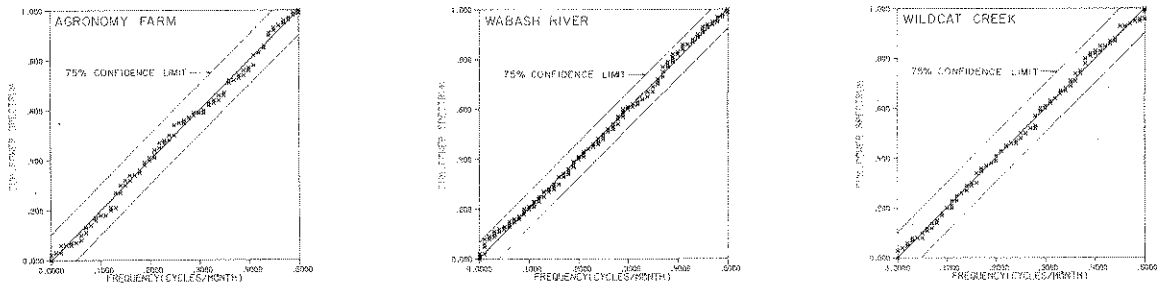
FIGURE 3.21   CUMULATIVE PERIODOGRAMS OF RESIDUALS
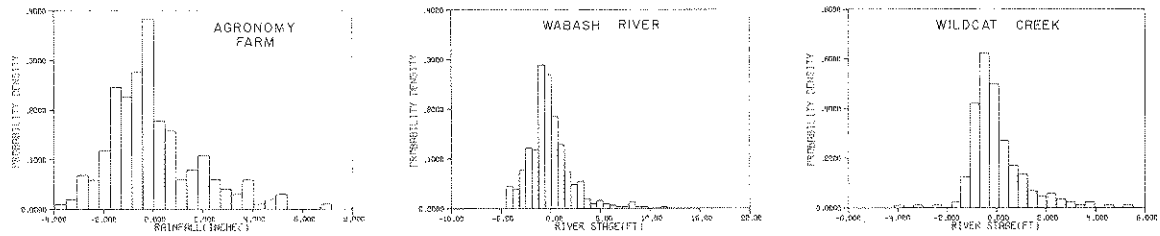
FIGURE 3.22   HISTOGRAMS OF RESIDUALS

$$I(f_k) = \frac{2}{N}\left[\left(\sum_{j=1}^{N} \bar{W}(j) \cos 2\pi f_k j\right)^2 + \right.$$

$$\left. \left(\sum_{j=1}^{N} \bar{W}(j) \sin 2\pi f_k j\right)^2\right] \qquad (3.5)$$

where $f_k = k/N$, $k=1,2, \ldots N-1$. The normalized cumulative periodogram C_k is given in Eq. 3.6.

$$C_k = \sum_{j=1}^{k}\left[I(f_j)/N \times VAR(\bar{W}(k))\right] \ , \ k=1,2, \ldots, N/2 \qquad (3.6)$$

where N is an even integer. The plot of C_k against f_k is known as the cumulative periodogram of the data. If the residuals are free from deterministic sinusoidal components, then their normalized cumulative periodogram should be tightly scattered around the straight line from (0,0) to (0.5, 1) and should lie within the 25% confidence limits. The values of the confidence limits are shown in Table 3.5. The cumulative periodograms of residuals from models R_A, S_W and S_{WC} are plotted in Fig. 3.21. In all the cases the periodograms lie within the 25% confidence limits and are tightly scattered around the straight line passing through (0,0) and (0.5, 1). Consequently, it was concluded that the residuals are free from any deterministic sinusoidal trend terms at the 75% probability level.

(iii) Portmanteau Test

This is a "goodness of fit" test to detect the whiteness of a sequence of residuals (*Box and Pierce, 1970*). The test statistic is given in Eq. 3.7

$$Q = N \sum_{j=1}^{K} d_j^2(w) \qquad (3.7)$$

where N is the number of data points and $d_j(w)$ are the serial correlation coefficients given in Eq. 3.4. The statistic Q is approximately distributed as χ^2 with ν degrees of freedom. The value of ν is given by $\nu = K - p - q$, where K is the number of lags considered and p and q are respectively the number of autoregressive and moving average terms used in the model. The critical values of χ^2-statistic for different values of ν may be obtained from statistical tables. They are also listed in Table 3.5 under the title "Portmanteau test (critical values)". The decision rule used in the Portmanteau test is explained next. We accept the hypothesis that the residuals $[\bar{W}(\cdot)]$ are white if the test statistic Q at any given lag is less than the corresponding critical statistic. We reject the hypothesis if it is otherwise. The results of the Portmanteau test for the residuals from all the three models are presented in Table 3.6. The test statistics for the residuals from the models R_A and S_{WC} are less than the respective critical values. Consequently, we can conclude that the residuals of these models are white.

TABLE 3.6

RESULTS OF PORTMANTEAU TEST, F-TEST AND

CHI-SQUARE TEST ON RESIDUALS

STATION	LAG	PORTMANTEAU TEST		F-TEST		CHI-SQUARE TEST	
		STATISTIC	DECISION	STATISTIC	DECISION	STATISTIC	DECISION
RAINFALL AG. FARM (MODEL R_A)	5	4.060	A	0.830	A	4.165	A
	10	8.447	A	0.903	A	9.072	A
	15	13.262	A	0.821	A	12.472	A
	20	18.597	A	0.849	A	17.221	A
	25	21.958	A	0.817	A	20.853	A
	30	23.615	A	0.693	A	21.695	A
STAGE WABASH R. (MODEL S_W)	5	2.312	A	0.463	A	2.327	A
	10	13.625	A	1.259	A	12.522	A
	15	28.047	R	1.526	A	22.509	A
	20	28.864	A	1.170	A	23.237	A
	25	30.575	A	1.001	A	25.012	A
	30	37.629	A	1.011	A	30.305	A
STAGE WILDCAT CR. (MODEL S_{WC})	5	1.242	A	0.262	A	1.333	A
	10	2.567	A	0.250	A	2.590	A
	15	11.064	A	0.680	A	10.417	A
	20	12.478	A	0.628	A	13.001	A
	25	13.664	A	0.562	A	14.783	A
	30	22.480	A	0.741	A	23.018	A

A = Accept the hypothesis that the residuals are uncorrelated at α = 0.05.

R = Reject the hypothesis that the residuals are uncorrelated at α = 0.05.

The test statistic at lag 15 for the residuals from model S_W is 28.047 which is higher than the critical value 23.362. In all the other lags, the test statistic is lower than the critical value which indicates that the residuals may be considered to be white at the other lags.

(iv) F-Test and χ^2-Test

The details of the F-test and the χ^2 test are documented in *Kashyap and Rao (1976)*. The critical values of F-test and χ^2-test at different lags are given in Table 3.5. The computed values of the F-test statistic and those of the χ^2-test statistic at different lags are shown in Table 3.6. The residuals were considered to be uncorrelated when the test statistic at any lag is less than the corresponding critical value.

The results of the F-test and the χ^2-test for the residuals from the three models are presented in Table 3.6. The test statistics at different lags are less than the respective critical values which indicate that the residuals from the three models are uncorrelated.

(v) Cross Correlation Test

One of the assumptions made in the estimation of the parameters of the models is that the

random input [W(·)] is indpendent of the signal [y(·)]. The validity of the above assumption was checked by determining the empirical cross correlations between the residuals and the input values (*Jenkins and Watts, 1968*). If the residuals are independent of the input values the cross correlation coefficients should be small in comparison to unity.

The cross correlation coefficients between the residuals and the observed values of all the three models are shown in Table 3.7. The values are very small in comparison to unity which confirms the assumption that the residuals are uncorrelated with the observed values.

TABLE 3.7

CROSS CORRELATION COEFFICIENTS BETWEEN OBSERVED DATA AND RESIDUALS

| STATION | CROSS CORRELATION COEFF. | | | | DECISION |
	LAG 1	LAG 2	LAG 3	LAG 4	
RAINFALL AG. FARM	-0.037	-0.083	0.042	-0.055	A
STAGE WABASH R.	0.003	0.056	-0.025	-0.038	A
STAGE WILDCAT CR.	0.066	0.082	0.034	0.069	A

A = Accept that residuals are uncorrelated with observed values.

3.4.4 *Simulation Results*

The final models and the criteria used for their selection were explained in Sec. 3.4.2. All the models selected have satisfied the validation tests presented in Sec. 3.4.3. In order to simulate monthly values by models such as R_A, S_W and S_{WC} (Table 3.4) on a digital computer, the probability distribution of the disturbance inputs W(·) must be known. The statistics of the residuals from the models R_A, S_W and S_{WC} are given in Table 3.8. The means of the residuals are very close to zero. The histograms of the residuals for the models R_A, S_W and S_{WC} are shown in Fig. 3.22. The residuals from the above models appear to fit a normal distribution satisfactorily. Consequently, random values were generated from a normal distribution using the mean and standard deviation of the residuals from the appropriate models. The random values were then used as disturbance inputs W(·) in the models R_A, S_W and S_{WC} (Table 3.4) in order to simulate the monthly values.

The above procedure was used in the model R_A for the simulation of 42 years of monthly precipitation values at the Agronomy Farm. Similarly the models S_W and S_{WC} were respectively used to simulate 83 years of mean monthly stages in the Wabash River and 42 years of mean monthly stages in the Wildcat Creek. The plots of the simulated values of rainfall and river stages for a period of 25 years are shown in Fig. 3.23. The results of the simulated data and their statistical
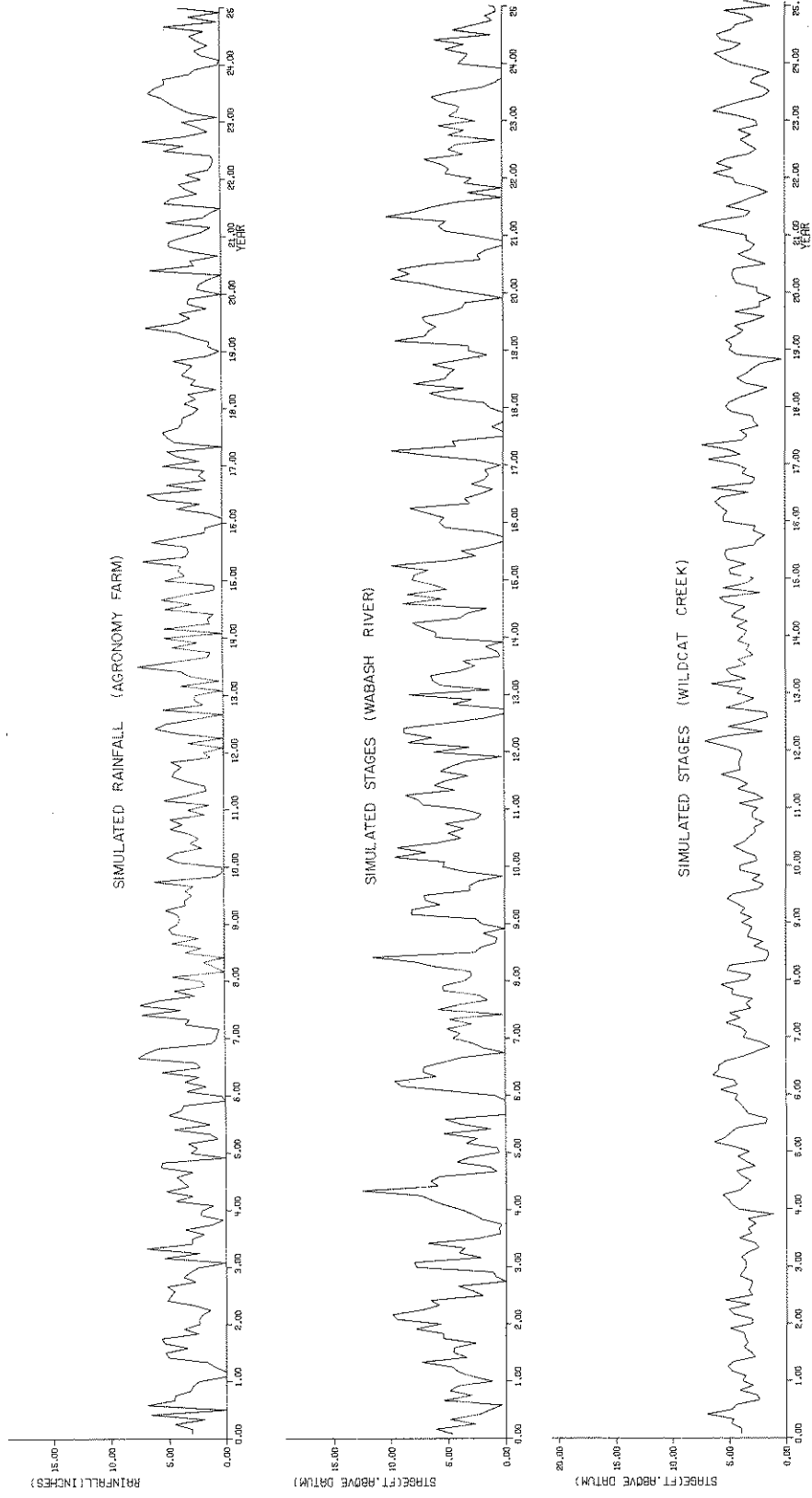
FIGURE 3.23 SIMULATED DATA

TABLE 3.8

STATISTICS OF RESIDUALS FROM THE BEST FITTED STOCHASTIC MODELS

STATISTIC	RAINFALL (IN.) AG. FARM	RIVER STAGE (FT.)	
		WABASH R.	WILDCAT CR.
MEAN	-0.01	-0.08	0.02
STD. DEV.	1.81	2.22	1.14
SKEWNESS COEFF.	0.95	1.41	1.29
KURTOSIS	4.09	7.00	7.38
MIN.	-3.97	-4.44	-4.15
MAX.	7.16	11.79	5.51

characteristics in comparison to those of the observed data are discussed below.

The elementary statistics of the simulated data are presented in Table 3.9. The statistics of the observed data are also presented in Table 3.9 for comparison. The mean and standard deviation of the simulated data for each set are close to their counterparts from the observed data. However, coefficients of skewness and kurtosis of the observed data are not preserved in the simulated values as these characteristics were not incorporated into the stochastic models.

TABLE 3.9

STATISTICS OF SIMULATED AND OBSERVED DATA

STATISITC	RAINFALL (AG.FARM) (in.)		STAGE (WABASH R.) (ft. above datum)		STAGE(WILDCAT CR.) (ft. above datum)	
	SIMULATED	OBSERVED	SIMULATED	OBSERVED	SIMULATED	OBSERVED
Mean	2.912	3.020	3.946	4.295	3.881	3.949
Std. dev.	1.944	2.034	2.812	3.028	1.283	1.371
Skewness Coeff.	-0.068	1.094	0.028	1.213	0.076	1.218
Kurtosis	2.709	4.281	2.730	4.028	2.758	5.583
Min.	0.0	0.080	0.0	0.400	0.284	2.260
Max.	8.182	11.700	12.52	17.600	7.610	9.520

Next the autocorrelations, power spectral densities, monthly means and the monthly standard deviations of the simulated data were examined for each process. The autocorrelations and the normalized power spectral densities of the observed and of the simulated data for all the three processes are shown separately in Fig. 3.24. The autocorrelations and the normalized power spectral densities of the simulated and the observed data are very close to each other. Thus the periodicities inherent in the observed data are also seen in the simulated data.
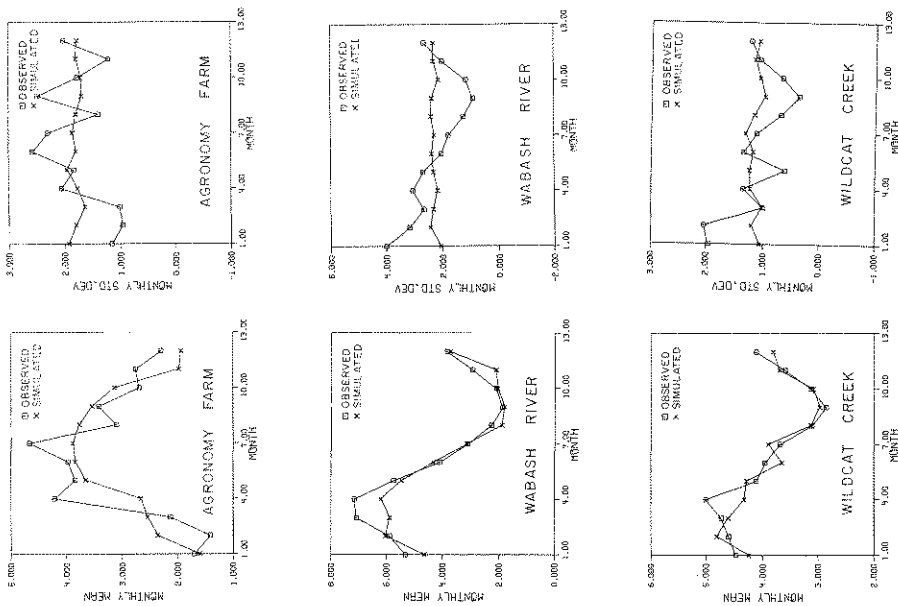
FIGURE 3.25 COMPARISON OF MONTHLY
MEANS AND STANDARD DEVIATIONS
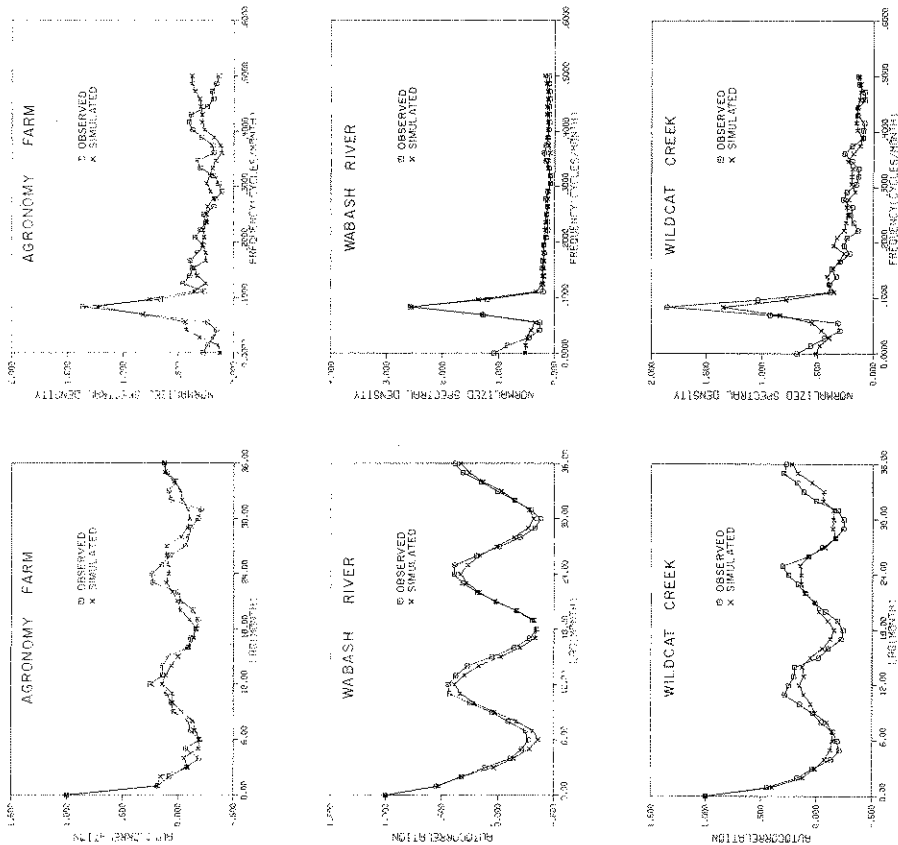
FIGURE 3.24 COMPARISON OF RESULTS
FROM SPECTRAL ANALYSIS

A comparison of the means and the standard deviations in individual months of the simulated and the observed data are presented in Fig. 3.25. The monthly means of the simulated data from all the three processes exhibit the seasonal pattern as their historical counterparts. However, the standard deviations of the simulated precipitation and river stage data in individual months do not exhibit any pronounced seasonality.

In conclusion, most of the statistical characteristics of the observed values of the precipitation and the river stage processes were retained in the respective simulated values.

IV. THE DETERMINISTIC GROUNDWATER MODEL

4.1 General Procedure

Groundwater models may be formulated by using either a lumped or a distributed parameter approach (*Domenico, 1972*). In a lumped-parameter, or *black box*, approach the output corresponding to a given input can be measured or estimated although the internal mechanism relating the input and output is not known. The analysis is made by considering the physical system, such as the groundwater basin, as a single point in space. Thus, the distinctive feature of a lumped-parameter approach is that a space coordinate system is not required in problem formulation and solution. However, the spatial characteristics of the partinent parameters over the area under investigation should be approximately uniformly distributed so as to arrive at satisfactory results. As a practical example, the average drawdowns from a closely spaced group of wells over a certain time interval may be related to pumping rates without regard to the aquifer properties, location of wells or to their spacing in the field (*Moench, 1971*). Several other groundwater problems have also been investigated (*Pinder, et al., 1969 ; Moench and Kisiel, 1970 ; Maddock III, 1972, 1974 ; and Morel-Seytoux and Daly, 1975*) by using the above approach.

In the distributed-parameter approach, the area under investigation is described by data at several points, each of which is examined in relationship to the others. Therefore, the initial data must include values of the partinent parameters at all the points of interest. In addition, the location of the boundaries are needed. Most of the problems on regional aquifer evaluation (*Prickett and Lonnquist, 1968 ; Pinder and Bredehoeft, 1968 ; Pinder and Frind, 1972 ; and Meyer, et al., 1975*) have been analyzed by the distributed-parameter approach. The above approach is recommended when the spatial variation of the partinent parameters such as hydraulic conductivity, aquifer thickness, storage coefficient, infiltration characteristics and pumping rates are significant. However, the validity of the results from the above method depends on the length and accuracy of the data, and the availability of computer time and manpower.

4.2 Procedure Used in the Present Study

In the present study, the glacial aquifer underlying the study area is highly heterogeneous (Sec. 3.3). The aquifer properties such as aquifer thickness, hydraulic conductivity, storage coefficient, soil conditions and the pumping rates vary significantly over the area. This suggests that the model be formulated using the distributed-parameter approach. But the available data regarding the spatial distribution of infiltration characteristics of the soil and of the Wabash River bed are not sufficient to incorporate the recharge due to rainfall and the induced infiltration due to the river as an integral part of the distributed-parameter model. Consequently, a mixed parameter approach was used in the present investigation using two-dimensional method of analysis.

The digital model was formulated as a distributed-parameter system using finite difference approximations as explained in Chapter II. The values of aquifer thickness, hydraulic conductivity and storage coefficient were specified at each node of the finite difference grid, as will be discussed later. Flow rates crossing the boundaries of the study area were introduced into the model as distributed-parameters at the boundary nodes.

Recharge due to rainfall and the gravel pit, and the net base flow contribution into the Wabash River were considered as lumped quantities at the appropriate nodes in the digital model. Recharge due to rainfall was assumed to be uniformly distributed within the different soil zones of the study area as shown in Fig. 3.14. In each zone, recharge was considered as a fraction of the total rainfall. This fraction was determined on the basis of the surface and near surface conditions of the study area as shown in Fig. 3.14. In addition a time lag of 8 months (Sec. 3.3.5) was used as a delay between rainfall and subsequent groundwater recharge. Recharge due to the gravel pit (Sec. 3.3.6) was introduced as a lumped input at the appropriate nodes. Net base flow into the Wabash River (Sec. 3.3.6) was represented as a constant withdrawal at each river node.

As discussed in Sec. 3.2, the static water level information is not sufficient to formulate a time-series model. Consequently, the different input variables such as static water levels, rainfall, stream stages and pumping rates were averaged over a period of time for use in the model. These details are discussed in Sec. 4.3.3.

4.2.1 *Convergence Criteria*

The convergence of the solution of the finite difference equations at the end of each iteration is tested in several ways and the conditions used in the present study are given below.

(1) The sum of the changes in heads between the previous iteration and the present iteration at all the nodes in the model should be less than 2 ft (0.61 m).

(2) The largest absolute value of the change in any single head between the current iteration and the previous iteration should be less than 1.0 in (2.5 cm).

The above values of error were chosen after considering the 'rule of thumb' given by *Prickett and Lonnquist (1971)* and the response of the computer program to the problem under study.

The computations were considered to have converged for a given time step if atleast one of the above conditions was satisfied at the end of any iteration. After the solution had converged for a given time step, the computed heads were used as initial values for the next time step and the computations were continued until the end of the pumping period. This completed a *simulation run*.

4.3 The Digital Model

The digital model for the study area was formulated as explained in Chapter II. The aquifer simulation program developed by *Prickett and Lonnquist (1971)* using the alternating direction implicit method

for the solution of finite difference equations was used in the analysis. The computer program was modified in several aspects so as to incorporate the mixed-parameter approach discussed in Sec. 4.2. Details of the specific aspects of the model are presented next.

4.3.1 *Initial and Boundary Conditions*

As discussed in Sec. 3.3.4, the piezometric surface in the study area does not fluctuate significantly with time. Consequently, the initial water levels for the digital model were represented by the average piezometric surface map for January (Fig. 3.12). Also the computed water levels that resulted from different trials during calibration of the ditigal model were verified by using these average water levels.

The boundaries of the digital model were fixed using the following criteria. The geology and the topography were examined to determine the location of geohydrologic boundaries in the study area. The Wabash River, which is hydraulically connected to the aquifer (Sec. 3.3.5), may be treated as a source of recharge although it does not penetrate the full thickness of this aquifer. Thus, the river was treated as a constant head source in the model. The outer boundaries of the model were fixed arbitrarily so that most of the municipal and industrial well fields located in Lafayette and West Lafayette are included in the model. The boundaries of the digital model and the location of well fields are shown in Fig. 4.1. The flow rates crossing these boundaries were estimated from the flow net shown in Appendix C and were introduced into the model as functions of the piezometric head at the boundary nodes. These estimates were then subsequently modified during the process of calibration according to the convergence criteria explained in Sec. 4.2.1. These final values for the flow rates crossing the boundaries are presented in Sec. 4.3.3.

4.3.2 *The Finite Difference Network*

The shape, size and the number of finite difference grids were fixed after considering computational time, computer storage requirements and accuracy of the available data. As a trial, a square node system with 500 ft. (15.25 m) spacing containing 47 columns, 65 rows and 3055 nodes was superimposed on the study area. The digital computer model was formulated with the above node system and several trial computer runs were made after introducing the pertinent input variables and boundary conditions. Although, the model performed satisfactorily, the computational time and the storage requirements were large. In addition, after evaluating the limitations imposed by the basic data (Sec. 3.2.4) used in the model, it was concluded that a coarser grid spacing could be satisfactorily used. Finally, a square node system with 1000 ft. (30.5 m) spacing was found to be most advantageous from the standpoints of programming ease, computational time and storage requirements. The resulting finite difference network, consisting of 24 columns and 33 rows containing 792 nodes, is shown in Fig. 4.1. The nodes corresponding to the various well fields, ponds and rivers in the study area are also indicated in this figure.
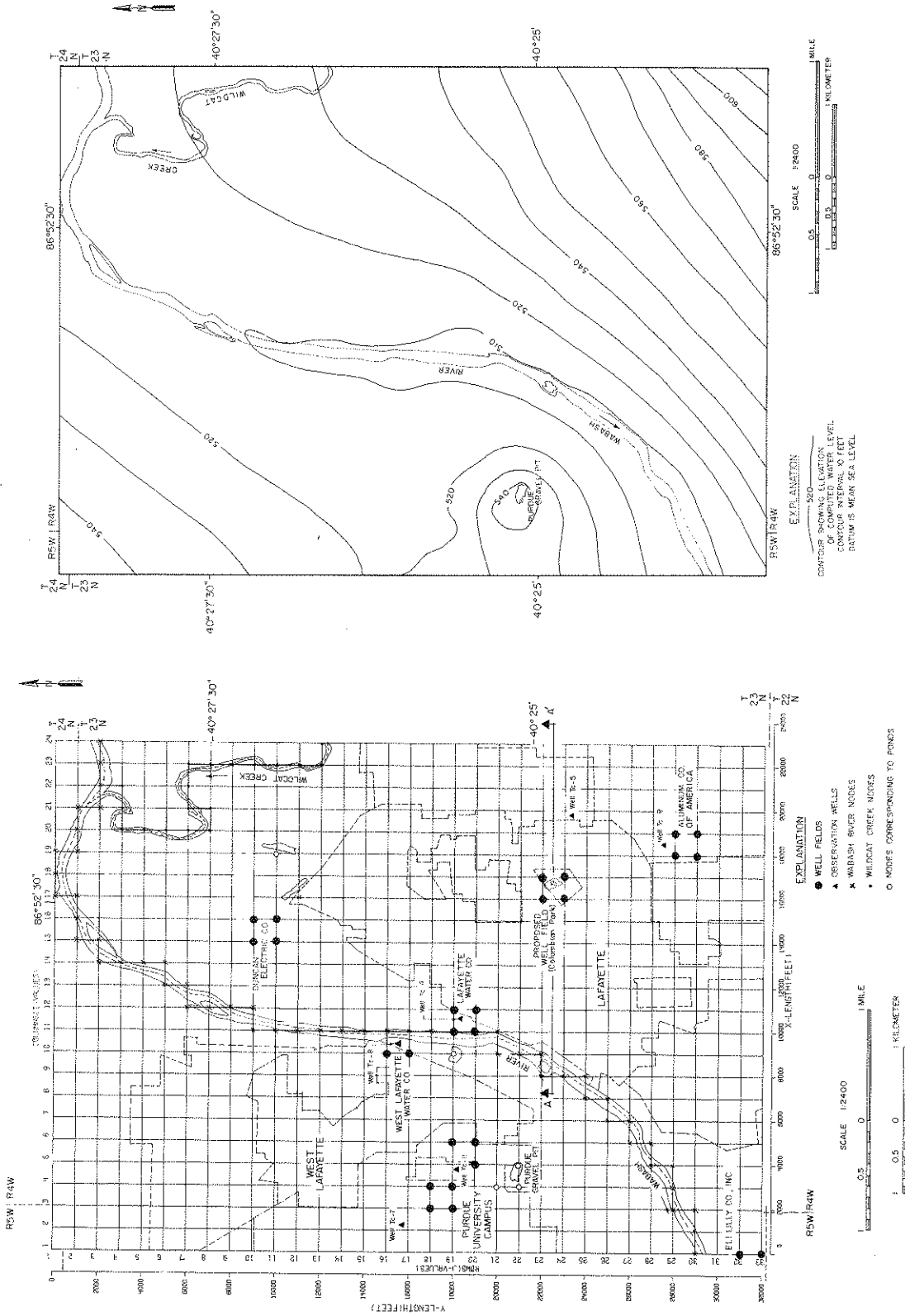
FIGURE 4.2 COMPUTED HEAD DISTRIBUTION FROM
THE CALIBRATED DIGITAL MODEL

FIGURE 4.1 FINITE DIFFERENCE NETWORK FOR
THE STUDY AREA

4.3.3 *Calibration of the Digital Model*

In the discussion of Sec. 3.3.4, it was concluded that steady or near steady conditions prevail in the aquifer system. This condition, in the form of a water budget analysis, was investigated further during the calibration of the model. In particular, if the aquifer system is in dynamic equilibrium, the total inflow into the model on an average, should approximately balance the total outflow from the model. This, along with the correct replication of the average piezometric surface (Fig. 3.12) were used as the calibration criteria.

(a) Input Variables

The average piezometric surface elevations of January (Fig. 3.12) were discretized and entered as initial water levels in the digital model. The values of hydraulic conductivity and the storage coefficients given respectively in Figs. 3.7 and 3.8 were introduced at each nodal point. The bedrock elevations and the values of aquifer thickness used in the model were obtained from Figs. 3.4 and 3.6.

The historical values of rainfall measured at the Purdue Agronomy Farm and the stages in the Wabash River and the Wildcat Creek (Fig. 3.2) averaged over a period of 15 years (1960-74) were used as inputs at the respective nodes. The average pumping rates from different well fields in the study area during the period 1960-74 were applied at the appropriate nodes. The above input values used in the model during the process of calibration are shown in Table 4.1.

TABLE 4.1

AVERAGE ANNUAL DATA USED IN THE DIGITAL MODELS

TEST NO.	INVESTIGATION		TYPE OF INPUTS	PERIOD FOR PUMPING DATA	RAINFALL AG. FARM (in)	RIVER STAGE (ft. above bed level)		PUMPAGE (m gals)			
	USE	PERIOD (Years)				Wabash	Wildcat	PURDUE	W. LAF	LAFAYETTE	
										CANAL ST.	COL. PARK
1	CALIBRATION	5	HISTORICAL	1960-'74	36	4.29	3.94	1999.2	712.4	2190	0
2	PREDICTION EXPERIMENT-A	5	HISTORICAL	1970-'74	34.2*	3.75*	3.59*	2196.6	872.9	2699.4	2125.6
3	PREDICTION EXPERIMENT-B	5	STOCHASTIC	1970-'74	32.6**	3.83**	3.70**	2196.6	872.9	2699.4	2125.6

*   Average values of 1953-'56

** Average values of simulated sequence 18-22.

(b) Calibration

In the present study, a parameter adjustment procedure was used to calibrate the digital model. The input variables, hydraulic conductivity, net recharge due to rainfall and the gravel pit, net base flow into the Wabash River and the flow rates crossing the boundaries of the study area were suitably adjusted after each simulation run until the computed heads at the end of the period of calibration compared

satisfactorily with the observed heads. In addition, the computed heads at the nodes representing the Wabash River and the gravel pit were also verified with the average observed stage in this river and the pit.

During the different trials for calibrating the digital model, the stage above the Wabash River bed throughout its length in the study area was maintained constant at the average value shown in Table 4.1. This was accomplished by proper manipulation of the values of base flow contribution at each node during each simulation run. The preliminary estimates of base flow contribution in different parts of the Wabash River were obtained from the flow net analysis as shown in Appendix C. However, the internal distribution at each node was a trial procedure as explained before. Lesser importance was given to maintaining constant stage above the bed level of the Wildcat Creek as the hydraulic connection between the creek and the aquifer was not well established (Sec. 3.3.5).

The stage in the gravel pit was maintained constant at the average elevation of about 545 ft (166 m) above mean sea level as discussed in Sec. 3.2.2. The value of recharge, 14.2 mgd (53960 m^3/day), estimated from the flow net (Appendix C) was used as the initial value during calibration.

As explained in Sec. 4.2, recharge due to rainfall was considered as a fraction of the average observed rainfall value shown in Table 4.1. During the initial trials with the digital model, 40, 30, 20 and 5 percent of the average observed rainfall value (Table 4.1) was used as infiltration into zones I through IV respectively. These percentage values and the estimates of flow crossing the boundaries (Sec. 4.3.1) were subsequently modified during the process of calibration so as to arrive at the correct piezometric surface replication.

A pumping period of 5 years was simulated in the digital model using 30 nonuniform time steps. The importance of nonuniform time increments in aquifer simulation studies is discussed in *Prickett and Lonnquist (1971)*. The model was calibrated using the parameter adjustment procedure explained before.

(c) Results

Several simulation runs were needed to calibrate the digital model while adjusting the input variables suitably. The computed head distribution that compared most satisfactorily with the average piezometric surface (Fig. 3.12) is shown in Fig. 4.2. The maximum absolute difference between the computed and the observed heads at any single node is less than 10 ft. (3 m). However, comparison of contours indicates good agreement. The final values of transmissivity resulting from the calibrated model are shown in Fig. 4.3. At the end of calibration, the adjusted recharge values due to rainfall constituted 50, 35, 25 and 15 percent of the observed rainfall values respectively in zones I through IV. The average recharge rates in these zones (Fig. 3.14) are respectively 0.89, 0.6, 0.4 and 0.26 mgd/sq. mile (1306, 880, 590 and 382 m^3/sq. km). Final values of flows crossing the boundaries of the study area and the distribution of net base flow contribution into the different regions of the Wabash River are pre-

FIGURE 4.4 FLOW CROSSING THE BOUNDARIES AND
BASE FLOW INTO THE WABASH RIVER

FIGURE 4.3 TRANSMISSIVITY OF THE AQUIFER

sented in Fig. 4.4. Most of the flow entering the study area is from the southern boundary. The average rate of flow from this boundary is about 1.5 gpd/sq. ft (0.06 m/day). The northern boundary of the study area towards the west of the Wabash River and the lower part of the eastern boundary also contribute considerable amount of inflow into the region. There is very little subsurface flow leaving the study region as the general hydraulic gradient of the piezometric surface is towards the Wabash River. The total base flow into the Wabash River throughout its length in the study area is 54.2 mgd (205,960 m^3/day). This is in close agreement with the value, 55.8 mgd (212,000 m^3/day) estimated from the flow net. The average rate of base flow contribution into the Wabash River is about 6.5 mgd/mile (15,342 m^3/km). However, it can be observed from Fig. 4.4 that the base flow into the river in reach GB, downstream of the gage in Lafayette is much higher than that in the reach GA, upstream of the gage. The average rate of base flow into the river in the reach GB is about 12.5 mgd/mile (29,503 m^3/km) whereas, it is about 3.6 mgd/mile (8497 m^3/km) in the reach GA. Obviously, considerable recharge from the gravel pit in the Purdue University campus reaches the Wabash River as base flow. The steep hydraulic gradients of the piezometric surface on the eastern side of the Wabash River near the southern boundary also contribute to larger volumes of base flow. At the end of calibration, the computed recharge from the gravel pit was 15.9 mgd (60,420 m^3/day) which is once again close to the value estimated from the flow net, 14.2 mgd (53,960 m^3/day).

During the process of calibration, a continuous check was maintained on the water budget of the groundwater system. These water budget results are presented in Table 4.2. The results given in this table indicates the magnitude of the various flow components when steady conditions prevail in the study area. The deviation from steady state in this water balance is about 5.5% and may be attributed to the errors in the estimation of input parameters and approximations in computation. The above discrepancy in water balance may be considered reasonable as seasonal variations in net recharge and the cycles of wet and dry years continuously alter the water balance in the field. Consequently, it can be concluded that the model is capable of duplicating the average piezometric heads and the steady state conditions in the aquifer system.

4.4 Estimation of Aquifer Capacity Using Stochastic Inputs

One of the primary objectives of the present study is to demonstrate the use of stochastic inputs in groundwater models for the long range determination of aquifer capacity. This was demonstrated by using two experiments designated experiment A and experiment B. The historical values of rainfall and river stages were used as inputs in experiment A. Experiment B was executed using stochastic inputs. In the above experiments, a hypothetical well field was simulated in the vicinity of the Columbian Park in Lafayette (Fig. 4.1) in order to examine its effect on the aquifer system. The aquifer underlying Columbian Park and vicinity is mostly confined with a transmissivity of about 23000 ft^2/day (2100 m^2/day)

TABLE 4.2

AVERAGE GROUNDWATER BUDGET FROM CALIBRATED MODEL

| S. No | Item | From Digital Model | | From Flow Net (mgd) |
		Recharge (mgd)	Discharge (mgd)	
1	Rainfall	17.4		
2	Purdue Gravel Pit	15.9		14.2
3	Other ponds	2.2		
4	Wabash River (Base flow)		54.2	55.8
5	Wildcat Creek (Base flow)		0.8	
6	Flow across boundaries	31.5	0.1	
7	Municipal and Industrial Pumpage		15.6	
	Total	67.0	70.7	
	Balance		3.7	
	Error		5.5%	

(Fig. 4.3). The water budget given in Table 4.2 indicates that the major source of recharge to the aquifer is rainfall. Consequently, the groundwater situation might become critical if the magnitude of rainfall were to drop considerably over a period of several years. The situation would be worse if there were to be considerable increase in pumping during this drought period. Therefore, in experiment A, the aquifer response was tested using a relatively low rainfall sequence which had been observed at the Agronomy Farm during the years 1953-56 (Fig. 3.2). Corresponding Wabash River and the Wildcat Creek stages were also used. Experiment B was carried out by using once again a relatively low sequence of rainfall and corresponding stream stages obtained from the simulated data presented in Fig. 3.23. In both the above experiments, pumpage rates at different nodes were represented by those observed during the years 1970-74 (Fig. 3.3). Obviously, these values are higher than most of the previous pumping records. The pumping rates of the hypothetical well field were simulated using the second stage pumping record of the Lafayette Water Works (Fig. 3.3) for the period 1970-'74. The average annual rainfall values used in the experiments A and B are respectively 34.2 in. (86.9 cm) and 36.2 in. (82.8 cm). These values are about 5 percent and 10 percent less than the long term average annual rainfall, 36 in. (91.4 cm) observed over the study area. The average annual data used in the above experiments are presented in Table 4.1.

4.4.1 *Aquifer Response*

The aquifer response was tested using the calibrated digital model (Sec. 4.3.3) and the average annual values of rainfall, stream stages and the pumpage data for both the experiments as shown in Table 4.1. Once again a pumping period of 5 years was simulated in each experiment with 30 nonuniform time increments. The base flow contribution into the Wabash River was appropriately adjusted until the

computed stage at the river nodes compared closely with the average stage shown in Table 4.1 for the different experiments. The final values of fractions of rainfall contributing to recharge (Sec. 4.3.3) and of flow rates crossing the boundaries (Fig. 4.4) that resulted after calibration were not disturbed during these experiments. A comparative analysis of the results obtained from the above experiments is presented below.

The computed head distribution that resulted from experiments A and B are respectively shown in Figs. 4.5 and 4.6. The effect of pumping at the Columbian Park and the increased pumping at the other well fields is obvious when the 530 ft (161.65m) contour line is compared with the same contour in the average piezometric surface elevations (Fig. 3.12). The head distribution maps from both the experiments (Figs. 4.5 and 4.6) with the exception of the 530 ft. (161.65) contour line, are in close agreement with the average piezometric surface map (Fig. 3.12). A comparison of the drawdown curves resulting from experiments A and B along the section AA' passing through the proposed well field (Fig. 4.1) is shown in Fig. 4.7. The drawdown curves are close to each other. The computed average drawdown at the well field is about 27 ft (7.2 m) in both the experiments, and it is about 6 ft (1.8 m) at a distance of about 1 mile (1.6 km) towards the Wabash River along the section AA'. The drawdowns away from the well field towards the eastern boundary are considerably large.

The water budgets resulting from the experiments are presented in Table 4.3. The differences in the recharge due to rainfall in comparison to that from the calibrated model (Table 4.2) are obviously due to the different magnitudes of rainfall used in the experiments.

TABLE 4.3

AVERAGE GROUNDWATER BUDGET FROM EXPERIMENTS A AND B

S. No	Item	EXPERIMENT - A		EXPERIMENT - B	
		Recharge (mgd)	Discharge (mgd)	Recharge (mgd)	Discharge (mgd)
1	Rainfall	16.2		14.3	
2	Purdue Gravel Pit	16.4		15.9	
3	Other ponds	2.2		2.2	
4	Wabash River (Base flow)		45.9		43.9
5	Wildcat Creek (Base flow)		0.8		0.8
6	Flow across boundaries	31.1	0.04	30.9	0.01
7	Municipal and Industrial Pumpage (a) Existing (1970-74) (b) Proposed at Columbian Park		18.4 5.8		18.4 5.8
	Total	65.9	70.94	63.3	68.9
	Balance		5.04		5.61

FIGURE 4.6   COMPUTED HEAD DISTRIBUTION USING
STOCHASTIC INPUTS (EXPERIMENT B)
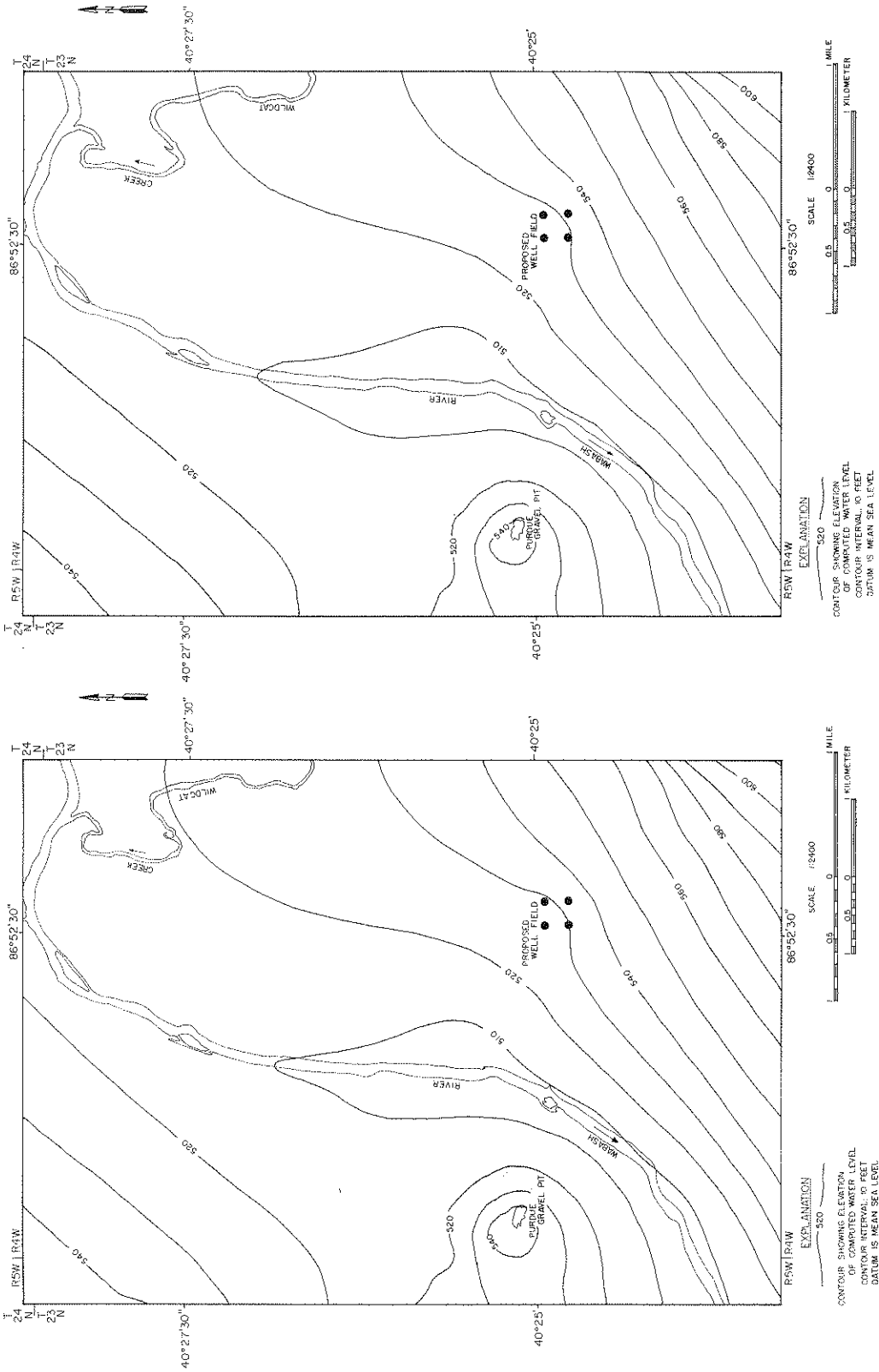
FIGURE 4.5   COMPUTED HEAD DISTRIBUTION USING
HISTORICAL INPUTS (EXPERIMENT A)
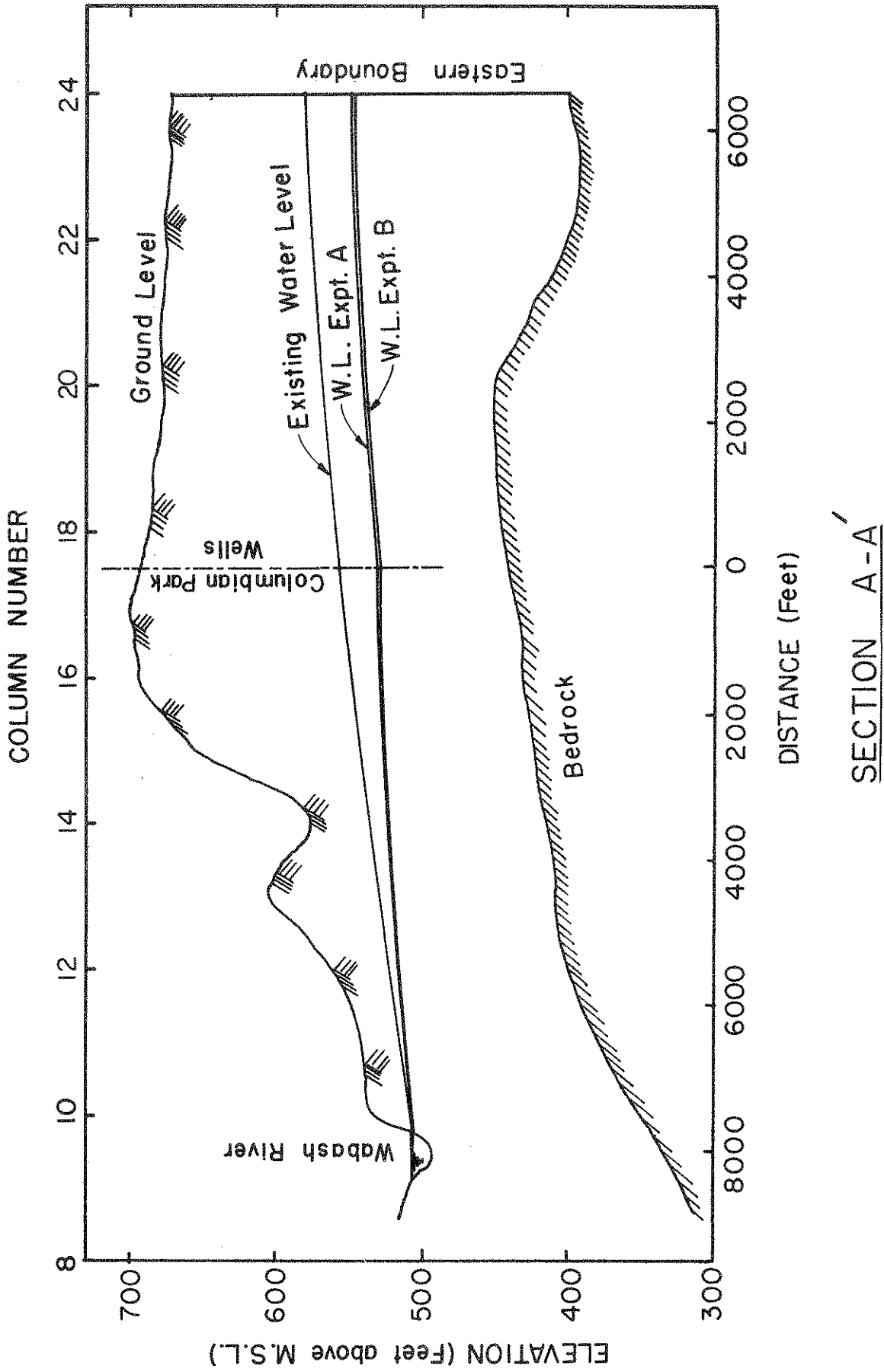
FIGURE 4.7 COMPARISON OF DRAWDOWNS FROM EXPERIMENTS A AND B

The base flow contribution into the Wabash River has decreased to 45.9 mgd (174400 m^3/day) in experiment A and 43.9 mgd (166800 m^3/day) in experiment B in comparison to 54.2 mgd (205900 m^3/day) obtained from the calibrated model (Table 4.2). This corresponds to about 15 percent and 19 percent decrease in the base flow respectively from the experiments A and B. The above discrepancies are essentially due to the additional pumpage of 5.8 mgd (22,040 m^3/day) at the Columbian Park, increased pumpage of 2.8 mgd (10,640 m^3/day) at the other well fields and about 2 mgd (7600 m^3/day) drop in recharge due to rainfall.
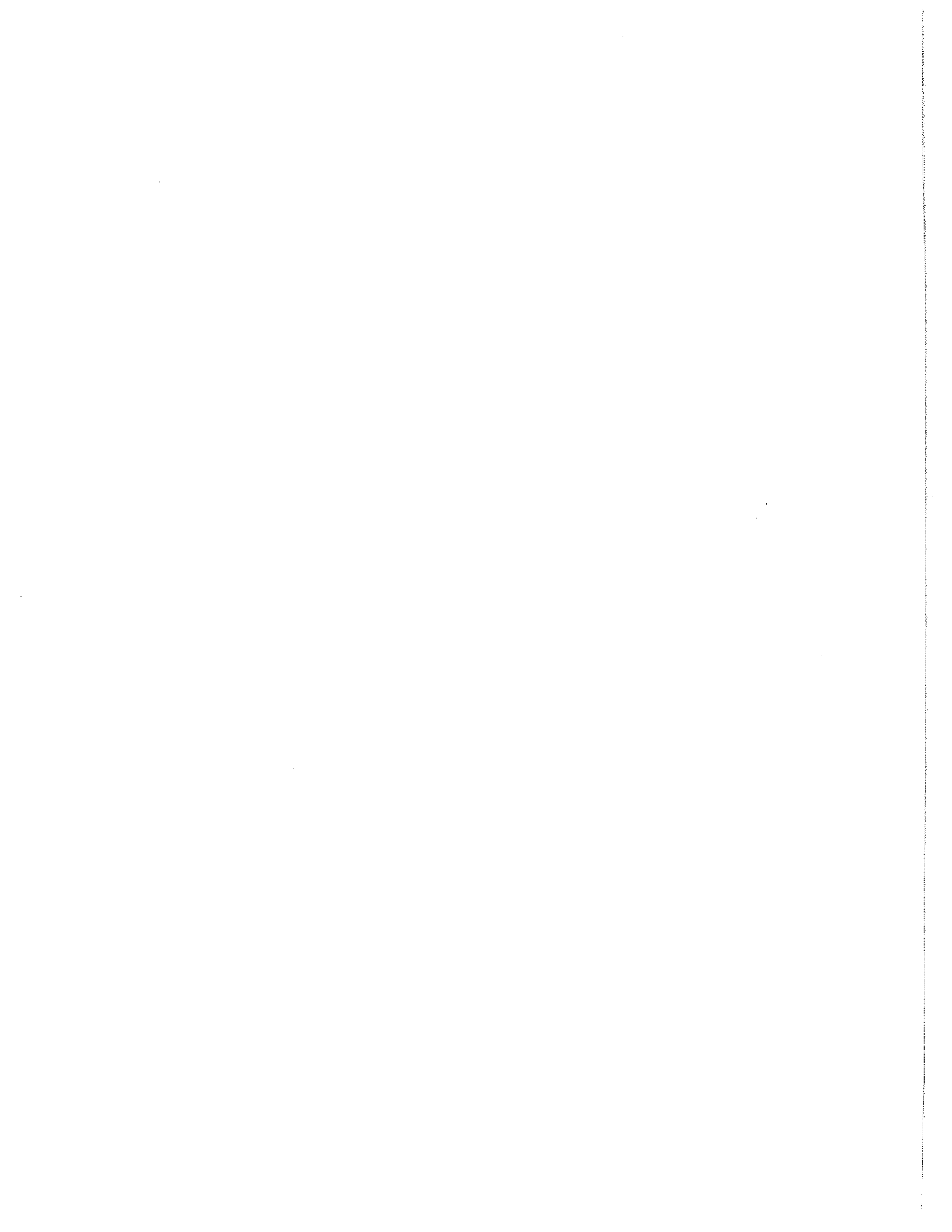
V DISCUSSION AND CONCLUSIONS

Problems encountered in formulating digital models for glacial aquifers, especially relating to the data and other constraints which arise when these models are to be developed for use by decision makers in medium size communities, have been previously discussed. Some of the other aspects such as costs and effort involved in the development of these models are discussed in this chapter. A set of conclusions are also presented.

5.1 Model Limitations

(1) As indicated by the geology of the glacial drift underlying the study area (Sec. 3.3.1), flow through this aquifer is three-dimensional. This fact should be considered in formulating the digital model. However, because of lack of data and budgetary constraints, only a two-dimensional model was used in the present investigation. Therefore, the conclusions presented herein should be interpreted with this approximation and other limitations, mainly the lack of data, in mind.

(2) In the present study, vertical leakage and induced streambed infiltration were handled as lumped quantities at the appropriate nodes in the digital model (Sec. 4.2). Consequently, the digital model was found to be well suited for calibration and water budget analysis. However, the estimation of aquifer capacity under increased pumping rates may not be very accurate in the sense that, the resulting drawdowns may be higher than the actual values.

(3) Because of the limitations imposed by the available data on the formulation and calibration of the model of the aquifer it was not possible to use the stochastic inputs (Sec. 4.4) as effectively as it was conceived initially. This aspect needs further investigation.

5.2 Data Limitations and Costs

Limitations imposed by the data available for the study at different stages of formulation of the model have been discussed in Secs. 3.2, 3.3, 4.2 and 4.4. The shape and the number of finite difference grids have a major bearing on the computational time and computer memory requirements. These limitations have been elaborated in Sec. 4.3.2. However, the cost of data analysis, computer time and the cost of different computer runs as a function of number of nodes and the overall computational expenditure may be of interest to decision makers in medium size communities. Consequently, a brief discussion of these aspects follows.

About 1000 skilled (undergraduate students guided by a graduate research assistant at Ph.D. level) man-hours were required for the preliminary phase in the model development. This phase consisted of data acquisition from past records, preparation of piezometric maps and flow nets, delineation of aquifers, analysis of pumping tests and estimation of aquifer properties. The effort expended in the specification of the aquifer characteristics such as hydraulic conductivity, storage coefficient, piezometric head, depth to bedrock and aquifer thickness at each nodal point of the finite difference grid is proportional to the

number of nodes in the grid. About 300 skilled man-hours were spent on this phase in the present study. The initial computer trial runs and calibration of the digital model were tedious and time consuming. These trials and the final computer runs required about 2500 hours at the skill level of a graduate research assistant.

The cost distribution of different computer runs as a function of number of nodes in the grid system using a CDC 6500 digital computer is shown in Table 5.1. The cost per single run for the Model X (3,055

TABLE 5.1

COST DISTRIBUTION OF DIFFERENT COMPUTER RUNS

Item	MODEL - X	MODEL - Y
Grid size (square)	500 ft	1000 ft
No. of nodes	3,055	792
Core storage (Octal)	110,000	67,000
Central processor time	1,100 Sec	400 Sec
Cost per run	$75 - $90	$25 - $40

TABLE 5.2

COMPUTATIONAL COST OF MODELING

S. No.	Item	Approx. Cost
1	Data processing and preliminary computer runs	$ 2,000
2	Calibration of the Digital Model	$ 4,500
3	Development of stochastic Models	$ 800
4	Estimation of Aquifer Capacity (Final Runs)	$ 2,900
5	Miscellaneous	$ 500
	Total	$10,700

nodes) is about three times as high as that for the Model Y (792 nodes). The above costs are based on an average rate of $250 per hour (Purdue internal rate structure) of central processor time. The major practical limitation to adopt larger number of grids (finer mesh) is the computing cost, a fact which has been emphasized by several other investigators also (Young and Bredehoeft, 1972 ; and Morel-Seytoux and Daly, 1975). The approximate overall computer related expenditure corresponding to different stages during the development of the digital model is presented in Table 5.2.

5.3 Conclusions

The following conclusions can be presented on the basis of the foregoing analysis.

(1) It is feasible to construct a digital model for the glacial aquifers underlying medium size communities with the available data from the past records. However, the results from such models should be

interpreted with caution.

(2) The following results were obtained regarding the location and characteristics of the aquifers underlying the study area.

(i) The alluvial deposits lying on both sides of the Wabash River valley have the highest ground-water potential. The aquifer to the east of the Wabash River, mostly underlying Lafayette, is under leaky artesian conditions. The average hydraulic conductivity of the aquifer underlying the Wabash River valley is about 240 ft/day (73 m/day) and that of the aquifer underlying the terraces is about 160 ft/day (49 m/day). The storage coefficient is about 0.05 on the east side of the Wabash River up to a distance of about 1400 ft (427 m) and about 0.0005 further away. The storage coefficient is about 0.1 for most of the aquifer towards the west of the Wabash River.

(ii) Rainfall is the major source of recharge to the aquifer in the study area. This recharge was computed to be 17.4 mgd (66,120 m^3/day). The average rate of recharge due to rainfall in the Wabash River valley is about 0.9 mgd/sq. mile (1320 m^3/sq. km) and that in the terraces varies from about 0.25 to 0.4 mgd/sq. mile (367 to 590 m^3/sq. km).

(iii) The Wabash River is hydraulically connected to the aquifer and the total base flow contribution into this river in its 8.2 miles (13.2 km.) reach in the study area is about 54.2 mgd (205,960 m^3/day). The average rate is about 6.5 mgd/mile (15,342 m^3/km) of the river. About 60% of the total base flow is from the aquifer on both sides of the river downstream of the stream gage in Lafayette.

(iv) The gravel pit in the Purdue University campus is hydraulically connected and forms a steady source of recharge to the aquifer. The average recharge from the gravel pit is about 15.9 mgd (60,420 m^3/day). A considerable part of this recharge leaves the aquifer as base flow into the Wabash River.

(3) The formulation and calibration of the digital model by using historical data from the past records were satisfactory only to the extent of replicating long term average piezometric surface observed at the test site. Based on this analysis, steady or near steady conditions prevail in the aquifer system.

(4) Cross correlation studies between rainfall, groundwater levels and river stages are quite useful in introducing recharge due to rainfall and in examining the hydraulic interaction between a river and the aquifer. The simulation results from the stochastic models fitted to the monthly precipitation and the mean monthly river stages are satisfactory.

(5) An additional quantity of about 6 mgd (22,800 m^3/day) can be pumped at the hypothetical well field in the Columbian Park without serious depletion of water levels. However, this is not the ultimate capacity of the aquifer.

(6) The approximate computational cost of modeling was $10,700. The computer runs required about 2500 hours at the skill level of a graduate research assistant. The preliminary phase of the model required about 1300 skilled man-hours.
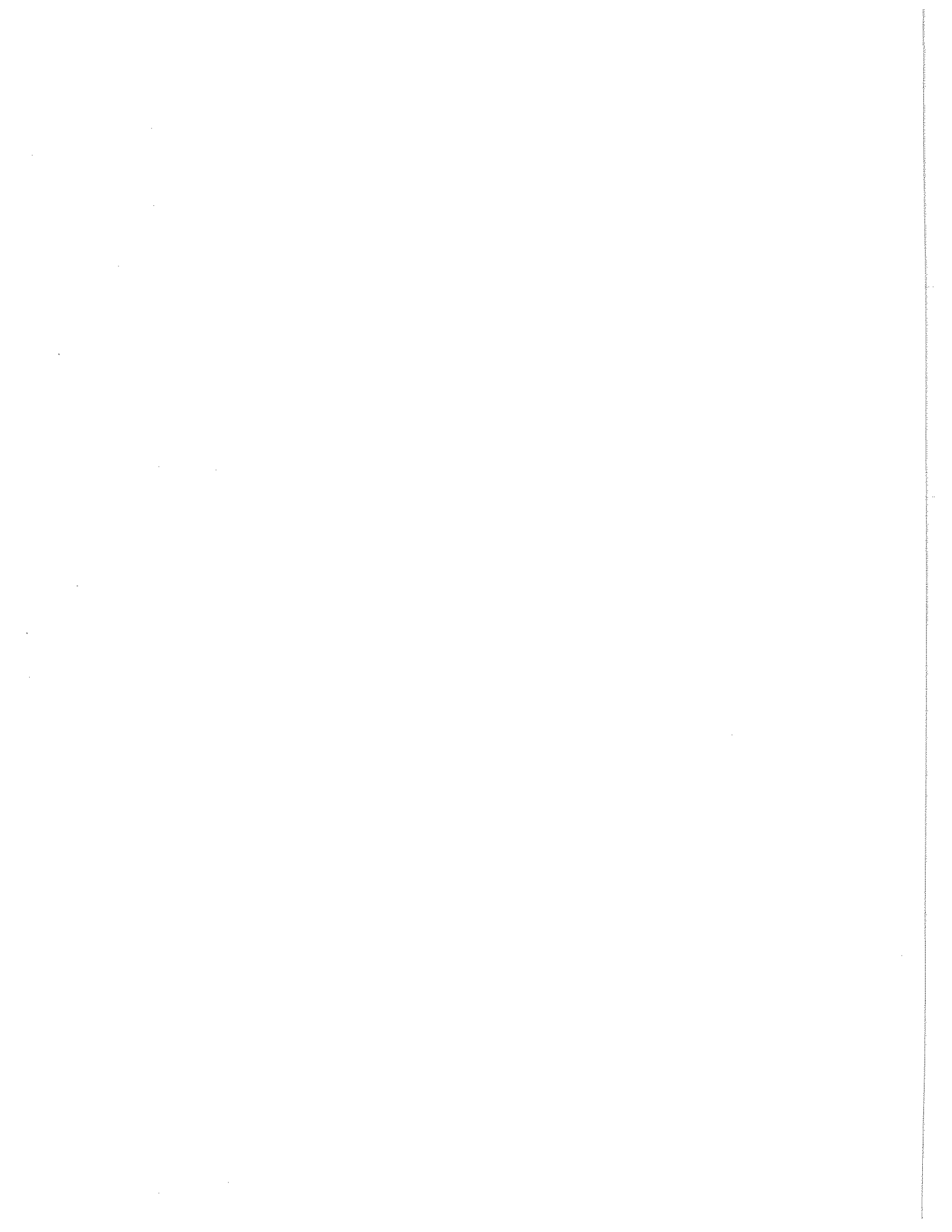
REFERENCES

1. Anderson, R. L., 1942. "Distribution of Serial Correlation Coefficient," Ann. of Math. Stat., Vol. 13, No. 1.

2. Bartlett, M. S., 1955. An Introduction to Stochastic Processes, Cambridge University Press, London.

3. Bear, J., 1972. Dynamics of Fluids in Porous Media, American Elsevier Publishing Co., Inc., New York.

4. Bjelke, W., 1960. "Recharge Capacity of the Purdue Gravel Pit," M. S. Thesis, Dept. of Civil Engineering, Purdue University, West Lafayette, Ind., August.

5. Box, G. E. P., and G. M. Jenkins, 1970. Time Series Analysis, Forecasting and Control, Holden Day, San Francisco.

6. Box, G. E. P., and D. A. Pierce, 1970. "Distribution of Residual Auto Correlations in Autoregressive-Integrated Moving Average Time Series Models," Jour. of Ann. Stat. Assoc., Vol. 64.

7. De wiest, R. J. M., 1965. Geohydrology, John Wiley and Sons, Inc., New York.

8. Dixon, W. J., 1971. Biomedical Computer Programs, Uni. of California Press, Berkeley, Ca.

9. Domenico, P. A., 1972. Concepts and Models in Groundwater Hydrology, McGraw-Hill Book Company, New York.

10. Ferris, J. G., Knowles, D. B., Brown, R. H., and R. W. Stallman, 1962. "Theory of Aquifer Tests," U.S. Geol. Survey, Water Supply Paper 1536-E.

11. Gorby, S. S., 1886. "Geology of Tippecanoe County," Ind. Dept. of Geology and Nat. History, 15th Ann. Rept., pp 61-96.

12. Guymon, G. L., 1973. "Finite Element Solution for General Fluid Motion," Journal of the Hydraulics Division, Proc. of the Am. Soc. of Civil Engineers, Vol. 99, No. HY6, June.

13. Harrell, M., 1935. Groundwater in Indiana, Ind. Dept. of Geology and Nat. History, 15th Ann. Rept., pp. 61-96.

14. Hurr, R. T., 1966. "A New Approach for Estimating Transmissibility from Specific Capacity," Vol. No. 2, No. 4, Water Res. Res., Fourth Quarter.

15. Jacob, C. E., 1940. "On the Flow of Water in an Elastic Artesian Aquifer," Trans. Am. Geophys. Union, pt. 2.

16. Javandel, I., and P. A. Witherspoon, 1968. "Application of the Finite Element Method to Transient Flow in Porous Media," Soc. Petrol. Engrs. Journal, 8(3), p. 241.

17. Jenkins, G. M., and D. G. Watts, 1968. Spectral Analysis and Its Application, Holden-Day, San Francisco.

18. Kashyap, R. L., and A. R. Rao, 1973. "Real Time Recursive Prediction of River Flows," Automatica, The Journal of the International Federation of Automatic Control, Vol. 9, No. 2, pp 175-183, Pergamon Press, Oxford, England, March.

19. Kashyap, R. L., and A. R. Rao, 1976. Stochastic Dynamic Models from Empirical Data, to be published by Academic Press, New York.

20. Leverett, F., and F. G. Taylor, 1915. "The Pleistocene of Indiana and Michigan and the History of the Great Lakes," U.S. Geol. Survey, Mon. 53.

21. Logan, J., 1964. "Estimating Transmissibility from Routine Production Tests of Water Wells," Ground Water, January.

22. Lohman, S. W., et. al., 1972. "Definitions of Selected Ground-Water Terms- Revisions and Conceptual Refinements," Geological Survey Water-Supply Paper 1988.

23. Maarouf, A. M. S., and W. N. Melhorn, 1975. Hydrogeology of Glacial Deposits in Tippecanoe County, Indiana, Tech. Rept. No. 61, Purdue University, Water Res. Res. Center, West Lafayette, Ind., June.

24. Maddock, T., III, 1972. "Algebraic Technological Function from a Simulation Model," Water Resources Research, Vol. 8, No. 1, pp 129-134, February.

25. Maddock, T., III, 1974. "The Operation of a Stream-Aquifer System Under Stochastic Demands," Water Res. Res., Vol. 10, No. 1, February

26. Meyer, W., Reussow, J. P., and D. C. Gillies, 1975. Availability of Ground Water in Marion County, Indiana, Open-File Report 75-312, U.S. Geological Survey, July.

27. Moench, A., 1971. "Groundwater Fluctuations in Response to Arbitrary Pumpage," Groundwater, Vol. 9, No. 2, pp 4-8, March - April

28. Moench, A. F. and C. C. Kisiel, 1970. "Application of Recharge from an Ephemeral Stream," Water Res. Res., Vol. 6, No. 4, August.

29. Morel-Seytoux, H. J., and C. J. Daly, 1975. "A Discrete Kernal Generator for Stream-Aquifer Studies," Water Resources Research, Vol. 11, No. 2, April.

30. Narasimhan, T. N., 1967. "Note on 'A New Approach for Estimating Transmissibility from Specific Capacity' by R. Theodore Hurr," Vol. 3, No. 4, Water Res. Res., Fourth Quarter.

31. Neuman, S. P., and P. A. Witherspoon, 1970. "Finite Element Method of Analyzing Steady Seepage with a Free Surface," Water Res. Res., Vol. 6(3), pp 889-897.

32. Ogden, L., 1965. "Estimating Transmissibility with One Drawdown," Ground Water, July.

33. Peaceman, D. W., and H. H. Rachford, Jr., 1955. "The Numerical Solution of Parabolic and Elliptic Differential Equations," Journal Soc. of Indus. and Applied Mathematics, Vol. 3, pp 28-41.

34. Pinder, G. F., and J. D. Bredehoeft, 1968. "Application of the Digital Computer for Aquifer Evaluation," Water Resources Research, Vol. 4(5).

35. Pinder, G. F., Bredehoeft, J. D., and H. H. Cooper, Jr., 1969. "Determination of Aquifer Diffusivity from Aquifer Response to Fluctuations in River Stage," Water Res. Res., Vol. 5, No. 4, August.

36. Pinder, G. F., and E. O. Frind, 1972. "Application of Galerkin's Procedure to Aquifer Analysis," Water Res. Res., Vol. 8, No. 1, February.

37. Prickett, T. A., and C. G. Lonnquist, 1968. "Aquifer Simulation Program Listing Using Alternating Direction Implicit Method," Illinois State Water Survey mimeographed report presented at International Association of Scientific Hydrology Symposium on Use of Computers in Hydrology, Tuscon, Arizona.

38. Prickett, T. A., and C. G. Lonnquist, 1971. Selected Digital Computer Techniques for Groundwater Resource Evaluation, Bulletin 55, Illinois State Water Survey, Urbana, Ill.

39. Rao, R. A., Kashyap, R. L., and R. G. S. Rao, 1973. "Stochastic Models for the Interaction of Rainfall and Groundwater Levels," Proc. of the International Symposium on Development of Groundwater Resources, College of Engineering, Guindy, Madras, India.

40. Rao, A. R., Rao, R. G. S., and R. L. Kashyap, 1975. Stochastic Models for Ground Water Levels, Tech. Rept. No. 67, Purdue University, Water Res. Res. Center, West Lafayette, IN., August.

41. Remson, I., Hornberger, G., and F. J. Molz, 1971. Numerical Methods in Subsurface Hydrology, Wiley-Interscience.

42. Rosenshein, J. S., and O. J. Cosner, 1956. Groundwater Resources of Tippecanoe County, Indiana, Appendix: Basic Data, Bulletin No. 8, Division of Water Resources, Dept. of Conservation, State of Indiana.

43. Rosenshein, J. S., 1958. Ground-water Resources of Tippecanoe County, Indiana, Bull. No. 8, Division of Water Resources, Indiana Dept. of Conservation.

44. Skibitzke, H. E., 1963. "The Use of Analog Computers for Studies in Groundwater Hydrology," Journal of the Institution of Water Engineers, London, England, Vol. 17.

45. Stallman, R. W., 1956. "Numerical Analysis of Regional Water Levels to Define Aquifer Hydrology," Trans. Am. Geophys. Union, Vol. 37, No. 4.

46. Theis, C. V., 1963. "Estimating the Transmissibility of a Water-Table Aquifer from the Specific Capacity of a Well," U.S.G.S., Water Supply Paper 1536-I.

47. Todd, D. K., 1959. Ground Water Hydrology, John Wiley & Sons, Inc., New York.

48. Walton, W. C., 1970. Groundwater Resource Evaluation, McGraw-Hill Book Company, New York.

49. Wiggert, D. C., 1974. Two-Dimensional Finite Element Modeling of Transient Flow in Regional Aquifer Systems, Tech. Report No. 41, Institute of Water Research, Dept. of Civil Eng., Michigan State Uni., East Lansing, Michigan, August.

50. Young, D. M., 1954. "Iterative Methods for Solving Partial Differential Equations of Elliptic Type," Trans. Am. Math Society, Vol. 76.

51. Young, R. A., and J. D. Bredehoeft, 1972. "Digital Computer Simulation for Solving Management Problems of Conjunctive Groundwater and Surface Water Systems," Water Res. Res., 8(3), pp. 533-556.

52. Zienkiewicz, O. C., 1971. The Finite Element Method in Engineering Science, McGraw-Hill Book Company, New York.

DATA SOURCES

I. Groundwater Levels and Well Data

    (1) *Water Levels and Artesian Pressure in Observation Wells in the United States,* Part 1, Northeastern States, U.S. Geological Survey Water-Supply Papers.

    (2) *Groundwater Unit,* Division of Water, Dept. of Natural Resources, State of Indiana, State Office Building, 100 North Senate Avenue, Indianapolis, Ind. 46204.

    (3) *Hydrogeology of Glacial Deposits in Tippecanoe County, Indiana,* by Maarouf, A.M.S., and W. N. Melhorn, Tech. Rept. No. 61, Purdue University, Water Res. Res. Center, West Lafayette, Ind. 47907, June 1975.

    (4) *Ground-Water Resources of Tippecanoe County, Indiana, Appendix: Basic Data,* compiled by Rosenshein, J.S., and O.J. Cosner, Bulletin No. 8, Division of Water Resources, Indiana Dept. of Conservation, State of Indiana, 1956.

II. Precipitation Data

    (1) *Climatological Data,* Indiana Section, published by the Weather Bureau, U.S. Dept. of Commerce.

    (2) *National Weather Service,* National Oceanic and Atmospheric Administration, Agricultural Advisory Meteorologist, Poultry Science Building, Purdue University, West Lafayette, IN 47907.

III. Pumping Data

    (1) *Water Annual Reports,* Public Service Commission, State of Indiana, State Office Building, 100 North Senate Avenue, Indianapolis, Indiana 46204.

    (2) Physical Plant, Heating & Power, Administrative Services Building, Purdue University, West Lafayette, Indiana 47907.

    (3) West Lafayette Water Company, 1007 Happy Hollow Road, West Lafayette, Indiana 47906.

    (4) Lafayette Water Works, City Hall, 20 N 6th Street, Lafayette, Indiana.

IV. River Stage Data

    (1) *Daily River Stages,* Weather Bureau, U.S. Dept. of Commerce.

    (2) *Water Resources Division,* Geological Survey, U.S. Dept. of Interior, 1819 North Meridian Street, Indianapolis, IN 46202.

PUMPING TEST ANALYSIS

Test No. 1: Well No. 6, West Lafayette Water Company
Node: Col 10, Row 16

Owner   : West Lafayette Water Co., W. Lafayette

Location of well field: T23N, R4W, Sec. 17, NE¼ SE¼ SW¼

Pumped well   : Well No. 6

Observation well   : 10 ft. west of Well No. 6

Tested by   : Layne-Northern Co., Inc., Mishawaka, Indiana

Test period   : 8:00 a.m. to 4:00 p.m., February 23, 1960

The driller's log of the pumped well is shown in Fig. A.1. The well partially penetrates the aquifer and the material mostly consists of sand, boulders and gravel with some clay. The time-drawdown data and the well particulars are given in Table A.1. Semi-log plots of the time-drawdown data are shown in Fig. A.2. The change in slope of the plots after about 95 minutes from the starting of pumping indicates the presence of a recharge boundary. Obviously, the recharge boundary is the Wabash River and the pumped well is located about 500 ft. away from the river. The horizontal part BC of the time-drawdown plot (Fig. A.2) for the pumped well indicates that an equilibrium state was reached after 90 minutes from the start of pumping.

TABLE A.1

TIME-DRAWDOWN DATA, PUMPING TEST NO. 1

Pumped Well   : Well No. 6
Observation Well   : 10 ft. west of Well No. 6
Well   : Depth 88 ft., Inside Dia. 34", Gravel Wall Dia. 36"
Screen   : Length 20 ft., Dia. 18", Slot Size 5, Depth to Top 48 ft.
Pumping Rate   : 1302 gpm
Static Water Level: 25' 7" below reference mark

Date & Time	t (min)	Drawdown (ft.)	
		Pumped Well	Obs. Well
2-23-60			
8:00 A.M.	0	0	0
8:15	15	12.33	2.1
8:30	30	12.75	3.6
8:45	45	13.42	5.0
9:00	60	13.58	5.8
9:15	75	13.92	6.3
9:30	90	14.00	6.8
9:45	105	14.08	6.9
10:00	120	14.08	7.1
10:30	150	14.08	7.3
11:00	180	14.08	7.4
11:30	210	14.17	7.4
12:00 Noon	240	14.0	7.3
1:00 P.M.	300	13.92	7.3
2:00	360	13.83	7.2
3:00	420	14.75	7.8
4:00	480	14.67	8.0

The aquifer transmissivity was computed from the unaffected portion DE of the time-drawdown plot of the observation well using Jacob's approximate formula as given in Eq. A.1.

$$T = \frac{264 \ Q}{\Delta s} \qquad\qquad (A.1)$$

where,

T = transmissivity, in gpd/ft

Q = pumping rate, in gpm

Δs = drawdown difference per log cycle, in feet

$$T = \frac{264 \ X \ 1302}{(7.10-1.07)} = \underline{57000} \ gpd/ft$$

Aquifer thickness m = 61 ft.

The hydraulic conductivity $K = \frac{T}{m} = \frac{57000}{61} = 934 \ gpd/ft^2$.

Since the pumping well is affected by the Wabash River, the storage coefficient of the aquifer was computed using image well theory (Ferris, et al., 1962). The distance of the image well from pumping well is given by Eq. A.2.

$$r_2 = \frac{t_2}{t_1} \ r_1 \qquad\qquad (A.2)$$

where,

r_2 = distance of image well from pumping well

r_1 = distance of observation well from pumping well

t_1 = time intercept on the unaffected portion of the time-drawdown graph at drawdown, s

t_2 = time intercept on the affected portion of the time-drawdown graph at drawdown, s

From Fig. A.2, we have

t_1 = 14.5 min. and t_2 = 245 min. for s = 2 ft.

Using Eq. A.2

r_2 = 41 ft.

Therefore, the distance from the pumped well to the river $= \frac{41}{2} = 20.5'$.

The above value is too small in comparison to the actual distance from the pumped well to the Wabash River. Such a large discrepancy in the estimated distance may be caused by several factors. A few of these are, (1) large deviations in the observational data, (2) the slope of the affected portion, EF of the time-drawdown graph (Fig. A.2) is small and the time intercept is poorly defined for small slopes, and (3) the slope of the time-drawdown graph (Fig. A.2) changes at very small value of time and consequently, small errors in the intercept locus result in appreciable errors in the distance value.

The storage coefficient was estimated using the following relations (Walton, 1970) which are valid under equilibrium conditions.
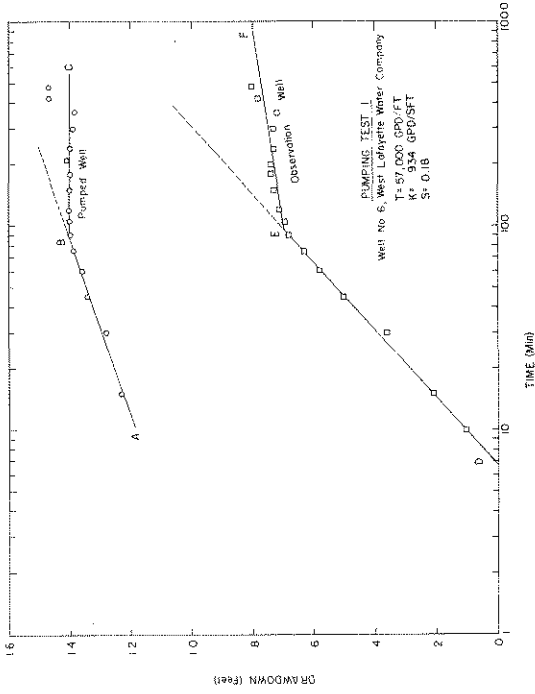
FIGURE A.1 GENERALIZED GRAPHIC
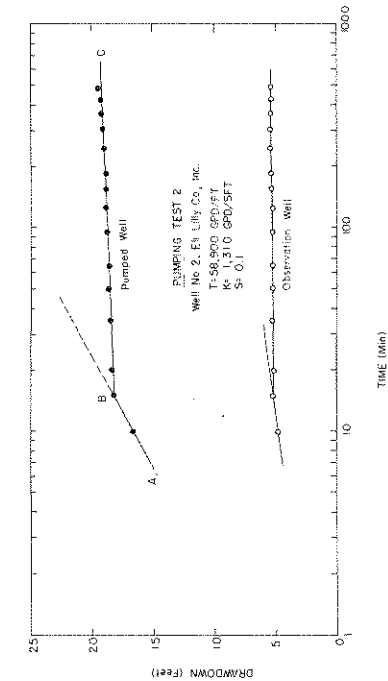LOG OF PUMPED WELLS

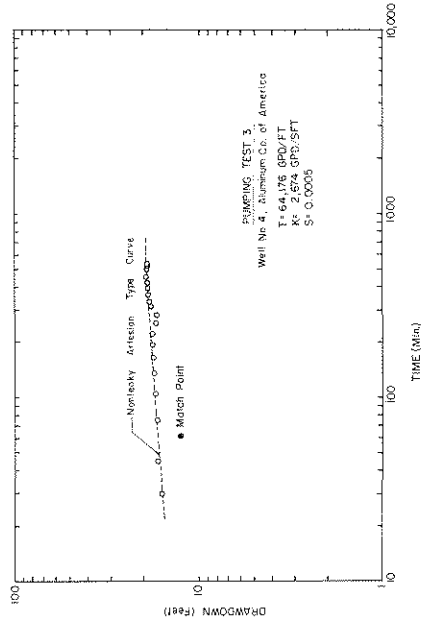FIGURE A.2 TIME-DRAWDOWN GRAPH,
PUMPING TEST NO. 1

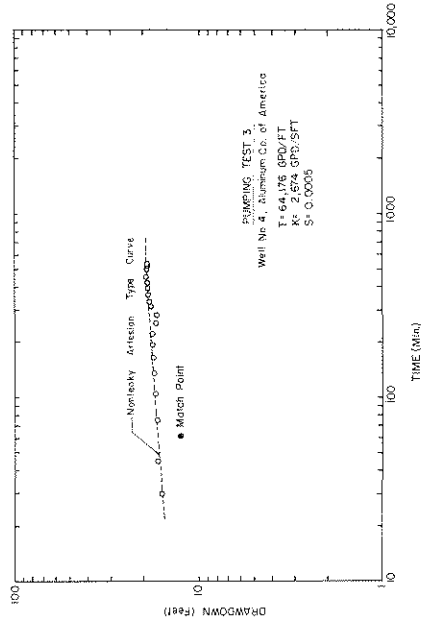FIGURE A.3 TIME-DRAWDOWN GRAPH,
PUMPING TEST NO. 2

FIGURE A.4 TIME-DRAWDOWN GRAPH,
PUMPING TEST NO. 3

$$s_i = s - s_r = \frac{114.6\ Q}{T}\ W(U_i) \qquad\qquad (A.3)$$

$$W(U_i) = -0.5772 - \ell_n\ U_i \quad \text{(Jacob's approximation)} \qquad (A.4)$$

$$U_i = \frac{1.87\ r_i^2 S}{Tt} \qquad\qquad (A.5)$$

where,

s_i = buildup due to image well, in feet

s = drawdown due to pumped well, in feet

s_r = drawdown in observation well near a recharge boundary, in feet

r_i = distance from observation well to image well, in feet

S = storage coefficient, fraction

t = time since pumping started, in days

At the end of pumping we have,

s = 14.67 ft, s_r = 8 ft, t = 480 min.

r_i = 10 + 41 = 51 ft

s_i = 14.67 - 10 = 6.67 ft

$$W(U_i) = \frac{6.67 \times 57000}{114.6 \times 1302} = 2.548$$

U_i = 0.046

$$S = \frac{0.046 \times 57000 \times 480}{60 \times 24 \times 1.87 \times 51 \times 51} = \underline{0.18}$$

The results are:

T = 57000 gpd/ft

K = 934 gpd/ft^2

S = 0.18

Test No. 2: Well No. 2, Ely Lilly Co., Inc.
Node: Col 1, Row 32

Owner   : Ely Lilly Co., Inc., Lafayette

Location of well field: T23N, R5W, Sec 36, NE¼ NE¼ SE¼

Pumped well   : Well No. 2

Observation well   : 15 ft. away from Well No. 2

Tested by   : Layne-Northern Co., Inc.

Test period   : 7:55 a.m. to 4:00 p.m., June 10, 1960

A plot of the well log is shown in Fig. A.1. The time-drawdown data for the pumped well and the observation well are presented in Table A.2 and the field data graphs for the wells are given in Fig. A.3. As these wells are very close to the Wabash River, equilibrium conditions are reached after 15 minutes of

pumping. The aquifer transmissivity was calculated using the unaffected portion, AB of the time-drawdown plot of the pumped well using Eq. A.1.

$$T = \frac{264 \times 2030}{(25.7 - 16.6)} = 58900 \text{ gpd/ft}$$

Aquifer thickness m = 45 ft.

The Hydraulic conductivity K = 58900/45 = 1310 gpd/ft^2.

The available data is not sufficient to compute the storage coefficient. However, after examining the geology of the area, the storage coefficient was assumed to be 0.1. The results are:

$$T = 58900 \text{ gpd/ft}$$

$$K = 1310 \text{ gpd/ft}^2$$

$$S = 0.1$$

TABLE A.2

TIME-DRAWDOWN DATA, PUMPING TEST NO. 2

Pumped Well   : Well No. 2
Observation Well : 15 ft. away from Well No. 2
Well   : Depth 55 ft., Inside Dia. 38", Gravel Wall Dia. 42"
Screen   : Length 20 ft., Dia. 26", Slot Size 5 & 7, Depth to Top 35 ft.
Pumping Rate   : 2030 gpm
Static Water Level: 16' 4" below G. L.

Date & Time	t (min)	Drawdown (ft.)	
		Pumped Well	Obs. Well
6-10-1960			
7:55 A.M.	0	0	0
8:05	10	16.59	4.75
8:10	15	18.25	5.17
8:15	20	18.34	5.17
8:30	35	18.50	5.25
8:45	50	18.67	5.25
9:00	65	18.67	5.25
9:30	95	18.75	5.25
10:00	125	18.84	5.25
10:30	155	18.84	5.33
11:00	185	18.84	5.42
12:00 Noon	245	18.92	5.42
1:00 P.M.	305	19.00	5.50
2:00	365	19.09	5.33
3:00	425	19.17	5.33
4:00	485	19.50	5.42

Test No. 3: Well No. 4, Aluminum Company of America

Node: Col 19, Row 29

Owner   : Aluminum Company of America, Lafayette

Location of well field: T23N, R4W, Sec. 34, NE¼ NW¼ NW¼

Pumped well   : Well No. 4

Observation well   : None

Tested by   : Layne-Northern Company, Inc.

Test period   : 7:15 a.m. to 4:15 p.m., March 25, 1943

The generalized log of the pumped well is shown in Fig. A.1. The time-drawdown data and other details are given in Table A.3. The observed drawdowns were plotted against time on a logarithmic paper (Fig. A.4). A match-point was obtained using the Theis nonleaky, artesian type curve. The values of transmissivity and storage coefficient were computed using Eqs. A.6 and A.7.

<div align="center">

TABLE A.3

TIME-DRAWDOWN DATA, PUMPING TEST NO. 3

</div>

Pumping Well   : Well No. 4
Observation Well   : None
Well   : Depth 233 ft., Inside Dia 8"x16", Gravel Pack
Pumping Rate   : 700 gpm
Static Water Level: 74' 6" below G. L.

Date & Time	t (min)	Drawdown (ft)
3-25-1943		
7:15 A.M.	0	0
7:30	15	15.84
7:45	30	15.75
8:00	45	16.50
8:30	75	16.75
9:00	105	17.00
9:30	135	17.25
10:00	165	17.50
10:30	195	17.67
11:00	225	17.67
11:30	255	17.00
12:00 Noon	285	16.75
12:30 P.M.	315	18.09
1:00	335	18.34
1:30	365	18.59
2:00	395	18.75
2:30	425	18.84
3:00	455	19.00
3:30	485	18.84
4:00	515	18.17
4:15	530	18.17

$$T = \frac{114.6\ Q}{s}\ W(U) \tag{A.6}$$

$$S = \frac{U\ T\ t}{1.87\ r^2} \tag{A.7}$$

The match-point coordinates are:

$W(U) = 10$

$s = 12.5$

$\frac{1}{U} = 10^6$

$t = 62$ min

$T = \frac{114.6 \times 700 \times 10}{12.5} = \underline{64176}$ gpd/ft

$S = \frac{64176 \times 62}{10^6 \times 1.87 \times (1.75)^2 \times 24 \times 60} = \underline{0.0005}$

Aquifer thickness m = 24 ft.

Hydraulic conductivity K = 64176/24 = 2674 gpd/ft^2

The results are:

T = 64,176 gpd/ft

K = 2674 gpd/ft^2

S = 0.0005

APPENDIX B
GRAPHICAL RELATIONSHIPS BETWEEN
SPECIFIC CAPACITY AND TRANSMISSIVITY

The relationships between specific capacity and transmissivity were computed from Eq. 3.1 for the most commonly used values of storage coefficient (S) and for different values of r_w^2/t. The graphs for these relationships are presented in Fig. B.1 and can be used to determine the transmissivity for given values of specific capacity, S and r_w^2/t.

APPENDIX C
FLOW NET ANALYSIS

The flow net for the study area is shown in Fig. C.1. The computational details for the estimation of recharge into the Purdue Gravel Pit and the base flow into the Wabash River are given below.

C.1 Recharge Due to Purdue Gravel Pit

The recharge into the aquifer due to the Purdue Gravel Pit was computed using Eq. 3.2.

$$Q_N = \frac{n_f}{n_d} K h_T m \tag{3.2}$$

Using the flow net enclosed by the 520-530 ft., contour lines around the gravel pit, $n_f = 13$, $n_d = 1$, $h_T = 530-520 = 10$ ft.

Average hydraulic conductivity K = 1500 gpd/ft^2 (Fig. 3.7)

Average ground water level = 525.00 above M.S.L. (Fig. C.1)

Average bed rock elevation = $\underline{415.00}$ (Fig. 3.4)

Thickness of saturated
material   = 110.00

The effective saturated aquifer thickness m = $\frac{2}{3} \times 110 = 73$ ft.
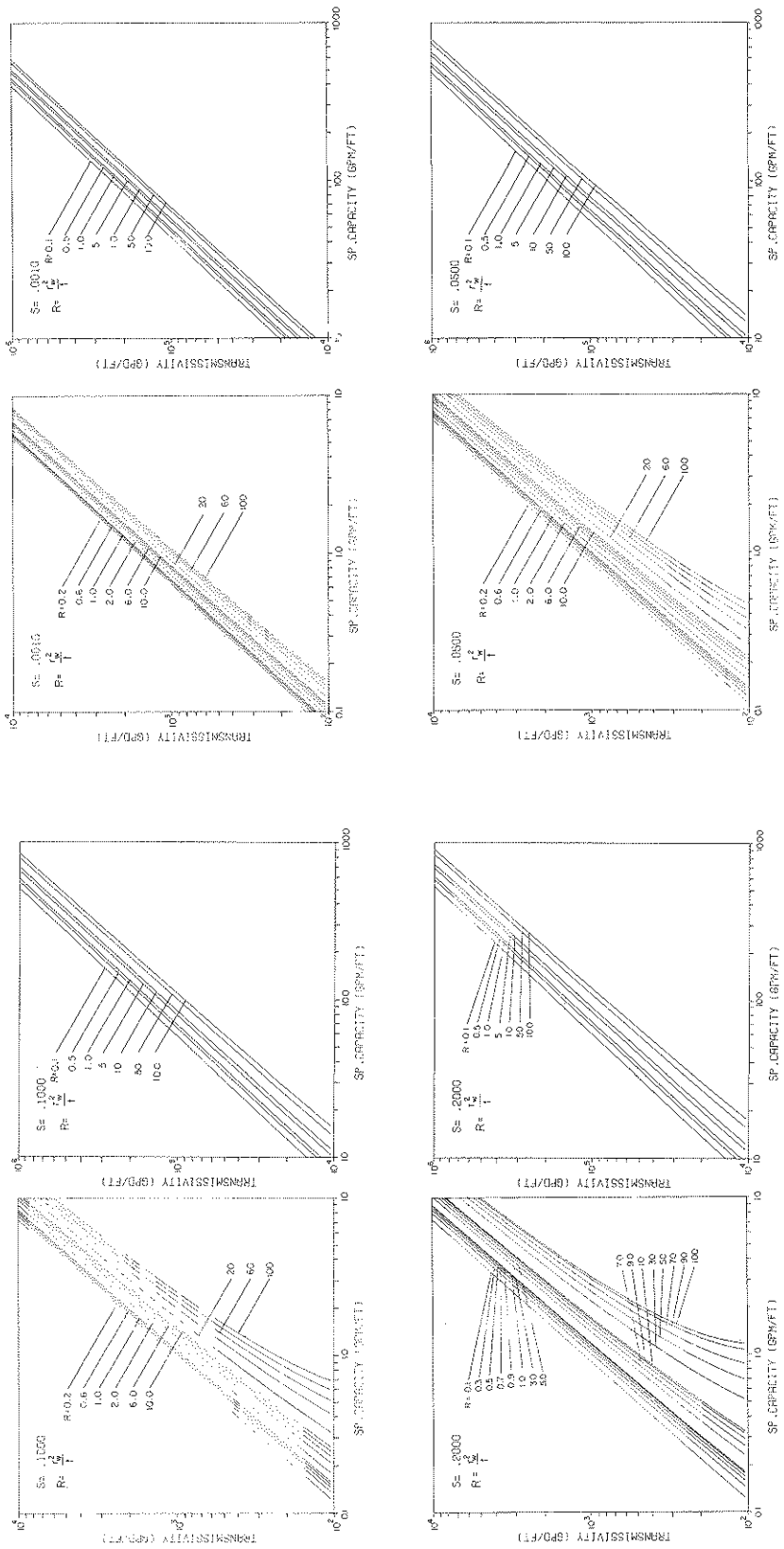
FIGURE B.1 GRAPHS OF SPECIFIC CAPACITY Vs TRANSMISSIVITY
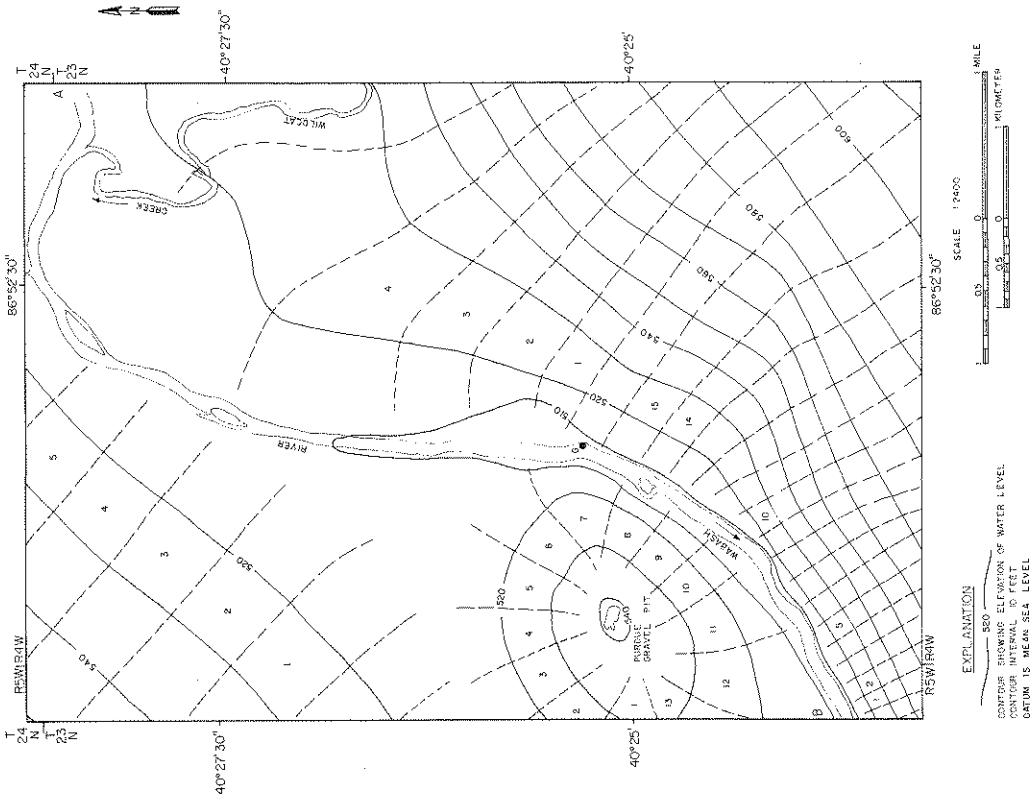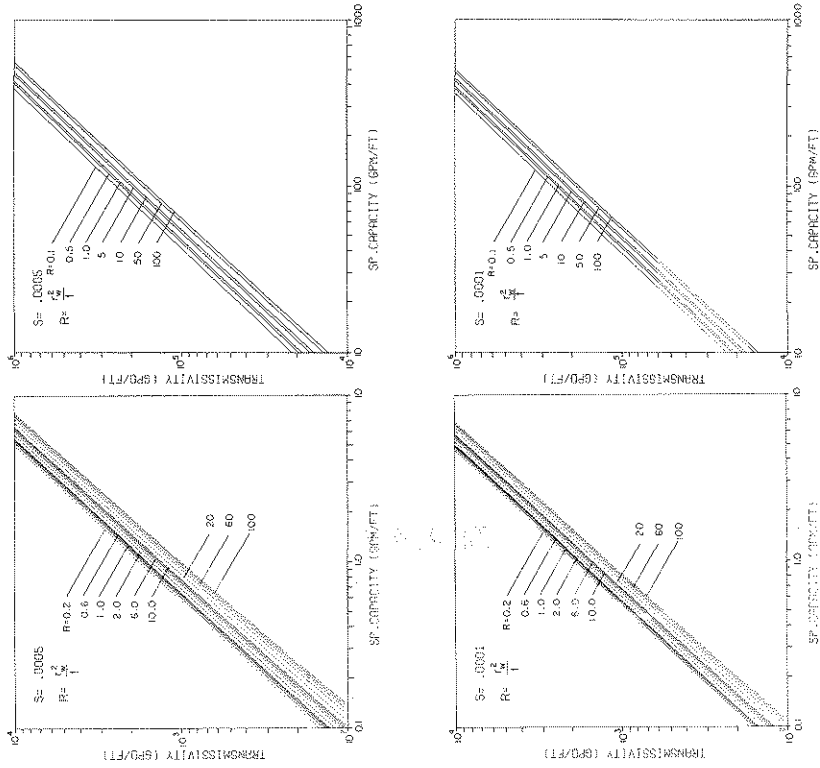
FIGURE C.1 FLOW NET FOR THE STUDY AREA

FIGURE B.1 GRAPHS OF SPECIFIC CAPACITY Vs
TRANSMISSIVITY (CONTD.)

Using Eq. 3.2

$$Q_N = \frac{13 \times 1500 \times 10 \times 73}{1} = 14.2 \times 10^6 \text{ gpd}$$

Therefore,

the recharge due to the gravel pit = 14.2 mgd.

C.2 Baseflow Into the Wabash River

(1) River Reach GA, Upstream of the Lafayette Gage

(a) Western Bank

The flow net between 520-530 ft. contours was used. Then, $n_f = 5$, $n_d = 1$, $h_T = 530-520 = 10$ ft.

Average K = 1600 gpd/ft^2 (213.9 ft/day) (Fig. 3.7)

Average ground water level = 525.00 (Fig. C.1)

Average bed rock elevation = 400.00 (Fig. 3.4)

Thickness of saturated
material   = 125 ft.

The effective saturated aquifer thickness $m = \frac{2}{3} \times 125 = 83$ ft.

Using Eq. 3.2, the average flow

$$Q_1 = \frac{5 \times 1600 \times 10 \times 83}{1} = 6.6 \times 10^6 \text{ gpd}$$

The approximate length of the flow path is 14000 ft. Therefore, the average base flow rate from the western bank $= \frac{6.6 \times 10^6}{14000} = 471$ gpd/ft. length of the river.

(b) Eastern Bank

Considering the flow net between 520-530 ft. contours, $n_f = 4$, $n_d = 1$, $h_T = 530-520 = 10$ ft.

Average K = 1600 gpd/ft^2

Average ground water level = 525.00

Average bed rock elevation = 400.00

Thickness of saturated
material   = 125 ft.

The effective saturated aquifer thickness $m = \frac{2}{3} \times 125 = 83$ ft.

From Eq. 3.2, the average flow

$$Q_2 = 4 \times 1600 \times 10 \times 83 = 5.3 \times 10^6 \text{ gpd}$$

The approximate length of flow path = 12000 ft. The average base flow rate from the eastern bank = $\frac{5.3 \times 10^6}{12000} = 442$ gpd/ft. length of river

(c) Average base flow rate from both banks of the river = 471 + 442 = 913 gpd/ft. length. Length GA of the river in the study area = 5.53 miles. Base flow in the river reach GA = 913 X 5.53 X 5280

$$Q_{GA} = \underline{26.7} \text{ mgd}$$

(2) <u>River Reach GB, Downstream of Gage in Lafayette</u>

(a) <u>Western Bank</u>

Most of the base flow into the Wabash River from the western side is from the Purdue Gravel Pit.

Average water level in the gravel pit = 545.00

Average stage in the Wabash River   = <u>508.00</u>

Differential head H = 37 ft.

Average distance from gravel pit to the river L = 6600 ft.

Average hydraulic conductivity K = 1600 gpd/ft^2

Average hydraulic gradient $I = \frac{H}{L}$

$$I = \frac{37}{6600} = 0.0056$$

From Darcy's Law,

Average velocity of flow V = K I

$$= 1600 \times 0.0056$$

$$= 1.2 \text{ ft/day}$$

Average effective saturated thickness of the aquifer m = 80 ft.

Length of river reach = 2.7 miles.

Base flow from western bank Q_{GBW} = 1.2 X 2.7 X 5280 X 80 X 7.48

$$Q_{GBW} = \underline{10.2} \text{ mgd}$$

(b) <u>Eastern Bank</u>

Considering the flow net enclosed by the 520-560 ft. contours, n_f = 15, n_d = 4, h_T = 560-520 = 40 ft.

Average K = 1800 gpd/ft^2 (240.6 ft/day)

Effective aquifer thickness m = 70 ft.

From Eq. 3.2 we get,

Base flow $Q_{GBE} = \dfrac{15 \times 40 \times 180 \times 70}{4} = \underline{18.9}$ mgd

(3) Total base flow into the Wabash River =

$$Q = Q_{GA} + Q_{GBW} + Q_{GBE}$$

$$= 26.7 + 10.2 + 18.9$$

$$Q = \underline{55.8} \text{ mgd}$$